Nano Energy 155 (2026) 112113

Contents lists available at ScienceDirect

Nano Energy

journal homepage: www.elsevier.com/locate/nanoen

Review

Nanoconfined iontronics: Modular nano-bricks for programmable ion transport

Lixue Yang [a,b], Ari Ivaska [c], Zhe Wang [a,d,e,*], Carita Kvarnström [f,**], Zhong Lin Wang [b,**], Di Wei [b,g,***]

[a] School of Chemistry and Life Sciences, Changchun University of Technology, Changchun 130012, China
[b] Beijing Institute of Nanoenergy and Nanosystems, Chinese Academy of Sciences, Beijing 101400, China
[c] Laboratory of Molecular Science and Engineering, Åbo Akademi University, Henriksgatan 2, Turku 20500, Finland
[d] Advanced Institute of Materials Science, Changchun University of Technology, Changchun 130012, China
[e] Key Laboratory of Advanced Functional Polymer Membrane Materials of Jilin Province, Changchun 130012, China
[f] Department of Chemistry, University of Turku, Henrikinkatu 2, Turku 20014, Finland
[g] Centre for Photonic Devices and Sensors, University of Cambridge, 9 JJ Thomson Avenue, Cambridge CB3 0FA, UK

ARTICLE INFO

Keywords:
Nanoconfined
Iontronics
Ion transport
Functional group structural design
Nanoblock architecture

ABSTRACT

Nanoconfined channels constructed from functional materials provide versatile platforms for regulating ion transport, enabling tailored ion dynamics and high-performance iontronic functionalities. The rational design of such nanoconfined systems is therefore central to advancing next-generation ion regulation and device architectures. In this Review, we establish a unified nano-brick framework that treats nanoconfined spaces as programmable building blocks defined by four key dimensions: geometry, surface charge, chemical functionality, and topology. We emphasize that nanoconfinement is the fundamental prerequisite for high-performance iontronic systems, as confined nanoscale architectures enable selective ion transport and unique ionic dynamics inaccessible in bulk environments. Within these confined spaces, interfacial surface charge governs cation–anion transport and ionic selectivity, while chemical functionalities regulate ion affinity and transport kinetics. Beyond local interfacial modulation, topological engineering introduces asymmetric transport pathways and hierarchical connectivity, enabling directional ion transport and enhanced device performance. We further discuss representative nano-brick platforms based on two-dimensional materials, metal-organic frameworks, and covalent organic frameworks, highlighting how their controlled assembly enables rational design of ion-selective systems for applications in energy harvesting, ionic information processing, and desalination. Finally, we outline the key challenges and future directions toward the practical implementation of nanoconfined iontronics.

1. Introduction

Biological systems offer a quintessential example of ion transport that combines exceptional precision and efficiency within nanoconfined spaces [1–3]. Ion channels and nanopores in biological membranes regulate ionic flux with remarkable selectivity, speed, and energy efficiency, enabling essential physiological processes such as neural signal transmission, osmotic regulation, and energy conversion [4–6]. The interest in and demand for understanding these biological ion transport mechanisms have led to extensive research on ion transport through nanoconfined channels. These phenomena arise from precisely defined nanoconfined spaces, where the channel geometry, chemical functionality, charge distribution, and topological connectivity govern ion motion that is markedly distinct from bulk behavior [7–9]. Inspired by these natural systems, researchers have developed artificial nanoconfined platforms to emulate controllable biological ion transport [10–12]. Unlike natural channels constructed from complex proteins, these systems feature tunable structures, controllable surface functionalities, and superior chemical stability and scalability [13–15]. Advances in nanofabrication and materials chemistry have enabled the construction of nanoconfined channels with precise dimensions and tailored physicochemical properties, providing new opportunities for

* Corresponding author at: School of Chemistry and Life Sciences, Changchun University of Technology, Changchun 130012, China.
** Corresponding authors.
*** Corresponding author at: Beijing Institute of Nanoenergy and Nanosystems, Chinese Academy of Sciences, Beijing 101400, China.
E-mail addresses: wangzhe@ccut.edu.cn (Z. Wang), carkva@utu.fi (C. Kvarnström), zlwang@binn.cas.cn (Z.L. Wang), weidi@binn.cas.cn (D. Wei).

https://doi.org/10.1016/j.nanoen.2026.112113
Received 31 March 2026; Received in revised form 27 May 2026; Accepted 7 June 2026
Available online 10 June 2026
2211-2855/© 2026 Elsevier Ltd. All rights are reserved, including those for text and data mining, AI training, and similar technologies.

the rational design of ion transport at the nanoscale. Moreover, nanoconfined systems exhibits several unique features, such as large surface area, abundant surface charge, scales comparable to the range of various surface/interfacial forces, and size similar to biomolecules or ions [5]. These unique physical and chemical features endow nanoconfined systems with exceptional ionic transport properties, including ion selectivity, ion rectification, surface-charge-governed ion transport, and ionic gating [16–19]. However, despite rapid progress, current research has largely focused on specific materials or device configurations, and a unified framework that systematically links nanostructure design with nanoconfined iontronic functionality is still lacking. Moreover, the latest advances in achieving precise ion transport control through nanoconfined structures and functionalized materials have not been fully reviewed.

Nowadays, various nanoconfined systems have been developed to construct high-performance ion transport channels, including platforms based on two-dimensional (2D) materials [6], metal–organic frameworks (MOFs) [5], covalent organic frameworks (COFs) [9], and functionalized nanoparticles [20]. These materials can form nanostructures of varying dimensionality and topology, such as stacked 2D materials creating nanoscale channels, three-dimensional interconnected networks composed of ordered pores, and heterogeneous architectures assembled from different materials. Through precise control of geometric dimensions, pore size distribution, chemical functionality, charge distribution, and topological connectivity, these nanostructures can be regarded as "modular nano-bricks", providing programmable pathways for ion transport. For example, graphene oxide membranes achieve selective transport of cations and anions by tuning the interlayer spacing and surface functional groups [1]. Graphene-like 2D materials, such as boron nitride [21] and molybdenum disulfide [22], can also realize ion rectification and molecular sieving through control of interlayer spacing and surface chemistry. MOFs, such as zeolitic imidazolate framework−8 (ZIF−8) [23] and university of oslo−66 (UiO−66) [24], offer tunable pore sizes and functional groups, enabling selective transport of specific ions while restricting diffusion rates. COFs provide highly controllable two-or three-dimensional scaffolds, where side-chain modifications-introducing carboxyl [25], amine [26], or sulfonic acid [27] groups-regulate the electrostatic environment and hydrophilicity/hydrophobicity within the channels, thereby enabling precise ion sieving and rectification. The combination of these materials and structures gives rise to 2D layered nanochannels, three-dimensional interconnected pores, and heterogeneous composite channels, enabling high-precision ion regulation within individual channels while establishing scalable ion transport networks across macroscopic or nanoscale membranes, thereby providing a foundation for device-level applications. The concept of modular design plays a key role in this context, with different materials, pore geometries, functional groups, and charge distributions regarded as programmable units. Through controlled assembly, customized ion transport systems can be constructed. For example, a carboxyl-functionalized COF combined with an amine-functionalized MOF can create regions of positive and negative charge within the same channel, enabling differential regulation of cations and anions [28]. Similarly, functionalized nanoparticles introduced into 2D layered materials can locally alter channel hydrophilicity or charge density, thereby modulating ion migration pathways and transport rates [29]. These nanoconfined systems achieve precise control over ion selectivity, rectification, surface charge–governed transport, and gating behavior through the synergistic effects of electrostatic interactions, molecular sieving, and confinement-induced dynamics [30–32]. They provide a foundation for functional applications such as energy harvesting, ion-based signal transmission, ionic logic devices, and seawater desalination, while also offering insights into the mechanisms of biological ion channels and opening new avenues for the development of nanoconfined iontronics.

Focusing on the ion transport behaviors in nanoconfined iontronic systems, this review covers the design and construction of nanoconfined platforms, the fundamental properties and basic principles of ion regulation, and their potential in functional applications (Fig. 1). First, we propose a unified theoretical framework that treats nanoconfined spaces as modular "nano-bricks", defined collectively by geometry, chemical functionality, charge distribution, and topological connectivity, which can be precisely designed to provide programmable pathways for ion transport. Then the fundamental properties and mechanisms of ion transport under nanoconfined conditions are systematically presented. These characteristics depend on the unique geometry of the nanostructures, channel design, and surface chemical environment, and strategies for achieving precise control of ion transport through functional group engineering and structural design are summarized. As the main part of this review, the diverse nano-bricks composed of 2D materials, MOFs, and COFs, as well as the ion transport systems are thoroughly discussed. We further demonstrate that controlled assembly and system integration can yield functional platforms with high ion selectivity and precise regulatory capability, enabling applications in energy harvesting, ion-based signal and information processing, and seawater desalination. Finally, we delineate the prevailing challenges, quantitatively assess the gaps between current achievements and practical benchmarks, and prospect future trajectories for advancing nanoconfined iontronics from concept to application.

2. A unified theoretical framework for modular nano-brick architectures

2.1. Nanoconfined domains as modular nano-bricks for iontronic design

In nanoconfined iontronic systems, each confined domain can be regarded as a discrete yet integrable functional unit. Distinct from continuum-based descriptions, nanoscale confinement introduces well-defined physical boundaries and interfacial characteristics, with dimensions often comparable to the Debye length, ion hydration radius, or even molecular scales [36–38]. Under such conditions, interfacial effects, surface charge interactions, and confinement-induced transport kinetics dominate ion behavior, rather than acting as perturbative corrections [39–41]. Key parameters, including channel geometry, pore size distribution, surface functionalization, charge density, and local potential profiles, can be precisely engineered to regulate ion migration,

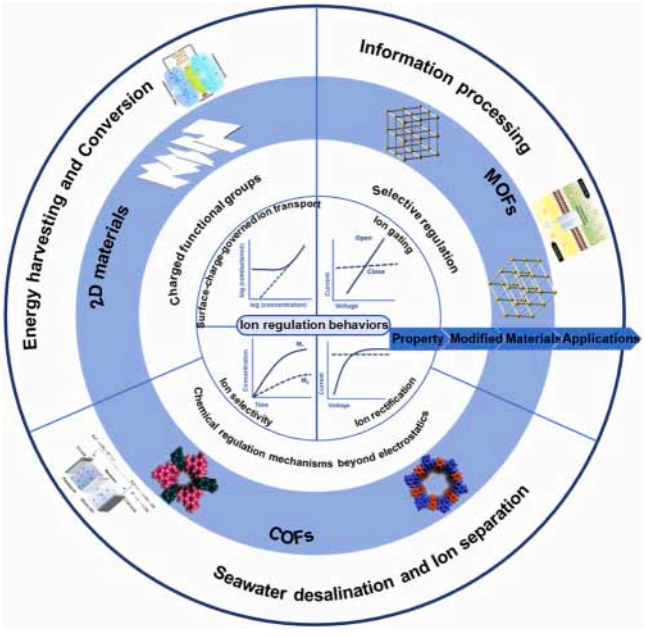


Fig. 1. Schematic diagram showing the main topics of this review: ion transport regulation and applications based on modular nano-brick design [33–35].

selectivity, rectification, and gating with high fidelity.

Importantly, these nanoconfined units exhibit not only functional autonomy but also inherent modularity and scalability. Diverse confinement motifs can be systematically assembled through stacking, arraying, or heterogeneous integration, forming hierarchical ion transport networks with emergent functionalities. At the system level, local transport behaviors, such as ion selectivity and rectification, can be amplified, coupled, or collectively orchestrated to achieve directional ion flux control. Conceptualizing nanoconfined domains as modular "nano-bricks" thus transcends a descriptive analogy, establishing a design paradigm with methodological significance. Rather than treating geometric dimensions, chemical functionality, charge distribution, and topological connectivity as isolated factors, the nano-brick framework views them as interconnected modules whose collective arrangement may give rise to emergent transport characteristics. This framework enables the explicit definition of structure–property relationships at the unit level and supports their hierarchical integration into complex systems, providing a robust theoretical foundation for the rational design of next-generation iontronic architectures.

2.2. Programmable dimensions of nano-bricks

The functionality of nano-bricks is not determined by a single factor but is defined synergistically by multiple programmable dimensions, including geometric dimensions, chemical functionality, charge distribution, and topological connectivity. First, geometric dimensions directly determine the degree of confinement and the overlap of the electrical double layer (EDL) [42]. When the channel size approaches or is smaller than the thickness of the EDL, ion distributions become significantly constrained, thereby affecting ion selectivity and transport rates. The size and shape of the pores also dictate the strength of molecular sieving effects, leading to differential sieving of ions with varying radii or hydration structures. Second, chemical functionalities regulate interactions between ions and the interface. By introducing functional groups such as carboxyl, amino, or sulfonic groups, the interfacial hydrophilicity, charge density, and local polarity environment can be modulated, thereby influencing ion adsorption, desorption, and migration kinetics. Furthermore, the spatial heterogeneity of charge distribution and its gradient structures affect the directionality and driving mechanisms of ion transport, with non-uniform charge domains capable of creating selective transport regions or functional partitions within the channels. Finally, the topological connectivity determines the coupling and synergistic effects between different "nano-bricks". For example, series arrangements can enhance selective sieving capabilities, while parallel or networked structures help improve overall ion flux and system stability [43–45]. These programmable dimensions are not independent of one another but collectively determine the overall ion transport behavior through synergistic regulation. A typical example [46] is the guanidinium-based COF membrane with 1D sub−2 nm channels (geometric dimensions), abundant guanidinium groups (chemical functionality), high positive surface charge (charge distribution), and ordered eclipsed stacking topology (topological connectivity). The synergistic effect of these four dimensions enables exceptional mono/divalent cation selectivity ($K^+/Mg^{2+}\approx202$). Specifically, the sub−2 nm geometry matches hydrated ion sizes; guanidinium groups provide charge-assisted hydrogen bonds; high positive charge creates strong electrostatic repulsion toward divalent ions; and the ordered topology ensures continuous low-resistance pathways, fully demonstrating the necessity of multidimensional synergy. Another representative case [47] is this biomimetic Janus NP-MXene membrane, which possesses sub-nanochannels of approximately 6.0 Å and stable interlayer spacing (geometric dimensions). Through chemical modification with EDTA and PDDA (chemical functionality), it achieves selective transport of cations and anions respectively, forms a Janus structure with asymmetric positive and negative charge distribution on the surface (charge distribution), and features a continuously connected topological structure stacked by two-dimensional nanosheets inside (topological connectivity), combining structural stability and scalable fabrication. Under a 50-fold salinity gradient, it delivers an osmotic potential of 181.5 mV and a power density of 85.1 $W{\cdot}m^{-2}$ with long-term stable performance, and enables gate-free iontronic logic control and signal transmission relying on salinity gradients. By systematically designing geometric, chemical functionality, charge distribution, and topological factors, it is possible to achieve a transition from single-function modulation to multifunctional synergistic integration, thereby laying a solid foundation for constructing high-performance, multi-responsive, and scalable iontronic systems.

These programmable dimensions suggest several structure-performance correlations that can guide nano-brick design. Confinement-charge interplay: When channel dimensions approach the Debye length, surface charge effects dominate over bulk behavior, leading to concentration-independent transport regimes. Asymmetric architecture: Gradient pore geometries combined with non-uniform charge distributions favor directional ion transport and rectification. Chemical selectivity: Pore sizes matched to hydrated ion dimensions, coupled with specific binding sites, enhance selectivity beyond pure electrostatic effects. Stimuli responsiveness: Responsive functional groups integrated into rigid frameworks enable dynamic gating of ion transport. These correlations are quantitatively analyzed in Section 3 and experimentally validated by the nano-brick systems discussed in Sections 4–6.

Despite the great potential of the four programmable dimensions for constructing advanced iontronic systems, several critical limitations remain to be addressed for practical applications. (1) Geometry dimensions: Sub-nanometer channels are vulnerable to structural collapse or pore clogging under realistic operating conditions, especially under pressure fluctuations or fouling environments. (2) Chemical functionality: Many functional groups exhibit limited chemical and thermal stability under harsh operating conditions (for example, hypersaline environments or extreme pH), resulting in progressive performance degradation. (3) Charge distribution: Surface charge is easily screened or attenuated in high-ionic-strength solutions, which weakens electrostatic control and reduces ion selectivity. (4) Topological connectivity: Complex hierarchical topologies require high-precision synthesis, which is difficult to scale up and increases manufacturing costs. Overcoming these limitations will be essential for translating nano-brick-based iontronics into real-world technologies.

3. Properties and basic principles of ion transport in nanoconfined systems

Based on recent advances in the field of nanoconfined iontronics, numerous theories and models have been proposed to elucidate ion transport behavior in nanoconfined systems [48–50]. Ion selectivity, ion rectification, and ion gating are the most fundamental characteristics of nanoconfined systems, primarily arising from surface charge distribution, EDL overlap, and localized chemical environments within the confined space. Ion selectivity is determined collectively by the geometric dimensions, surface functional groups, and charge characteristics of the nanoconfined channels, typically enabling differential transport through electrostatic interactions and molecular sieving effects. Ion rectification manifests as asymmetric transport behavior in different directions, while ion gating refers to the channel's ability to switch or modulate ion transport under specific conditions. This work first provides an overview of the fundamental properties and principles of ion transport in nanoconfined systems, where such behaviors are closely related to precisely engineered nanostructures, controlled channels, and chemical functionality, thereby laying the foundation for understanding and designing high-performance iontronic systems.

3.1. Surface-charge-governed ion transport

In nanoconfined channels with surface charges, ion transport behavior is highly dependent on the fixed charges on the channel walls. Typically, counter-ions preferentially pass through the channel, while co-ions are repelled. This phenomenon, known as ion selectivity, is primarily governed by the EDL effect [51]. The EDL composed of the Stern layer tightly adsorbed on the surface and the outer diffuse layer, forms the basis for various ion transport phenomena in nanoconfined channels (Fig. 2A). At the nanoscale, when the channel radius is comparable to the Debye length, the charge distribution within the EDL significantly affects ion concentration and migration kinetics, thereby determining the channel conductivity and ion selectivity [18,52]. As the channel radius further decreases to approach the thickness of the double layer, surface-charge-governed transport becomes increasingly pronounced, and the system exhibits high ion selectivity.

Surface charge density and solution concentration are key parameters that determine the thickness of the EDL. Under conditions of high salt concentration or low surface charge density, the double layer is relatively thin, and ion transport approaches bulk solution behavior. In contrast, at low salt concentration or high surface charge density, the double layer becomes significantly thicker, and ion transport is dominated entirely by surface effects, resulting in excellent ion selectivity. For example, measurements of ionic conductivity in nanoconfined channels as a function of solution concentration show that at high concentrations, the conductivity increases approximately linearly with concentration, consistent with the bulk solution conductivity γ_{bulk}, but at low concentrations, the conductivity deviates from bulk behavior and reaches a plateau, indicating the dominant role of surface charge in ion transport (Fig. 3) [52].

$$\gamma_{bulk} = \sum \mu_i c_i N_A e = (\mu_{K^+} + \mu_{Cl^-}) c N_A e \quad (1)$$

Here, μ_i is the ion mobility, c_i is the ion concentration, N_A is Avogadro's number, and e is the elementary charge. The conductivity plateau observed at low concentrations is primarily attributed to the excess mobile counter-ions present at the channel surface, which carry the majority of the current within the channel. Under the condition of overall electroneutrality, the concentration of mobile counter-ions within the channel can be calculated based on the surface charge density and the channel geometry, providing a theoretical basis for explaining the deviation of conductivity from bulk solution behavior at low concentrations. This indicates that in nanoconfined systems, even at very low bulk solution concentrations, surface effects can still dominate ion transport, enabling highly controllable ion selectivity and conductivity [52,53].

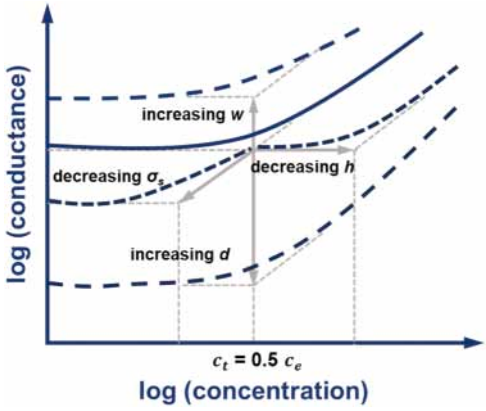


Fig. 3. Schematic illustration of ion conductance in a nanoconfined system as a function of KCl concentration, showing the impact of the surface charge density σ_s, the width w, the length d, and the height h of the nanofluidic system on its conductance.

$$c_e = \frac{2\sigma_s}{hN_A e} \quad (2)$$

Here, σ_s refers to the effective surface charge density, and h is the channel height. When the bulk salt concentration is lower than the concentration of excess mobile counter-ions inside the channel, the negative surface charge of the nanoconfined channel attracts cations to maintain electroneutrality, while anions are repelled due to electrostatic interactions. The total channel conductance G can be considered as the sum of the bulk conductance and the contribution from excess counter-ions:

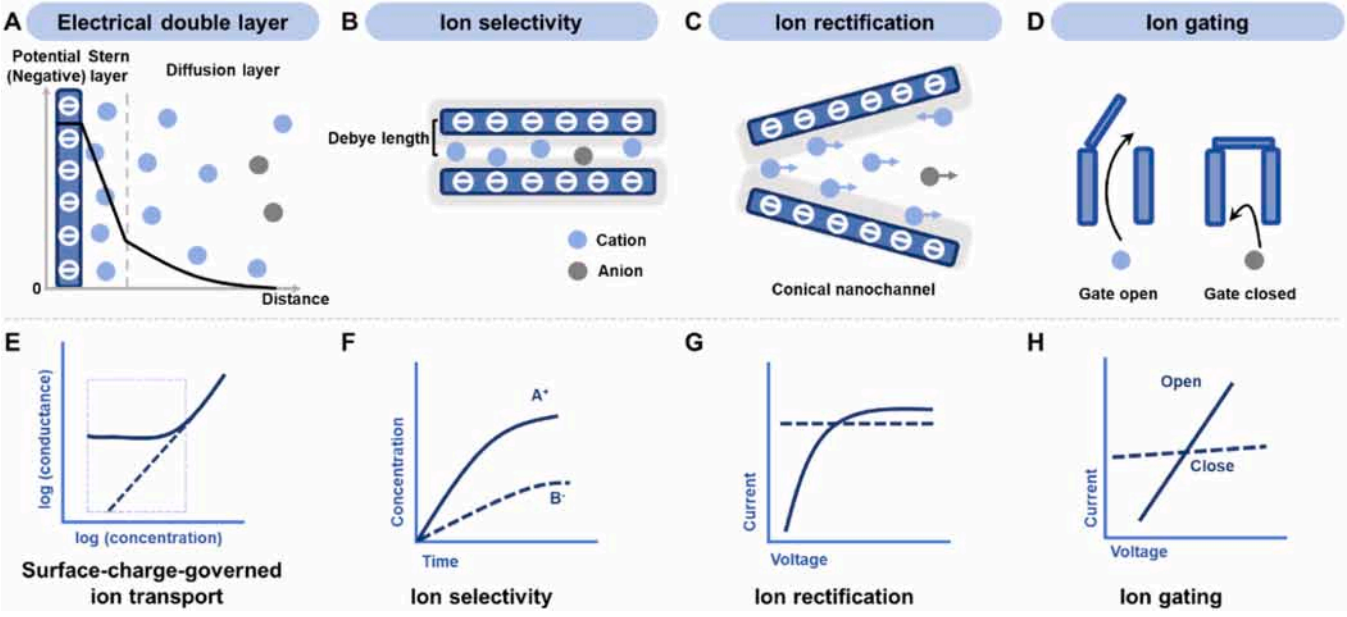


Fig. 2. Properties and basic principles of ion transport in nanoconfined and the typical curves. (A) Schematic diagram of the EDL mechanism and the potential profile as a function of distance from the charged surface (solid line). (B) Ion selectivity in a surface-charged nanochannel. (C) Ion rectification in a conical charged nanochannel. (D) Schematic representation of ion gating. (*E*)-(H) Typical curves of surface-charge-governed ion transport, ion selectivity, ion rectification, and ion gating in nanoconfined systems.

$$G = (\mu_{K^+} + \mu_{Cl^-})cN_A e\frac{wh}{d} + 2\mu_{K^+}\sigma_s\frac{w}{d} \quad (3)$$

Here, w and d refer to the channel width and length, respectively. This model not only explains the conductance plateau observed at low concentrations but also highlights the central role of surface charge in governing ion transport in nanoconfined systems.

When the bulk salt concentration exceeds the concentration of excess mobile counter-ions in the channel (c_e), the conductance of the nanoconfined channel is primarily governed by the channel geometry, corresponding to the first term in Eq. (3) The second term in Eq. (3) indicates that when the salt concentration is below (c_e), ion conduction is dominated by the effective surface charge density (σ_s) and is insensitive to the channel height, exhibiting the typical characteristics of surface-charge-governed ion transport. When the contributions of the two terms in Eq. (3) are equal, the transition salt concentration (c_t) can be defined. Below this concentration, the channel enters the conductance plateau region, where the conductance shows a weakened dependence on salt concentration. This analysis clearly illustrates the dominant role of surface charge in ion transport within nanoconfined channels, as well as the regulatory interplay between channel geometry and surface effects.

The geometric dimensions of the channel have a significant impact on the conductance behavior of nanofluidic systems: increasing the channel width (w) enhances the overall conductance, whereas reducing the channel height (h) decreases it. Although decreasing the height does not alter the magnitude of the conductance plateau, it results in an increase in the critical salt concentration (c_e) required to reach the plateau. The effective surface charge density (σ_s) is a key parameter influencing the conductance of nanofluidic systems. When$\sigma_s$decreases, both the conductance plateau and its corresponding critical concentration shift toward lower values (Fig. 3). This pronounced sensitivity to surface charge density provides a new strategy for the precise regulation of ion transport. For instance, the responsiveness of surface charge density to solution pH can enable differential selectivity between cations and anions under varying conditions, thereby inducing ion rectification behavior. Furthermore, from the perspective of energy conversion, increasing the surface charge density or reducing the thickness of nanomembranes can enhance osmotic energy harvesting efficiency, providing theoretical guidance for the design of high-performance iontronic devices [54,55].

$$I_{osm} = \frac{2\pi R\sigma_s}{L}\frac{k_B T}{\eta\lambda_B}\log(C_s) \quad (4)$$

where I_{osm} is the osmotic current, and R, η, λ_B, k_B, and T are the channel radius, the viscosity, the Bjerrum length, the Boltzmann constant, and the absolute temperature, respectively. C_s is the concentration gradient. L and σ_s refer to the channel length (membrane thickness) and surface charge density, respectively.

In conclusion, surface charge not only determines the transport preference of counter-ions versus co-ions, but also provides precise control over ion selectivity and conductivity in nanoconfined systems by regulating the local ion concentration and electric potential distribution.

3.2. Ion selectivity

Ion selectivity is one of the fundamental characteristics of nanoconfined systems, referring to the preferential transport of certain ions (such as cations versus anions, or ions of different valence or size) over others through the channel. This property directly influences rectification, gating, and energy conversion functions in nanoscale iontronic systems. In nanoconfined channels, ion selectivity primarily arises from the synergistic effects of surface charge, channel geometry, chemical functionality, and topological structure. In nanoconfined channels with fixed surface charges, the wall charges repel co-ions and attract counter-ions through electrostatic interactions. Due to thermal fluctuations and Brownian motion, counter-ions are not strictly confined to the channel walls but instead form a concentration profile that gradually decays from the surface toward the channel center [56]. This region is known as the diffuse layer, where the electric potential decays exponentially along the direction perpendicular to the channel wall (as illustrated by the solid line in Fig. 2A). The thickness of the EDL is typically characterized by the Debye length, (λ_D), which depends on parameters such as the ionic concentration, temperature, and dielectric constant of the solution. It provides a quantitative measure of the range over which surface charges in the nanochannel influence the ion distribution [57].

$$\lambda_D = \left(\frac{\varepsilon_r\varepsilon_0 kT}{2n_{bulk}z^2e^2}\right)^{\frac{1}{2}} = \left(\frac{\varepsilon_r\varepsilon_0 RT}{2c_{bulk}z^2F^2}\right)^{\frac{1}{2}} \quad (5)$$

Here, ε_r is the relative permittivity of water, ε_0 is the vacuum permittivity, k is the Boltzmann constant, c_{bulk} is the bulk solution concentration, z is the ion valence, and e is the elementary charge. T, F, and R represent the absolute temperature, the Faraday constant, and the universal gas constant, respectively. As the solution concentration increases, the Debye length gradually decreases. When the channel width approaches the Debye length, the EDL inside the nanochannel significantly overlap. This overlap leads to a concentration profile dominated by counter-ions, while co-ions are excluded from the channel, resulting in highly selective ion transport. The combined effects of geometric confinement at the channel entrance and surface charge enable controlled and predictable ion transport at the nanoscale. The ion selectivity of nanofluidic systems can be quantitatively characterized by measuring the diffusion rates of tracer ions, fluorescent probes, or dye molecules, thereby revealing the channel's ability to discriminate between different ions (Figs. 2B and 2F) [14,15,58,59]. In recent years, sub-nanometer nanofluidic membranes based on MOFs and COFs have attracted widespread attention, owing to their ordered channel structures, sub-nanometer pore sizes, rich channel topologies, and tunable chemical functionalization [60–62]. For example, in ZIF−8 nanomembranes, efficient selective filtration of cations with different hydration diameters is achieved through sub-nanometer pores, which endows the system with excellent ion selectivity and energy conversion performance [24]. It is worth noting that the high output current of the nanomembrane is not solely dependent on ion selectivity, for instance, in the case of a single-layer 1,3,5-triformylphloroglucinol–p--phenylenediamine (TpPa−1) COF membrane, its high porosity plays a decisive role in achieving high current density, with ion selectivity being just one of the contributing factors [63].

3.3. Ion rectification

Ion rectification refers to the directional asymmetry of ion transport in nanoconfined systems, where ions preferentially pass through the channel in one direction while being hindered in the opposite direction. This phenomenon is typically reflected in the current–voltage (I–V) characteristics (Fig. 2G), where the current at the same absolute voltage differs significantly under opposite polarities, exhibiting diode-like behavior [64–66]. Ion rectification is a hallmark of nonequilibrium transport in nanofluidic systems, primarily arising from the combined effects of structural asymmetry in the nanochannels, surface charge distribution, and electrostatic interactions within the confined space.

Mechanistically, ion rectification typically relies on asymmetric geometries of nanopores or nanoslits, or on nonuniform surface charge distributions. In asymmetric channels, the local potential distribution creates energy barriers that hinder ion transport in one direction while allowing freer movement in the opposite direction. This asymmetric potential typically arises from the overlap of the EDL with the channel walls, which alters the local ion concentration profile and thus generates directional differences in ion transport. Rectification efficiency is typically quantified by the rectification ratio (r_{rec}), defined as the ratio of forward to reverse current. A higher rectification ratio indicates stronger

control over the directionality of ion transport [64,67,68].

$$r_{rec} = \left| I_{-U} / \; I_{+U} \right| \quad (6)$$

A classic example is a conical nanopore with a negatively charged surface. Siwy et al. proposed the "ratchet model" to qualitatively explain its rectification behavior [66]. In the conical pore, the electric field is stronger at the tip, producing an asymmetric, sawtooth-like potential distribution. When a forward voltage is applied, the electrostatic potential forms an energy well that suppresses ion flow; under reverse voltage, this energy well is absent, allowing increased ion transport. This indicates that, to achieve significant rectification, nanopores generally require high surface charge density, small channel dimensions, and low bulk solution concentration.

In addition to geometric asymmetry, the spatial distribution of surface charge can also induce rectification. Nanopores can be functionalized with chemical groups to create uneven charge distributions at the entrance and exit, or heterostructures can be formed by combining membrane materials with different pore sizes and surface functionalities. For example, heterostructured nanofluidic membranes based on COFs and ZIF−67, composed of highly ordered angstrom-scale pores and cavities, can achieve efficient ion rectification through differences in pore size distribution, surface charge density, and wettability [69]. Another example is a three-layer continuous pore membrane constructed by integrating an ultrathin, dense Zr-based UiO−66-NH_2 MOF layer with highly aligned anodic aluminum oxide (AAO) nanochannels: the angstrom-scale windows of UiO−66-NH_2 provide highly selective ion transport, while the geometric gradient promotes directional ion flow, significantly enhancing rectification performance and osmotic energy harvesting efficiency [70].

Overall, by tuning the channel geometry, surface charge, and the combination of membrane materials, ion rectification can not only achieve unidirectional transport but also simultaneously optimize overall ion permeability and selectivity. In osmotic power harvesting, ion-selective membranes, and bioinspired ion transport systems, precise control of ion flow is crucial for enhancing performance. With advances in material design, surface functionalization, and environmental regulation, the controllability and efficiency of ion rectification are expected to improve further, offering more effective solutions for energy conversion, separation technologies, and sensing applications.

3.4. Ion gating

Ion gating refers to the ability of a nanoconfined system to actively regulate or switch ion transport, enabling the channel to alternate between "open" and "closed" states in response to external stimuli or intrinsic triggers, or to modulate the magnitude of ion flux (Fig. 2D). When the gate is in the closed state, ions cannot pass through the channel, resulting in negligible ion current; when the gate is open, ions can flow freely, generating a significant ion current (Fig. 2H) [55]. Unlike passive ion selectivity or ion rectification, ion gating enables dynamic control over ion flow. This feature is crucial in both biological ion channels and artificial nanofluidic devices, providing a foundation for applications in signal transduction, sensing, and energy conversion [71–74]. Depending on the triggering mechanism, ion gating can be classified into voltage-gated, light-gated, ligand-gated, pressure-gated, and other types. By designing smart materials and applying specific external stimuli, ion-gated systems can precisely regulate the transport of chemical or biomolecular species. The on-off ratio ($r_{on\text{-}off}$) is an important metric for evaluating gating performance, typically determined by measuring the transmembrane ion current. It is defined as the ratio of the current in the open state to that in the closed state.

$$r_{on-off} = \left| I_{open} / \; I_{closed} \right| \quad (7)$$

Ion gating is a mechanism that enables the regulation of ion transport and can be realized through various strategies. One approach involves controlling the surface charge density, where altering the local electrostatic potential modulates the energy barrier for ion migration, thus enabling controllable ion transport. Another key mechanism relies on the responsive changes of the channel's internal structure, such as the expansion or contraction of polymeric, MOF, or COF frameworks under external stimuli like pH, temperature, light, or chemical triggers. Additionally, stimulus-responsive functional groups, such as protonatable amines, carboxyls, or azobenzene moieties, can dynamically modify the channel's internal surface charge or hydrophilicity/hydrophobicity, thereby achieving reversible gating behavior. Many studies have demonstrated effective ion gating in nanoconfined systems [26]. For example, carboxyl-functionalized COF membranes exhibit pH-responsive gating behavior: at low pH, protonation of the carboxyl groups reduces the negative charge, thereby suppressing cation transport through the channel; at high pH, deprotonation of the carboxyl groups reopens the channel, restoring ion transport. Similarly, embedding stimulus-responsive polymer or MOF layers within nanoconfined channels allows the channel permeability to be modulated under external stimuli, enabling precise control over ion flux [75]. Ion gating not only enables selective and switchable ion transport at the level of a single channel, but can also be integrated across multi-channel arrays to construct programmable ionic circuits and logic systems [76–78]. This capability opens new avenues for applications of nanofluidic systems in ion-based signaling, energy conversion, sensing, and information processing.

In addition, the tunability of nanofluidic systems can be further enhanced through chemical modification with smart materials or by incorporating stimuli-responsive elements [79,80]. By designing functional molecules that respond to light, temperature, or chemical stimuli and integrating them into nanofluidic systems, multi-responsive ion regulation mechanisms can be realized [79,81]. For example, photoresponsive molecules such as azobenzene and spiropyran have been used to construct light-driven isomerizable nanofluidic systems, achieving ion gating by altering channel dimensions and surface wettability [82]. Thermoresponsive nanofluidic channels, on the other hand, rely on the expansion or contraction of temperature-sensitive polymers to modulate pore size, thereby enabling controlled ion transport [83]. For example, Sheng et al. [84] reported a COF membrane with a thickness of less than 2 nm, which exhibited high permeability for monovalent cations and extremely low permeability for multivalent cations, achieving a K^+/Mg^{2+} selectivity of approximately 765, demonstrating ultrahigh monovalent ion sieving performance. This study not only advanced the understanding of ion selectivity and rectification effects but also provided new insights for achieving efficient energy harvesting and sensing.

These derived theoretical formulas quantitatively correlate channel geometric parameters, interfacial surface charge properties and solution environmental conditions with macroscopic ionic transport performances, and their respective applicable regimes and internal physical mechanisms are fully clarified throughout the above discussion, which provides systematic theoretical guidance and quantitative criteria for the rational design and performance optimization of various nanochannel-based ion transport systems.

4. Functional group engineering and structural design strategies

In nanoscale confined systems, ion transport behavior is governed not only by geometric confinement effects within channels but also more profoundly by the delicate regulation of interfacial chemical environments and local structural features. Therefore, systematic optimization of charge distribution, chemical interactions, and spatial configuration inside channels through functional group engineering and structural design strategies has emerged as a core pathway for achieving highly selective, high-flux, and multifunctional ion regulation [85–87]. On the one hand, the introduction of charged functional groups can effectively modulate the EDLstructure and local electrostatic potential, enabling

precise control over ion sieving and transport directionality. On the other hand, chemical regulation mechanisms beyond purely electrostatic interactions, such as coordination interactions, hydrogen bonding, and specific ion–framework interactions, further expand the regulatory dimensions and application potential of nanofluidic systems under complex environments. Based on this, the following sections will systematically elaborate on charged functional group regulation and chemical mechanisms beyond electrostatics.

4.1. Charged functional groups and selective regulation

In nanoscale confined systems, charged functional group engineering is one of the most direct and effective strategies for achieving selective ion regulation. By introducing tunable charge sites on the inner walls of channels, a stable electrostatic potential gradient can be constructed across spatial scales, thereby altering the EDL structure and modulating ion migration pathways. The type, density, and spatial arrangement of functional groups all exert significant influences on the local potential distribution. Generally, high-density and uniformly distributed charged sites help form a continuous charge screening effect, enabling the channel to exhibit stronger ion sieving capability, whereas irregularly distributed charges may induce local ion accumulation or create heterogeneous transport pathways.

Negatively charged functional groups (such as carboxyl, sulfonic, and phosphoric groups) primarily facilitate cation transport while suppressing anion migration through electrostatic attraction, thereby regulating ion selectivity and the transport kinetics of hydrated ions. Among them, sulfonic groups, owing to their strong electronegativity and stable ionization behavior, can generally endow nanochannels with higher cationic conductivity. In contrast, the ionization behavior of carboxyl groups is more strongly influenced by environmental pH, making them more suitable for constructing environment-responsive ion regulation systems. Based on the above design concept, various negatively charged functionalized nanochannel membranes have been developed sequentially. For example, the freestanding TpPa-SO_3H COF membrane with vertically aligned one-dimensional nanochannels introduces sulfonic groups onto the pore walls to provide abundant negative charge sites, achieving not only high water flux but also excellent size and charge-dependent sieving performance for various water-soluble drugs and dyes (Fig. 4A) [88]. Furthermore, sulfonated poly (ether ether ketone) (SPEEK) nanochannel membranes with high spatial charge density enhance cation selectivity and ionic conductivity by regulating channel structures, achieving high power density output under salinity gradient conditions while maintaining good mechanical stability (Fig. 4B) [89]. In addition, carboxylate-functionalized nanochannel network membranes with pore sizes of 1–3 nm can achieve highly selective separation based on differences in molecular charge and size, while also exhibiting excellent water flux and considerable potential for tunable functionalization [90].

Positively charged functional groups mainly include amino groups, quaternary ammonium groups, and other protonatable moieties. Among them, amino groups tend to undergo protonation under low pH conditions, rendering the interior of channels positively charged and thereby promoting anion transport. In contrast, deprotonation under high pH conditions weakens electrostatic attraction and reduces anion flux. Compared with amino groups, quaternary ammonium groups, owing to their structural stability, can generally maintain a constant charge state over a relatively wide chemical environment, making them more suitable for constructing long-term stable ion sieving systems. Based on the above charge regulation mechanisms, researchers have further developed various positively charged nanomembrane design strategies. For example, Zhao et al. constructed a positively charged nanofiltration membrane system with coexisting polyamine and quaternary ammonium groups, increasing the surface charge density of the membrane and enhancing the Donnan exclusion effect, thereby enabling efficient selective separation of Mg^{2+} and Li^{+}[91]. On this basis, biomimetic structural design has also been introduced into the development of ion separation membranes. Inspired by the charge-embedded structure of sandstorms, Wang et al. constructed an anti-Janus biomimetic nanofiltration membrane, where quaternary ammonium groups provide a stable positively charged environment, significantly improving Li^{+} selectivity, permeability, and lithium recovery stability under complex electrolyte conditions (Fig. 4C) [92]. In addition, interfacial polymerization technology has provided an effective approach for the fabrication of high-performance positively charged nanofiltration membranes. Zhao et al. (Fig. 4D) [93] developed a polyamine nanofiltration membrane with an ultrathin selective layer of approximately 95 nm, an effective pore size of 6.5 Å, and a high positive zeta potential. The membrane enables efficient divalent salt ion separation, significantly reducing the Mg^{2+}/Li^{+} ratio in a three-stage nanofiltration process, while also

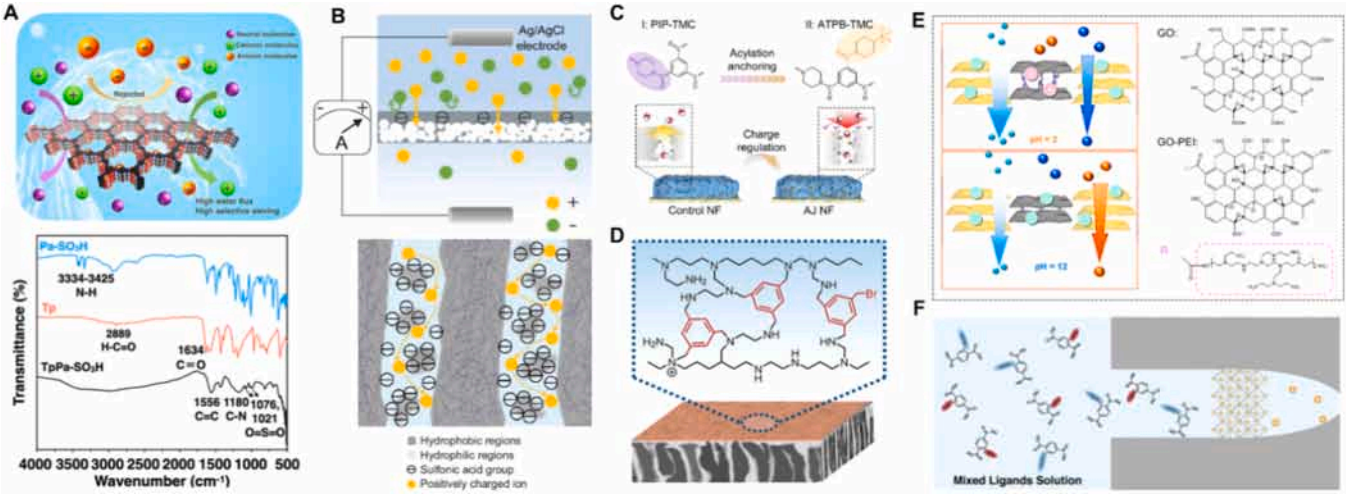


Fig. 4. Schematic illustration of ion transport regulation mediated by functional groups with different charge characteristics, including negatively charged functional groups: (A) Sulfonic acid COF membrane [88]. Copyright 2024, American Chemical Society. (B) SPEEK nanochannel membrane [89]. Copyright 2020, Oxford University Press on behalf of China Science Publishing & Media Ltd. Positively charged functional groups: (C) Quaternary ammonium-based reverse Janus nanofiltration membrane [92]. Copyright 2025, Nature. (D) Polyamine nanofiltration membrane [93]. Copyright 2023, American Chemical Society; pH-responsive functional groups: (E) GO–PEI functionalized pH-responsive nanofiltration membrane [94]. Copyright 2021, American Chemical Society. (F) Amphoteric MOF sub-nanometer channel membrane [95]. Copyright 2023, Royal Society of Chemistry.

exhibiting excellent water flux and long-term operational stability.

In addition, pH-responsive functional groups provide important dynamic regulation capability for nanoscale confined systems. By modulating the acidity or alkalinity of the solution environment, reversible surface charge conversion can be achieved, thereby dynamically tuning the transport characteristics of channels. For example, under low pH conditions, carboxyl groups undergo protonation, reducing surface negative charge and thereby suppressing cation transport. Conversely, under high pH conditions, deprotonation enhances electrostatic repulsion, significantly increasing cation flux. This reversible regulation mechanism enables nanofluidic systems to adapt to complex and variable external environments, holding significant application value in intelligent sensing and controllable separation. Based on the above regulatory mechanisms, such strategies have been widely applied in the design of smart nanofiltration membranes. Inspired by the glomerular filtration mechanism, Zhang et al. (Fig. 4E) [94] constructed a pH-responsive smart graphene oxide (GO) nanofiltration membrane based on GO-PEI (polyethyleneimine) modification. By synergistically regulating nanochannel size, surface hydrophilicity, and electrostatic interactions, the membrane achieves high water flux and efficient selective removal of organic molecules, demonstrating excellent tunable gating separation performance. Similarly, Hou et al. (Fig. 4F) [95] developed an amphoteric MOF sub-nanochannel membrane containing amino and carboxyl groups, which enables reversible switching of ion selectivity through pH regulation. Under acidic conditions, the membrane exhibits excellent anion sieving capability, whereas under alkaline conditions, cation sieving performance is significantly enhanced, further validating the application value of pH-responsive strategies in intelligent ion separation.

Recent studies have shown that functionalized COF membranes exhibit excellent performance in monovalent ion sieving. Sub-nanochannels constructed from molecular recognition units can achieve preferential ion transport through host–guest interactions. Crown ether structural motifs can selectively encapsulate cations with specific sizes and hydration states, enabling efficient ion recognition in complex electrolyte systems [96–98]. This structure-matching and chemical affinity-based sieving mechanism has become an important research direction for surpassing the limitations of traditional electrostatic sieving.

4.2. *Chemical regulation mechanisms beyond electrostatics*

In addition to traditional electrostatic repulsion and attraction, ion transport in nanoscale confined systems can also be regulated through higher-level chemical recognition mechanisms. This mechanism is essentially similar to the selective filtering process in biological ion channels, where specific molecular sites form weak and reversible interactions with target ions, thereby enabling high-precision sieving.

Coordination interaction is an important means of achieving chemically selective regulation. MOF materials often contain metal center sites that can form coordination bonds or coordination complexes with specific ions, thereby altering ion hydration structures and migration energy barriers. For example, MOF channels containing transition metal nodes may exhibit stronger binding affinity toward soft alkali metal ions, thereby enhancing the preferential transport of target ions [99]. Chi et al. (Fig. 5A) [100] investigated Zr metal nodes and coordination defects in a 2D UiO−66-NH_2 membrane, which impart positive charge to the framework. By strengthening electrostatic interactions between ions and metal nodes within the membrane, ion migration behavior was regulated to preferentially promote K^+ transport while suppressing Mg^{2+} diffusion, synergistically combining with pore-size sieving effects to achieve high ion selectivity. Mo et al. (Fig. 5B) [101] regulated the functional groups and pore size of MOF sub-nanochannels, utilizing coordination and binding interactions within the channels to modulate ion transport energy barriers and selectivity, thereby achieving efficient separation of monovalent and divalent cations. Notably, the K^+/Mg^{2+} selectivity of the UiO−66-$(OCH_3)_2$ membrane reached 1567.8. Hydrogen-bond networks also play an important role in ion regulation. Hydrogen-bond donor or acceptor sites constructed within channels can form transient interactions with hydrated ions, thereby modulating the energy barrier of the ion dehydration process. Since transmembrane ion transport usually involves partial dehydration, reducing the dehydration energy barrier is an important strategy for improving ion permeation efficiency. Wang et al. [102] clarified the regulatory mechanism of hydrogen bonding and water structure evolution on nanochannel ion selectivity by tuning the hydrophobicity and rigidity of polymer side

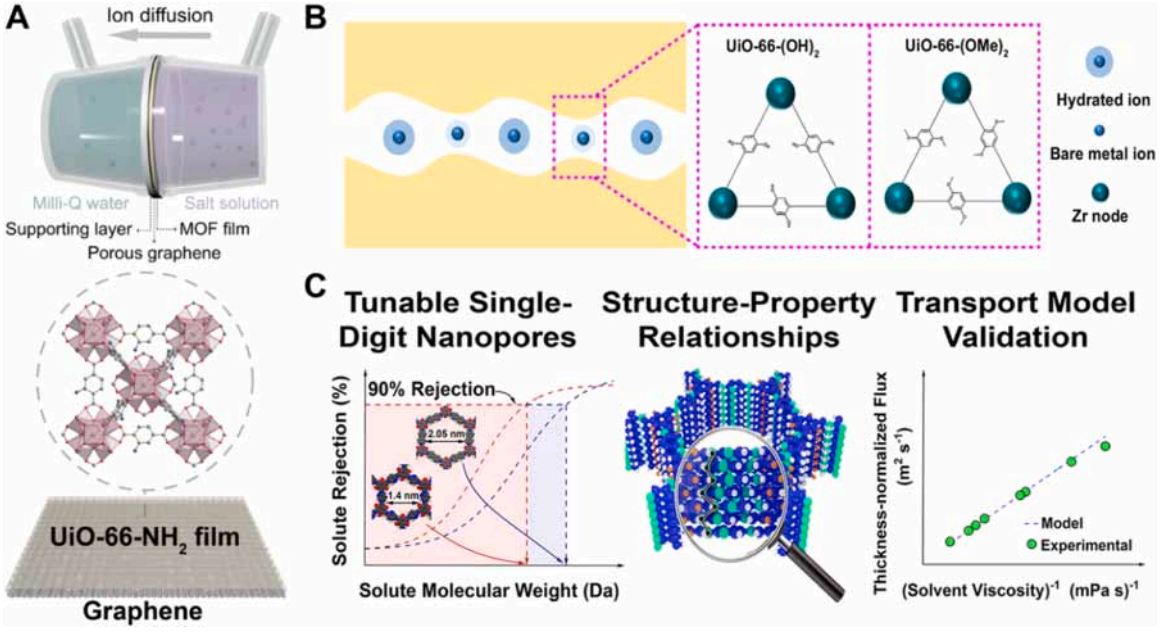


Fig. 5. Chemical regulation mechanisms beyond electrostatics. (A) Zr node coordination defects in UiO−66-NH_2 membranes [100]. Copyright 2025, American Chemical Society. (B) Coordination–binding interactions in MOF sub-nanometer channels [101]. Copyright 2024, Nature. (C) Aromatic π-system coupled COF ion channel membranes [103]. Copyright 2022, American Chemical Society.

chains. By restricting the hydration shell and constructing a confined water environment, the membrane significantly enhanced monovalent cation transport selectivity while suppressing divalent ion migration. π-electron systems can also participate in ion regulation processes. Some COF structures contain aromatic conjugated backbones that can influence the solvation environment surrounding ions through induced dipole interactions, thereby indirectly regulating ion migration behavior. Lin et al. constructed large-area, ultrathin TpPa-series 2D COF separation membranes via interfacial polymerization, achieving angstrom-scale pore size regulation and revealing the significant influence of the coupling between aromatic π systems and ion channels on solvent and ion transport flux as well as sieving selectivity (Fig. 5C) [103].

Notably, chemical regulation mechanisms beyond electrostatics can often overcome the limitation of the traditional Debye screening effect, enabling nanoscale confined systems to maintain good selectivity even under high-salinity conditions. This is of great significance for seawater energy harvesting, complex electrolyte separation, and biomedical ion regulation. Lin et al. [104] proposed an ion regulation strategy by confining highly spatially charged polyelectrolyte hydrogels within ordered nanochannels. The sieving mechanism differs from conventional approaches relying on Debye screening and instead mainly depends on the synergistic regulation of nanochannel structural confinement and interfacial chemical interactions. This strategy suppresses hydrogel swelling and reduces concentration polarization while achieving highly selective ion transport, leading to relatively high power density and energy conversion efficiency under salinity gradient conditions.

Overall, the combination of functional group engineering and chemical recognition strategies provides a multiscale synergistic optimization pathway for ion regulation in nanoscale confined systems, enabling ion transport to be governed not only by macroscopic structural design but also by the fine control of the microscopic chemical environment.

5. Ion transport system based on nanoblock architecture

With the continuous advancement of controllable synthesis techniques for nanomaterials, constructing ion transport systems based on the nanobuilding block concept has emerged as an important strategy for achieving precise structural regulation and functional integration. Various materials, such as 2D layered materials, MOFs, and COFs, provide highly designable platforms for constructing sub-nanoscale confined transport channels [105–107]. These materials not only enable geometrical confinement of ion migration pathways with high precision but also offer abundant chemically tunable sites, allowing ion transport behavior to be synergistically optimized across structural, interfacial, and molecular recognition dimensions. By treating these structural units as programmable functional modules, hierarchical architectures can be constructed ranging from single-component homogeneous channels to multicomponent heterogeneous systems. The synergistic assembly of different nanobuilding blocks not only integrates their respective advantages but also generates new transport mechanisms and coupling effects at interfaces, thereby overcoming the trade-offs among selectivity, flux, and stability that are inherent in single-material systems. Therefore, nanobuilding block–based ion transport systems provide a systematic design framework for constructing efficient, tunable, and integrable nanofluidic platforms. In this section, the design strategies and functional realization pathways of nanobuilding block–based ion transport will be systematically discussed from four aspects: hierarchical confinement structures of 2D materials, programmable pore networks of MOFs, ordered and stable frameworks of COFs, and the synergistic construction of homogeneous and heterogeneous systems.

5.1. Hierarchical structures of two-dimensional materials

2D materials (such as graphene, transition metal dichalcogenides (TMDs), and black phosphorus) have become important platforms for constructing nanoconfined ion transport channels due to their atomic-scale thickness, high in-plane crystallinity, and excellent electronic/ionic conductivity [108–110]. Their unique structural characteristics confer significant advantages in ion transport regulation, particularly in the tunability of interlayer spacing and the ordered confined spaces formed by the stacking of monolayers or few-layer assemblies. Compared with conventional porous materials, 2D materials primarily rely on interlayer nano-gaps or artificially engineered sub-nanoscale pores to establish ion migration pathways. Such layered confinement structures enable the formation of vertically aligned, size-precise, and highly ordered ion transport channels, thereby demonstrating superior performance in ion selectivity, transport rate, and channel regulation precision. Building on these structural advantages, researchers have further explored specific strategies for constructing 2D confined transport channels. Liu et al. (Fig. 6A) [111] assembled polymeric carbon nitride nanosheets with intrinsic nanopores and combined them with a MXene defect-healing strategy to fabricate a 2D layered separation membrane. Relying on the ordered intralayer nanopore structure and tightly stacked arrangement, this system achieved efficient molecular sieving performance and revealed the critical role of precisely regulating interlayer spacing and pore size in governing transport behavior. While maintaining high selectivity, the membrane also exhibited a hydrogen permeance as high as 8046 GPU, highlighting the role of structural regulation in promoting the synergistic optimization of flux and selectivity. Similarly, Hong et al. (Fig. 6B) [112] employed a vacuum filtration method to assemble $Ti_3C_2T_x$ MXene nanosheets, constructing a high-density sub-nanoscale interlayer channel network. Through the synergistic regulation of channel size confinement and surface chemical environment, the system achieved highly selective cation transport under different ionic concentration conditions and attained a power density of approximately 21 W m^{-2} during salinity gradient energy harvesting, demonstrating the application potential of 2D confined channels in blue energy conversion. Furthermore, ion channel regulation in 2D materials depends not only on intrinsic structural design but also on precise modulation through various external stimuli. For example, applying an electric field can alter the interfacial potential distribution and regulate the ion migration energy barrier; mechanical pressure can affect interlayer spacing and channel geometry; and surface chemical modification can optimize interfacial charge states and the localized chemical microenvironment [113]. Through these multiscale regulation strategies, 2D material systems can dynamically balance the relationship between ion selectivity and transport flux under different operating conditions, thereby maintaining stable and efficient ion transport performance.

In 2D material ion transport systems, interlayer spacing is one of the key structural parameters for achieving confinement regulation. The interlayer spacing of 2D materials can be precisely tuned through various approaches, including chemical modification, molecular intercalation, environmental control of solution conditions, temperature variation, and mechanical compression, thereby endowing nanoconfined channels with programmable geometric design capability. Taking GO as a representative example, its layered structure can be optimized by regulating the degree of oxidation–reduction and the distribution state of water molecules within the interlayers, allowing the channel dimensions to gradually approach the hydration structural characteristics of target ions. When the confined space scale approaches the hydrated diameter of ions, ions typically undergo partial dehydration or hydration shell reconstruction during transport across the nanochannel [114]. Such structural and dynamic transformations further enhance ion sieving selectivity while also significantly influencing migration energy barriers and overall transport kinetics. Based on the above confinement-size regulation concept, Joshi et al. (Fig. 6C)

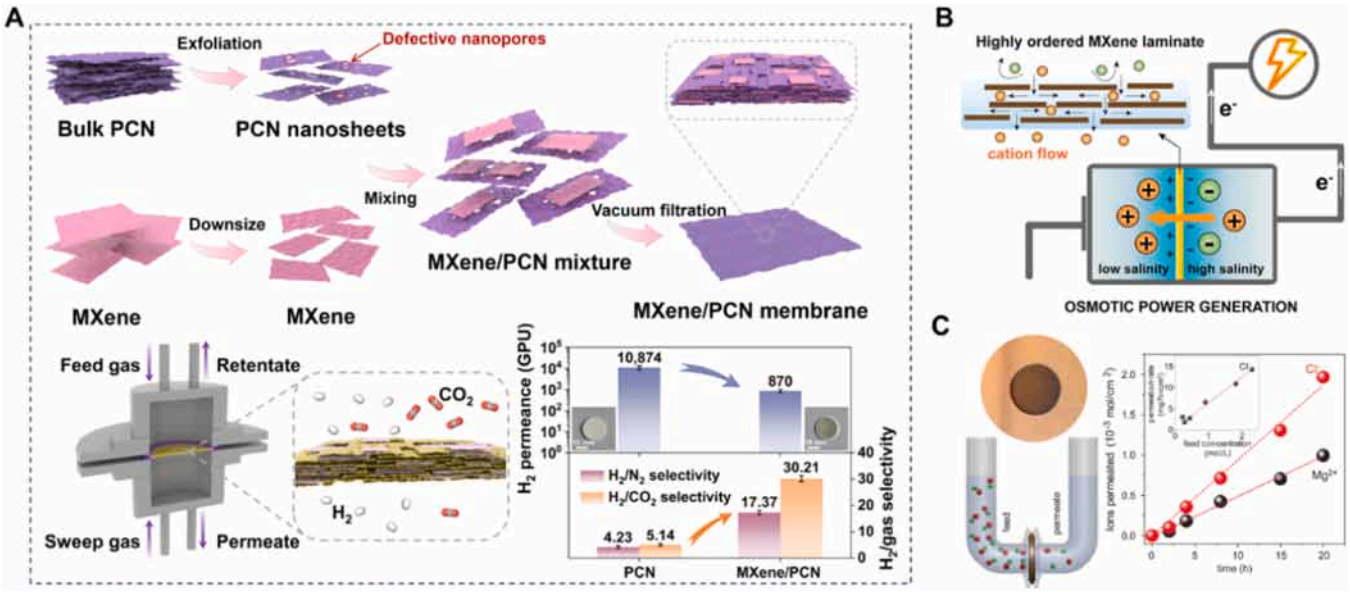


Fig. 6. Ion transport systems based on hierarchical 2D material nano-building blocks. (A) Nanoporous polymeric carbon nitride nanosheets coupled with MXene defect-repair ion transport systems [111]. Copyright 2026, Science. (B) Vacuum-filtrated $Ti_3C_2T_x$ MXene membranes with high-density sub-nanometer interlayer ion transport channels [112]. Copyright 2019, American Chemical Society. (C) Vacuum-filtrated graphene oxide-based micron-scale layered ion transport systems [115]. Copyright 2014, Science.

[115] precisely controlled the interlayer spacing of graphene oxide to construct hydration-confined nanochannels of approximately 9–10 Å, bringing the channel dimensions close to the hydration structural size of specific ions and thereby achieving efficient sieving of ions with hydrated diameters smaller than 4.5 Å. This work not only verified the critical role of size matching in regulating ion selectivity but also revealed the partial dehydration mechanism induced by interlayer nanochannels as well as the ultrafast ion transport characteristics driven by capillary pressure, highlighting the profound influence of geometric confinement in nanoscale spaces on transport kinetics.

In addition to geometric size regulation, the transport performance of 2D material systems is also significantly influenced by the interfacial chemical environment. The surfaces of 2D materials are typically rich in tunable functional sites such as hydroxyl, carboxyl, and phosphate groups. These functional groups can modify the interfacial charge distribution, the strength of localized electrostatic interactions, and the wettability of channel walls, thereby further regulate the degree of EDL overlap and exerting a systematic influence on ion migration pathways and transport rates. Based on this, Zhang et al. (Fig. 7A) [115] constructed an electrostatically tunable ion transport interface by

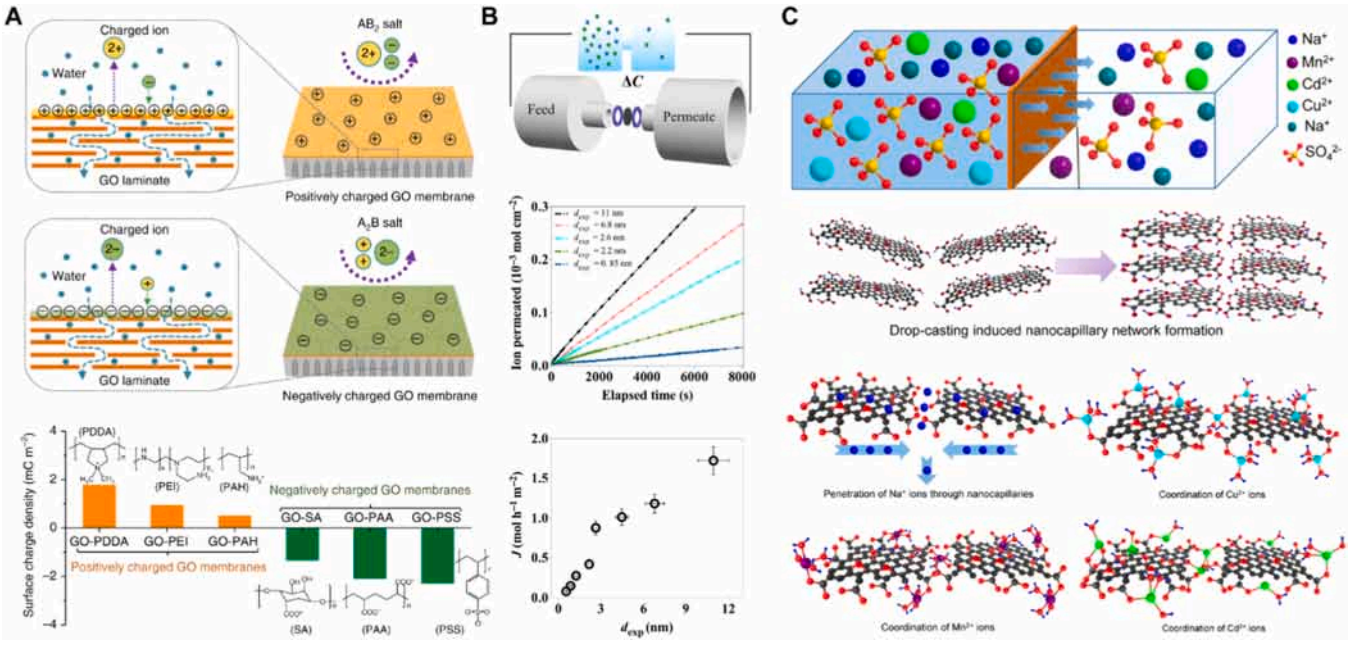


Fig. 7. Ion transport systems based on hierarchical 2D material nano-building blocks. (A) Charge-regulated GO membrane ion transport system achieved by polyelectrolyte modification on pre-stacked GO surfaces [116]. Copyright 2019, Nature. (B) Ion transport system of graphene hydrogel membranes regulated via chemical transformation [117]. Copyright 2016, Science. (C) Self-supporting GO membrane ion transport system fabricated by drop-casting GO colloidal suspension followed by drying and peeling at room temperature [119]. Copyright 2013, American Chemical Society.

regulating the surface charge density and distribution of charged functional groups in graphene oxide membranes. The results demonstrated that the EDL structure and electrostatic repulsion effect can effectively regulate the migration behavior of monovalent and divalent salt ions. While maintaining the high water flux characteristics of 2D capillary channels, the membrane achieved efficient rejection of multivalent ions, systematically revealing the coupled regulation mechanism of interfacial electrostatic interactions on ion flux and sieving performance. Furthermore, Cheng et al. (Fig. 7B) [117] used a layered graphene hydrogel membrane as a structural regulation platform and combined experiments with theoretical simulations to investigate transport behaviors within cascaded graphene nanochannels ranging from sub−10 nm to sub-nanometer scales. The study found a pronounced synergistic regulation relationship among the distribution of interlayer functional groups, interfacial charge states, and channel structural parameters. By modulating the local EDL overlap and the stability of hydration structures, anomalous nonlinear enhancement of ionic conductivity was induced, and the mechanisms by which multiscale structural factors influence ion migration and conductivity regulation were systematically elucidated. Furthermore, surface chemical modification of 2D materials provides more refined molecular recognition strategies for regulating ion selectivity. By introducing specific functional groups at channel interfaces, size exclusion effects, electrostatic interactions, and the cooperative interactions between solvated ions and interfaces can be comprehensively utilized to achieve differential screening of various ions. For example, Chen et al. [118] prepared amine-functionalized graphene oxide (am-GO) membranes and constructed heterogeneous nanochannel structures with tunable positive and negative interfacial potentials. Through functional group–induced interfacial charge reconstruction and hydration structure regulation, the system achieved highly selective anion sieving. Strong electrostatic interactions effectively blocked multivalent anions such as SO_4^{2-} and PO_4^{3-} while facilitating the rapid transport of Cl^-, demonstrating the application value of interfacial charge engineering in ion transport regulation. In addition, the chemical selective transport mechanism is not limited to electrostatic interactions but also involves more complex intermolecular interactions. Sun et al. (Fig. 7C) [119] further revealed the specific interactions between oxygen-containing functional groups in graphene oxide membranes and various ions and organic molecules, including coordination interactions and π–π stacking interactions. This multi-level chemical recognition mechanism enables rapid transport of Na^+ while effectively blocking ions or organic molecules such as Cu^{2+}, Mn^{2+}, Cd^{2+}, and rhodamine B, highlighting the important role of selective interactions between interfacial functional groups and target transport species in regulating transport behavior. Overall, this regulation strategy relies not only on geometric size matching of ions but is also influenced by multiple factors, including ionic charge density, solvation structure stability, and the localized chemical microenvironment, thereby providing an important theoretical foundation for the design of high-performance 2D confined ion transport systems.

In addition, 2D materials can be assembled into hierarchical structures through layer-by-layer stacking or ordered self-assembly methods, enabling the material to exhibit processable membrane morphologies at the macroscopic scale while maintaining continuous and stable nanoconfined transport networks at the microscopic level. Such hierarchical architectures help establish a dynamic balance between high ion flux and high selectivity, providing a robust structural foundation for functional applications such as osmotic energy harvesting, ion rectification transport, intelligent gating regulation, and environment-responsive ion transport. More importantly, hierarchical structures are not merely simple spatial stacks but are achieved by regulating the synergistic coupling effects among channels of different length scales, enabling ion migration pathways to exhibit continuous and low-energy-barrier characteristics, thereby significantly improving overall transport efficiency. Based on the above structural design concept, Zhang et al. (Fig. 8A) [120] combined vacuum filtration with micro-electro-mechanical systems (MEMS) microfabrication technology to construct graphene oxide membranes with vertically preferential growth characteristics. Relying on the hierarchical architecture, this system significantly shortened ion migration pathways and established a continuous network of confined nanochannels, allowing ions to maintain low energy dissipation during transmembrane transport. The results showed that structural optimization not only promoted the synergistic enhancement of flux and selectivity but also effectively reduced ion

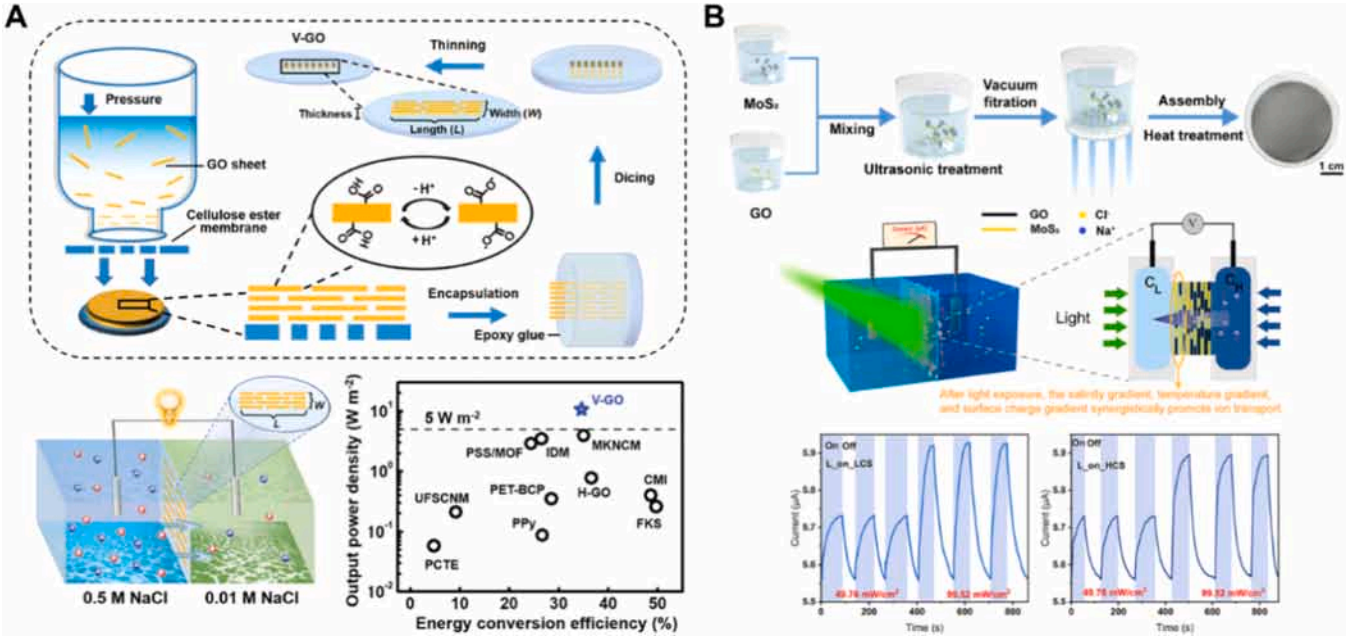


Fig. 8. Ion transport systems based on hierarchical 2D material nano-building blocks. (A) Graphene oxide membrane ion transport system with vertically preferential growth characteristics constructed by combining vacuum filtration and MEMS microfabrication [120]. Copyright 2020, Wiley-VCH GmbH. (B) MoS_2/GO composite membrane ion transport system prepared by vacuum filtration of a mixed dispersion of graphene oxide and MoS_2 on a polycarbonate substrate [121]. Copyright 2025, Elsevier B.V.

migration energy barriers. Under salinity gradient energy conversion conditions, the membrane achieved a power density output of up to 10.6 W m^{-2}, demonstrating the advantages of vertically confined structures in osmotic energy harvesting. On this basis, researchers further explored multicomponent composite strategies to enhance the functional complexity of confined transport systems. He et al. (Fig. 8B) [121] constructed a 2D molybdenum disulfide (MoS_2)/GO composite nanochannel membrane that synergistically regulated interlayer spacing distribution, interfacial charge states, and external field-responsive properties through a multilevel layered architecture. This system exhibited tunable transport responses to external environmental stimuli such as pH variation, light irradiation, and temperature perturbation, thereby expanding the application dimensions of intelligent ion regulation. The results demonstrated that hierarchical structures not only play an important role in osmotic energy harvesting but also enable ion rectification transport and gate-controlled transport modulation while exhibiting high cation selectivity. Benefiting from the synergistic optimization of structural and interfacial properties, the system ultimately achieved a power density output of approximately 17.68 W m^{-2}, further validating the potential of multiscale structural engineering in improving energy conversion efficiency. In addition, 2D material systems typically possess high mechanical strength and structural flexibility, enabling them to maintain relatively stable transport performance under complex flow conditions, pressure fluctuations, and external disturbances [122]. Such structural stability is particularly critical for practical applications, as ion transport membranes must not only exhibit high-performance transport characteristics but also ensure structural reliability during long-term operation. By strengthening interlayer interactions and optimizing composite interface structures, 2D confined systems can preserve the overall integrity of channel architectures under mechanical stress, thereby providing important support for the practical implementation of highly stable ion transport devices.

Taken together, these 2D material systems reveal three design principles centered on interlayer engineering and surface chemistry. First, interlayer spacing matched to hydrated ion diameter enables size-selective sieving, as demonstrated by GO membranes with approximately 9–10 Å channels. Second, surface charge density modulates EDL overlap and thus ion selectivity, with higher σ_s enhancing cation selectivity but simultaneously increasing electrostatic repulsion that may reduce flux. Third, hierarchical architectures, namely vertical versus horizontal channels, determine the flux-selectivity balance: vertically aligned channels shorten transport pathways and enhance flux, while horizontal stacking maximizes interlayer confinement for higher selectivity. However, narrower interlayers improve sieving precision but increase hydraulic resistance and vulnerability to swelling-induced structural instability. Furthermore, interlayer spacing controlled by hydration or intercalants fluctuates with environmental humidity, compromising long-term operational reliability.

5.2. *Metal–organic frameworks (MOFs)*

MOFs are a class of porous crystalline materials constructed through the ordered coordination assembly of metal ions or metal clusters with organic ligands. Owing to their highly ordered structures and excellent designability, MOFs have gradually become important functional platforms in nanoconfined ion transport systems. The core advantages of MOF structures lie in their programmable pore topologies, high specific surface areas, and tunable pore sizes, enabling the construction of ordered ion migration networks within nanoconfined spaces. By rationally selecting metal centers and organic ligand structures, the pore geometry, charge distribution characteristics, and localized chemical microenvironment can be systematically regulated, allowing the precise design of ion transport processes. The pore architecture of MOF systems not only exhibits static geometric designability but can also be further optimized through synthesis regulation or post-modification strategies, enabling promising applications in chemical separation, electrochemical energy storage, and energy conversion.

In ion transport systems, the pore sizes of MOFs typically range from the angstrom scale to the sub-nanometer scale, enabling effective sieving of hydrated ions through spatial confinement effects. When the pore size is comparable to the hydration structure size of target ions, ions may undergo partial dehydration or hydration configuration rearrangement during migration, which alters the migration energy barrier and significantly influences transport kinetics. Based on this mechanism, many studies have explored ion selectivity regulation strategies within sub-nanoscale confined spaces from different perspectives. For example, Zhang et al. (Fig. 9A) [24] reported the ion sieving mechanism of sub-nanometer channels in ZIF−8 MOF membranes, systematically revealing the partial dehydration process induced by pore confinement and the dominant role of effective ionic size differences in governing the transport behavior of alkali metal ions. Both experimental results and molecular dynamics simulations demonstrated that partial hydration shell removal is a key factor leading to migration differences among monovalent ions such as Li^+, Na^+, and K^+, as the structural changes in ion hydration directly affect the energy barrier for ions entering the pores. In terms of anion-selective transport, Li et al. (Fig. 9B) [123] inspired by biological fluoride ion channels, constructed UiO−66-X MOF sub-nanometer synthetic channels. By regulating pore size, functional group type, and surface charge state, they successfully achieved a window structure of less than 1 nm and obtained high conductivity and highly selective sieving performance for anions such as F^-. In particular, the positively charged UiO−66-$N^+(CH_3)_3$ channel, owing to its minimum pore size and highest local positive charge density, exhibited an F^-/Cl^- selectivity of approximately 240 and an F^- conductivity of about 10 S m^{-1}. The study further confirmed that when the pore size approaches the ion dehydration scale, functional group regulation can significantly enhance anion transport performance.

In addition to spatial confinement and electrostatic interactions, the abundant metal nodes within MOF frameworks can also provide potential coordination-active sites, enabling selective regulation mechanisms beyond traditional electrostatic repulsion. Peng et al. (Fig. 9C) [124] immobilized thylenediaminetetraacetic acid (EDTA) functional groups within the MOF−808 framework to construct a broad-spectrum heavy metal capture material. By utilizing the metal–ligand selective binding microenvironment formed by multidentate ligands, the material achieved highly efficient removal of up to 22 types of heavy metal ions, including hard acids, soft acids, and borderline acids (all with removal efficiencies exceeding 99%). The study further revealed the critical role of differences in metal–ion coordination affinity within the framework-anchored ligands in selective capture processes. Furthermore, Sun et al. (Fig. 9D) [125] constructed a Fe-BTC/polydopamine composite adsorption system. This work utilized open metal sites in the MOF framework to induce in situ polymerization of dopamine within the channels, forming a high-density metal-chelating network. Through coordination chemistry–mediated regulation of metal ion affinity, the system significantly enhanced the capture rate, adsorption capacity, and selectivity for target metal ions such as Pb^{2+} and Hg^{2+}, while also demonstrating the important role of open metal sites in metal ion separation. Overall, the differences in localized chemical environments formed by various metal nodes (such as Cu^{2+}, Zn^{2+}, and Al^{3+}) can significantly regulate ion migration pathways and sieving efficiency. In particular, during multivalent ion separation and specific metal ion recognition processes, the synergistic regulation of metal node chemistry and confined structural features is of great significance. In addition, the ion transport performance of MOFs is also influenced by the synergistic regulation between metal nodes and organic ligands. Through rational design of functionalized ligand structures, the interfacial potential distribution within the channels and the interactions between solvated ions and channel walls can be precisely tuned. Among these, nitrogen-based ligands (such as imidazole and pyridine moieties) can enhance local electron density and coordination interactions, thereby improving the material's recognition capability for specific ions or

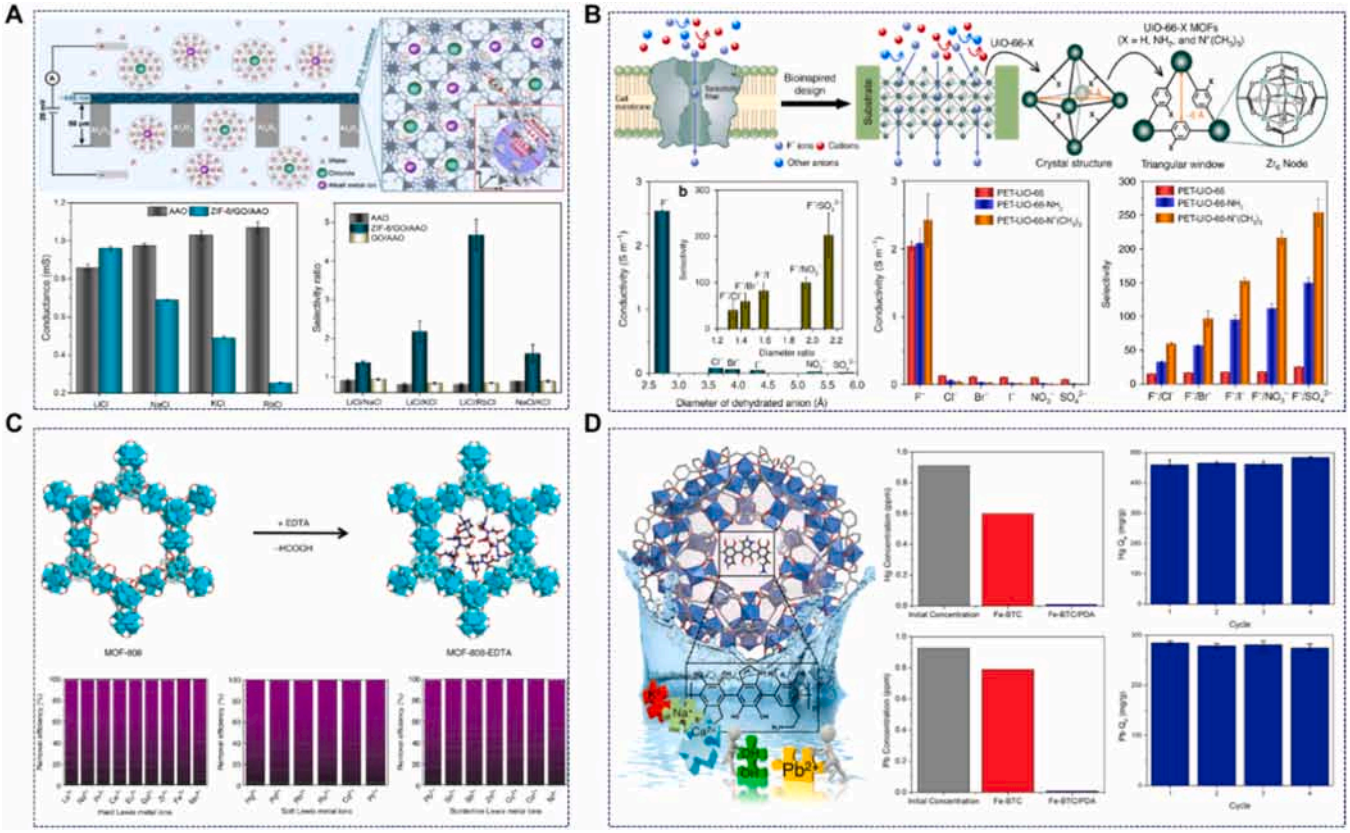


Fig. 9. Ion transport systems based on MOF nano-building blocks. (A) ZIF−8/GO/AAO composite membrane ion transport system constructed via the "nanoporous GO-assisted interfacial growth" strategy [24]. Copyright 2018, Science. (B) Ion transport system of Zr-based UiO−66-X crystals grown in situ within single-nanochannels of PET membranes [123]. Copyright 2019, Nature. (C) Ion transport system of EDTA-grafted MOF−808 heavy metal ion capture materials (MOF−808-EDTA) constructed via solvent-assisted ligand exchange [124]. Copyright 2018, Nature. (D) Fe-BTC/PDA composite ion transport system formed by anaerobic polymerization of dopamine induced by open Fe^{3+} metal sites in porous Fe-BTC, with polydopamine immobilized on the inner surface of MOF channels [125]. Copyright 2018, American Chemical Society.

molecular guests [126]. Meanwhile, the introduction of charged functional groups can reconstruct the charge distribution inside the channels, further modulating the migration energy barriers and transport kinetics encountered by ions when traversing confined spaces [127].

Regulation of the interfacial chemical environment is particularly important in hierarchical MOF systems. Tonnah et al. (Fig. 10A) [128] constructed a MOF-on-MOF bilayer heterostructure membrane based on functionalized UiO−66-NH_2 and MIL−88B layered architectures. Through amine functionalization and polystyrene sulfonate (PSS) intercalation strategies, the study achieved synergistic regulation of interfacial charge gradients and asymmetric channel structures, highlighting the critical role of ligand functional design in modulating interfacial ion potential and transport pathways. Benefiting from the coupled optimization of structural and chemical environments, the membrane achieved highly selective cation transport under salinity gradient conditions and generated an osmotic energy output power density of up to 32.47 W m^{-2}. The electronic structure and spatial configuration of ligands themselves can also profoundly influence the

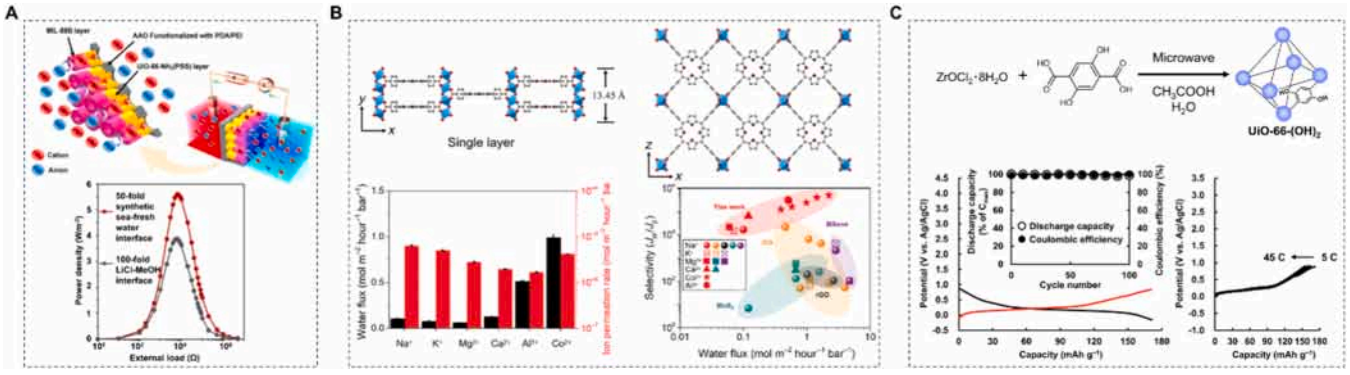


Fig. 10. Ion transport systems based on MOF nano-building blocks. (A) UiO−66-NH_2(PSS)/MIL−88B bilayer membrane ion transport system constructed via a layer-by-layer deposition strategy [128]. Copyright 2024, Elsevier B.V. (B) Laminated ion transport membrane assembled by exfoliation of bulk Al-MOF followed by vacuum filtration [133]. Copyright 2020, Science. (C) UiO−66-$(OH)_2$ ion transport system synthesized via microwave-assisted method [134]. Copyright 2025, Nature.

microenvironment of MOF channels. Marshall et al. [129] constructed a doubly interpenetrated Zr/Hf MOF modified with peb^{2-} ligands and systematically synthesized a series of functionalized Zr-MOFs containing substituents such as methyl, fluorine, naphthyl, and benzothiadiazole groups. The results showed that although ligand structural variations did not alter the overall topological framework, they induced subtle yet important structural rearrangements in ligand torsion angles, local crystal symmetry, and channel polarity environments, thereby modifying the binding affinity of the material toward guest molecules and providing an experimental basis for understanding ligand-mediated regulation of internal MOF potential and chemical recognition capability. Meanwhile, the regulation of channel interfacial hydrophilicity or hydrophobicity also significantly affects ion transport behavior in confined aqueous environments. Yang et al. [130] systematically revealed the synergistic regulation mechanism of hydrophilic/hydrophobic functional groups on channel water adsorption states, hydration ion structural stability, and ion–pore wall interaction strength through combined experimental and molecular dynamics simulation studies. The work primarily clarified the physical basis of water cluster network formation and partial dehydration processes within channels for achieving highly selective ion transport. Furthermore, free energy calculations provide an important theoretical tool for understanding gated transport mechanisms. Nordquist et al. [131] employed umbrella sampling and metadynamics methods to reveal the energetic nature of hydrophobic gating. The study found that the free energy barrier associated with transitions between hydrated and dehydrated states within the channel directly determines the open–closed equilibrium of ion channels, and demonstrated that variations in channel hydrophobicity can enable fine regulation of ion migration behavior by modulating hydration free energy.

Some MOF systems can also exhibit structural responsiveness, such as framework breathing effects or reversible pore-size variation phenomena, enabling materials to dynamically regulate ion flux under external environmental stimuli. This allows MOFs to function not only as static sieving materials but also as intelligent ion transport platforms with adaptive regulation capabilities. Wannapaiboon et al. [132] constructed alkyl ether–functionalized copper-based pillared-layer MOF flexible membranes through a surface anchoring strategy, revealing guest adsorption–induced structural phase transition behavior and the underlying mechanism governed by crystal size and interfacial interactions. This work demonstrated the fundamental role of controllable structural flexibility in intelligent sieving, flux regulation, and sensing applications. Overall, the advantages of MOFs in ion transport mainly arise from tunable pore structures, synergistic chemical regulation effects between metal nodes and ligands, and multiscale interfacial interaction mechanisms. Through chemical modification strategies, environmental condition regulation, and external physical stimuli (such as electric fields or temperature variation), the ion permeation performance of MOF systems can be further precisely optimized.

However, the stability of MOFs in aqueous environments remains one of the key factors limiting their practical applications. Water molecules may affect framework integrity and channel stability through hydrolysis or coordination competition effects. To address this issue, research efforts have commonly adopted strategies such as constructing ultrathin MOF layers or introducing multicomponent composite systems to enhance structural stability and long-term operational performance. For example, interfacial coupling between MOFs and 2D materials, polymer matrices, or other nanofunctional materials can improve both the mechanical stability and environmental tolerance of the material. Jian et al. (Fig. 10B) [133] reported an ultrathin water-stable 2D membrane constructed from single-layer aluminum–porphyrin MOF nanosheets. The membrane achieved high water flux and near-complete ion rejection by combining intrinsic nanopore size sieving with vertical through-channel transport, while the π–π interaction–induced self-locking structure enhanced long-term operational stability. Akai et al. (Fig. 10C) [134] reported a water-resistant UiO−66-$(OH)_2$ redox-active MOF that achieved excellent structural stability in acidic aqueous solutions by strengthening Zr–O coordination bonds and integrating conductive composite strategies, enabling high-capacity storage performance, long cycling lifetime, and high Coulombic efficiency, thereby providing an important paradigm for designing functional MOF materials for aqueous environments. Meanwhile, the structural designability of MOFs also allows their applications to extend beyond ion sieving membranes to multifunctional fields such as gas separation, environmental monitoring, as well as energy conversion and storage.

Drawing from the diverse MOF systems discussed above, three distinctive design principles emerge. First, pore aperture matched to hydration diameter induces partial dehydration, enabling high ion selectivity as seen in ZIF−8 and UiO−66 systems. Second, metal-node chemistry, specifically open metal sites and coordination defects, provides specific recognition beyond electrostatics, exemplified by the Zr nodes in UiO−66-NH_2 and the EDTA-functionalized MOF−808. Third, framework flexibility, namely breathing effects, enables dynamic pore tuning for stimuli-responsive gating. However, inherent trade-offs limit practical deployment, smaller apertures enhance selectivity but increase transport resistance and susceptibility to pore blockage; open metal sites enable specific binding but are prone to hydrolysis and coordination competition in aqueous media. Additionally, the aqueous instability of many MOF frameworks, particularly under extreme pH or high salinity, remains a fundamental barrier, and scalable fabrication of defect-free ultrathin MOF membranes remains technically demanding.

5.3. Covalent organic frameworks (COFs)

COFs are a class of crystalline porous materials formed by the ordered linkage of organic monomers through covalent bonds, possessing both high structural regularity and excellent chemical stability, and exhibiting unique advantages in nanoconfined ion transport. Unlike MOFs, COFs do not contain metal nodes in their structures and are composed entirely of light elements such as C, H, N, O, and B. This all-organic covalent skeleton endows the material with superior corrosion resistance, thermal stability, and environmental adaptability, allowing it to maintain structural integrity under relatively harsh conditions such as strong acid, strong base, high salinity, or elevated temperature. Meanwhile, the absence of metal centers that may trigger hydrolysis or coordination competition enables COFs to generally demonstrate more stable long-term operational performance in certain aqueous systems.

At the structural design level, the pore system of COFs is mainly constructed in a controllable manner based on the geometric configuration and linkage modes of organic monomers. By regulating monomer symmetry and condensation reaction pathways, precise control of pore size, porosity, and pore topology can be achieved. Meanwhile, solvent systems, reaction conditions, and post-treatment processes further influence the crystallinity and channel dimensions of the framework, enabling the formation of regular and continuous nanoconfined transport networks. Such highly predictable and programmable structural features make COFs an important platform for constructing ordered ion transport channels. In particular, 2D COFs are more suitable for constructing well-oriented sub-nanometer ion transport channels due to their relatively rigid planar frameworks and layered stacking characteristics. When membrane thickness is reduced to the nanoscale or even the single-layer limit, ion migration pathways are significantly shortened. While preserving the size exclusion effect, ion flux can be effectively enhanced, thereby achieving a better balance between selectivity and transport efficiency. Based on this structural advantage, Wang et al. (Fig. 11A) [135] designed a “confined cascade separation” architecture with alternating acidic and non-acidic microdomains within functionalized 2D COF ordered nanochannels. By constructing a multilevel chemical environment to regulate ion migration processes, this strategy achieved high-flux and high-selectivity synergistic separation of K^+/Li^+, overcoming the traditional trade-off between permeability and selectivity in membrane materials and demonstrating the application

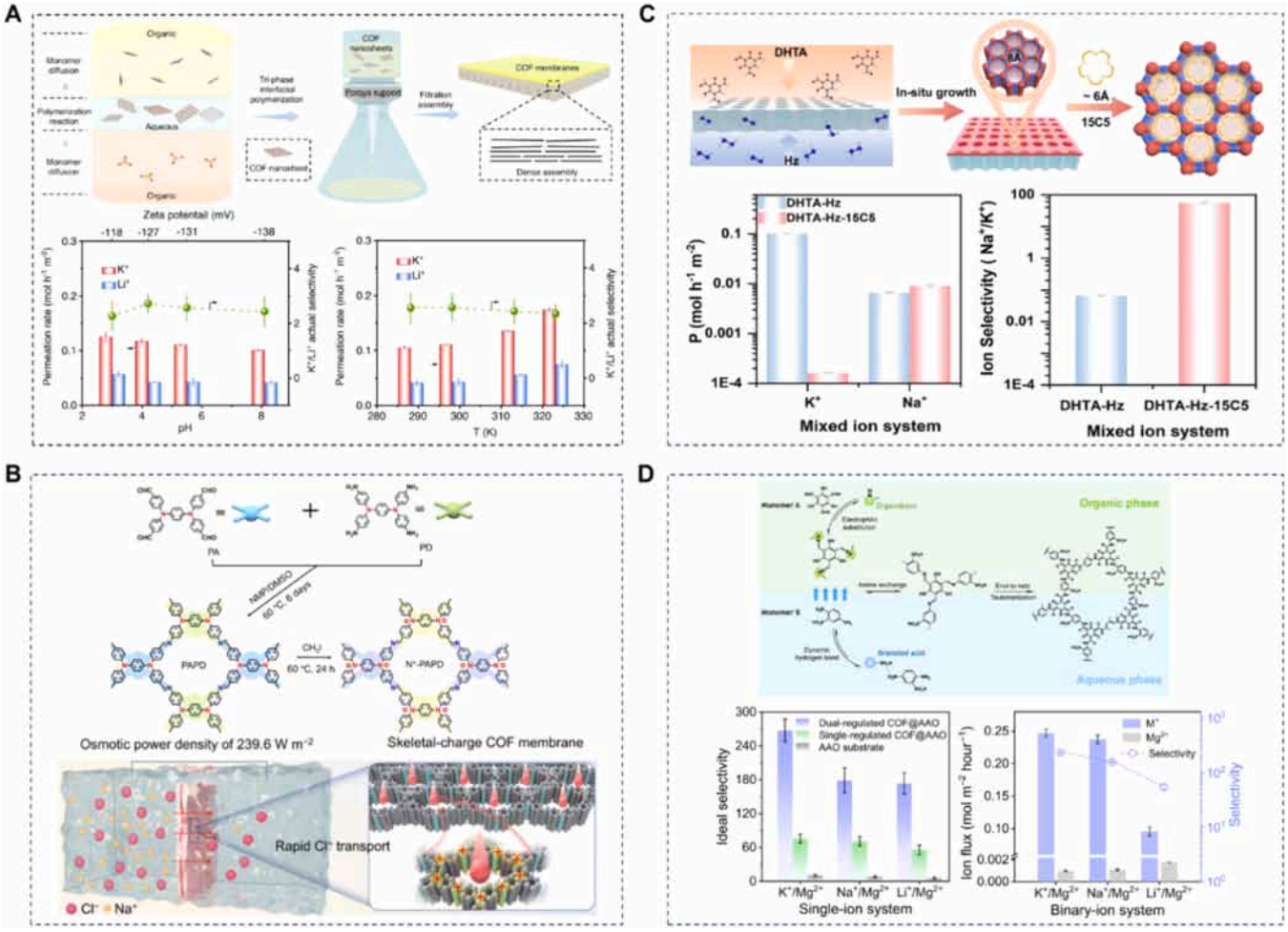


Fig. 11. Ion transport systems based on COF nano-building blocks. (A) COF nanosheets prepared via an oil–water–oil three-phase interfacial polymerization strategy and assembled into a PTFE-supported membrane by vacuum filtration [135]. Copyright 2022, Nature. (B) N^+-PAPD COF membrane ion transport system constructed via condensation reaction and in situ ionization [136]. Copyright 2025, American Chemical Society. (C) DHTA-Hz−15C5 ion transport system constructed via interfacial polymerization and pore post-modification [86]. Copyright 2025, Nature. (D) TpPa-SO_3H COF membrane fabricated on an AAO substrate via a dual-regulation interfacial polymerization strategy [140]. Copyright 2025, Science.

potential of 2D COF nanochannels in complex ion separation. Furthermore, framework charge engineering provides a more precise means of regulating ion transport. Zheng et al. (Fig. 11B) [136] introduced high-density atomic-scale positive charges into 2D COF ordered nanochannels and quantitatively tuned the charge distribution within the framework, achieving deep regulation of anion migration behavior. The high charge density not only strengthened electrostatic adsorption but also reconstructed the internal potential gradient of the channels, thereby promoting rapid directional transport of anions and exhibiting excellent energy output performance in osmotic energy conversion scenarios.

In addition to channel orientation regulation, the fine design of the interfacial chemical environment is also an important factor influencing the transport performance of COFs. COF frameworks possess high designability during synthesis or post-modification processes, allowing various functional units to be introduced into the channels, such as charged groups, hydrogen bond donors or acceptors, π-conjugated systems, and other active sites capable of selective interactions [137–139]. These functional sites can reconstruct the local electric field distribution inside the channels and regulate the interfacial charge environment as well as the stability of solvated ions, thereby influencing the migration energy barrier and hydration structure rearrangement processes when ions traverse confined spaces. Meanwhile, molecular intercalation or post-modification strategies can further tune the hydrophilic and hydrophobic characteristics of channel surfaces, enabling the material to maintain good selective sieving performance across different electrolyte systems. In terms of functional ion recognition design, Wang et al. (Fig. 11C) [86] constructed an artificial sodium-ion selective transport channel by introducing 15-crown−5 ether functional units into COF pores. By integrating size confinement effects and chemical affinity interactions, the structure achieved specific recognition and efficient directional transport of Na^+ and revealed that functional groups can enhance ion sieving performance by modulating local transport energy barriers, providing important inspiration for biomimetic ion channel design. Furthermore, interfacial charge engineering offers a more effective strategy for regulating multivalent ion sieving. Hu et al. (Fig. 11D) [140] constructed a COF membrane with pore sizes approaching the theoretical limit through a dual-regulation interfacial polymerization method and introduced –SO_3H sulfonic acid groups to synergistically modulate channel charge distribution and spatial structure. This strategy enabled rapid transport of K^+ while significantly suppressing the migration of multivalent ions such as Mg^{2+}, systematically revealing the functional group–mediated ion sieving mechanism in confined spaces. In addition, the introduction of high-density fixed charges has also been proven to significantly enhance electrostatic confinement effects. You et al. [141] constructed charged COF nanochannels by incorporating sulfonic acid groups into the framework to establish a strong local electric field environment. While

maintaining excellent water permeation performance, the structure effectively improved ion-selective sieving capability, highlighting the important role of charge regulation in nanoconfined transport systems.

In addition, COFs also exhibit favorable processability, enabling them to be constructed into continuous membrane structures through interfacial polymerization, solution transformation, and other controllable synthesis strategies, thereby forming large-area, integrable ion transport networks. Such structural programmability and potential scalability make COFs not only highly valuable in the field of ion-selective transport but also promising for applications in molecular sieving, electrochemical energy storage, and osmotic energy conversion. In terms of membrane fabrication and scalable applications, Pan et al. (Fig. 12A) [142] proposed an inverse microemulsion interfacial polymerization strategy. This method enables the rapid construction of high-crystallinity, large-area COF membranes, which improves water flux and desalination performance while effectively overcoming technical limitations associated with the large-scale fabrication of conventional COF membranes, providing an important implementation pathway for the application of COF materials in energy conversion and separation fields. Furthermore, interfacial charge regulation and three-dimensional transport network construction are considered key directions for enhancing ion sieving performance. Zhu et al. (Fig. 12B) [27] successfully prepared a three-dimensional sulfonic acid–functionalized COF membrane through a dual-acid–mediated interfacial polymerization strategy, constructing highly interconnected sub-nanometer ion transport channels. By introducing high-density fixed negative charges, this structure generated an enhanced EDL confinement effect, improving ion selectivity while maintaining relatively high ion migration efficiency, fully demonstrating the application potential of functional interface design in energy conversion systems. In addition, directional regulation of ion transport pathways can also significantly influence overall transport efficiency. Shin et al. (Fig. 12C) [143] constructed a negatively charged asymmetric COF membrane through a surface asymmetrical modification strategy. Based on a continuous vertical nanochannel architecture, the membrane achieved directional ion transport and enhanced selectivity. This structure effectively improved ion flux and increased power output in energy conversion processes such as osmotic and reverse osmotic energy harvesting. Overall, by systematically optimizing pore topology, surface functional group distribution, and interfacial chemical environment, COFs are expected to achieve more precise ion transport regulation in complex electrolyte systems and play an important role in the design of high-performance nanofluidic devices.

By contrast, COF systems leverage covalent bond stability and programmable organic linkages, offering three design principles. First, rigid backbones with precisely defined pore geometries enable angstrom-level size sieving, as demonstrated by TpPa-series membranes. Second, post-synthetic modification allows high-density charge introduction without compromising framework integrity, exemplified by sulfonic acid-functionalized COFs with enhanced EDL confinement. Third, π-conjugated backbones modulate local solvation environments, influencing ion migration energetics. However, high crystallinity ensures selectivity but fabrication defects (grain boundaries, misaligned channels) reduce effective flux; post-synthetic functionalization enhances tunability yet requires preserving crystallinity, limiting modification extent. Moreover, π–π stacking between layers may cause irreversible aggregation during processing, and controlled crystallization for large-area membranes remains challenging, hindering scalable manufacturing.

In conclusion, in nanoconfined ion transport systems, geometric dimension serves as the primary prerequisite for achieving nanoconfinement effects. Only when the channel size is reduced to the nanoscale can the unique confinement effect be activated, making ion transport behaviors distinct from macroscopic mass transfer and laying a structural foundation for the controllable regulation of ions. On the premise of satisfied geometric dimensions conditions, chemical functionality, and charge distribution act as core approaches to modulate ion dynamics. They effectively regulate ion adsorption, migration and diffusion, enabling fine optimization of ion selectivity and transport efficiency. As a higher-level design dimension, topological connectivity further optimizes the transport pathways and overall architecture of devices. It overcomes the performance limitations of individual regulation strategies and improves the comprehensive performance and operational stability of devices. In summary, the four dimensions including geometric dimensions, chemical functionality, charge distribution and topological connectivity form a progressive and synergistic design system. Covering basic confinement conditions, ion modulation strategies and device performance optimization, they jointly realize the optimal design of nanoconfined iontronic systems.

Overall, distinct nano-brick platforms exhibit significant differences in programmable dimensions, performance characteristics, and applicable scenarios, with their key properties, ion transport behaviors, and typical applications summarized in Table 1. Table 2 provides a quantitative comparison of key ion transport properties among representative nanofluidic materials, including ion selectivity, conductivity, rectification ratio, and gating performance.

6. Applications

Nano-confined ion transport systems are gradually advancing from fundamental transport mechanism studies toward engineering and system-level applications. Unlike conventional electron-conducting

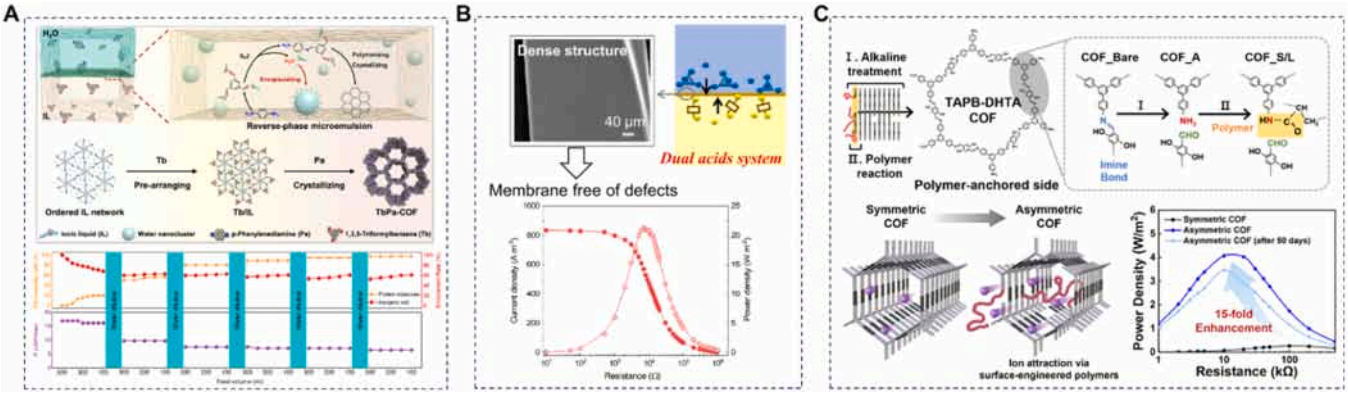


Fig. 12. Ion transport systems based on COF nano-building blocks. (A) Large-area, highly crystalline TpPa-COF composite membrane ion transport system rapidly fabricated within seconds via an inverse microemulsion interfacial polymerization strategy [142]. Copyright 2025, Nature. (B) Self-supporting membrane ion transport system based on 3D sulfonic acid-functionalized 3D SCOF constructed via dual acid-mediated interfacial polymerization [27]. Copyright 2023, Nature. (C) Asymmetric polymer-anchored COF membrane ion transport system constructed via a three-step strategy [143]. Copyright 2025, American Chemical Society.

Table 1
Summary of programmable dimensions, key advantages, limitations, ion transport performance, and typical applications of representative nano-brick platforms.

Materials	Programmable dimensions	Key Advantages	Main Limitations	Ion Transport Performance	Application	Ref.
2D materials						
MXene/PCN	PCN pores + MXene repair, C/N + -OH, Strong chemical group-CO_2 interaction, Layered stacking	Simple and scalable, Long-term stability (over 130 h)	Selectivity and permeability trade-off, Poor homogeneity in large-area membranes, Competitive adsorption reduces actual selectivity	H_2 Permeance of 870 GPU, $H_2/CO_2 \approx 30.2$	H_2 Separation and Purification	[111]
MXene	0.64 nm interlayer channels, pH/temperature-tunable surface charge, Ordered stacking	Simple, scalable fabrication via vacuum filtration	Water/oxygen stability, Homogeneity in large-scale fabrication	$t_+ \approx 0.95$, 21 $W \cdot m^{-2}$–54 $W \cdot m^{-2}$	Salinity gradient energy	[112]
GO	~9 Å capillary network, Hydrophobic graphene regions and oxygen-containing functional group regions	Perfectly blocks solutes with hydration radii > 4.5 Å, Small ion permeability enhanced by several thousand times	Functionality dependent on hydration, Poor pore size tunability	Ultrafast diffusion in capillary, confinement, Precise 4.5 Å size sieving	Nanofiltration, Water treatment	[115]
GO/PDDA/PSS	Surface charge (positive/negative)	Breaking the selectivity-permeability trade-off	Poor selectivity for monovalent salts, Performance declines at high salt concentrations	High rejection rate (~96%), High water flux (~57 LMH/bar)	Water softening Selective desalination	[116]
am-GO	Amino/carboxyl charge distribution, Nanochannel size (~7.5 Å)	Tunable Cl^-/N_3 transport, Cl-gated chemtronic effect	High energy barrier for high-valence anion permeation	Cl^- fast, NO_3^- tunable, SO_4^{2-}/PO_4^{3-} blocked	Anion exchange membrane (electrolysis, batteries, water treatment)	[118]
MoS_2/GO	pH-modulated surface charge, GO doping controlled interlayer spacing, Light-programmable	Good stability	Poor scalability, Weak performance in real seawater	17.68 W/m^2	Salinity gradient energy, Light-salt co-generation	[121]
MOFs						
ZIF−8/UiO−66	Ångström-scale windows (ZIF−8 ~3.4 Å, UiO−66 ~6.0 Å) - Nanoscale cavities, Neutral pores	High selectivity for alkali metals	Stringent requirements for structure/chemical properties	LiCl/RbCl≈ 4.6	Efficient extraction and purification of lithium Ions	[24]
UiO−66-X (X = H, NH_2, $N^+(CH_3)_3$)	~6 Å windows, ~1 nm cavities, Functional groups (-H, -NH_2, -$N^+(CH_3)_3$) regulate charge/size	–	High selectivity dependent on high F^- concentration	F^-/Cl^- ≈ 13–240 UiO−66-$N^+(CH_3)_3$ exhibits optimal performance	Water defluoridation F^--selective Separation Membrane	[123]
MOF−808-EDTA	EDTA ligand, ~11.3 Å Pore Size	Broad-spectrum and high-efficiency, Multi-component processing capability, Stable and recyclable	Performance/stability degradation under extreme conditions	High adsorption capacities for La^{3+}, Hg^{2+}, Pb^{2+} (205, 592, 313 mg/g)	Broad-spectrum adsorption, Resource recovery	[124]
Fe-BTC/PDA MOF	PDA amino/catechol groups, MOF small pore-large cage (pore sizes 5.5/8.6 Å)	High capacity, Anti-interference/stable and recyclable	Complex mercury treatment	Removes > 99.8% Pb^{2+}/Hg^{2+}, Adsorption capacity: Pb^{2+} 394 mg/g; Hg^{2+} 1634 mg/g	Rapid treatment of drinking water lead/mercury contamination	[125]
UiO−66-NH_2(PSS)/MIL−88B	~6 Å pores, PSS-induced negative surface charge	–	–	32.47 W/m^2	Salinity gradient energy	[128]
Al-MOF	6.1 Å channels, AB stacking	Stability (>750 h)	Water flux affected by ion species	Ion rejection rate: > 99.99%, Water flux: 2.22 mol m^{-2} h^{-1} bar^{-1}	Desalination, Wastewater reuse	[133]
UiO−66-$(OH)_2$	Tunable particle size (~70 nm), Strong bonds (Zr-O)	Long cycle life (>98%@100 cycles), Recyclable	Poor intrinsic conductivity Particle-size sensitive	Discharge capacity: 171.2 mAh g^{-1} Coulombic efficiency: 99.9%	Aqueous MOF-air battery anode	[134]
COFs						
TpPa-PO_3H_2/TpPa-SO_3H/TpPa-CO_2H	1.4 nm ordered channel, Acidic group chemistry	Programmable hydration energy	Binary ion competition reduces selectivity, Performance depends on acidic groups with high hydration energy	$K^+/Li^+ \approx 4.2$–4.7	Lithium extraction from salt lake	[135]
N^+-PAPD	Pore size: ~1.2 nm, High-density framework positive charge	Crystalline straight channels, Wide pH applicability, Stable operation	High synthesis control demand, Performance depends on anion type	High Cl^- selectivity (t_+ ~0.2–0.3) Power density: 239.6 W m^{-2} (50000 folds gradient)	Anion-selective salinity gradient power generation	[136]
DHTA-Hz−15C5	Pore size: ~8.4 Å → 6.0 Å, Na^+ recognition by hydroxyl/crown ether sites	High selectivity/high flux	Binary ion competition affects performance	$Na^+/K^+ \approx 58.31$, Na^+ permeability: 9.33 mmol·m^{-2}·h^{-1}	Artificial Na^+ channels	[86]
TpPa-SO_3H	Pore size: 8.4 Å - 6.3 Å, Sulfonate groups (high negative charge)	High selectivity/high flux	Ion coupling in binary system reduces actual selectivity	High K^+/Mg^{2+} selectivity (ideal ~267, actual 234)	Water purification recovery	[140]

(*continued on next page*)

Table 1 (*continued*)

Materials	Programmable dimensions	Key Advantages	Main Limitations	Ion Transport Performance	Application	Ref.
iCOFM	Large-pore geometry (~1.4 nm), High surface charge density (~200 mC m^{-2})	Electrostatic sieving, Stable & durable (200 h)	Driving pressure sensitive	Na_2SO_4: ~93.5% H_2O: 357.0 L m^{-2} h^{-1} bar^{-1}	Nanofiltration for water purification	[141]
C_8-IL-TbPa-COF	Membrane continuity/ thickness regulation	Ultrafast fabrication, Large-area, high crystallinity	–	High water flux (111.3 LMH/ bar), High Evans blue dye rejection (99.4%)	Dye separation, protein desalting, water treatment	[142]

Table 2
Comprehensive comparison of material properties including ion selectivity, ionic conductivity, ion rectification, and ion gating mechanisms.

Materials	Ion selectivity	Ionic conductivity	Ion rectification	Ion gating	Ref.
Cu-TCPP@SNF	t_+= 0.995, Cation (10- fold NaCl), V_{oc}= 136 mV (0.5 M/0.001 M)	1 M KCl, Surface-charge-dominated, P_{max}= 29.5 W/m^2 (5 M/0.01 M NaCl)	–	–	[150]
ZnTPP-COF	t_+= 0.35, Anion (0.5 M/0.01 M NaCl), σ_s= + 4.1 mC m^{-2}	I_{os}= 20 kA m^{-2}, P_{max}= 135.8 W m^{-2} (0.5 M/0.01 M NaCl)	–	–	[151]
UiO−66-NH_2 / TFP-TPA	–	< 10 mM NaCl Surface-charge-dominated, J_{sc}= 4483 A/m^2 (100-fold HCl)	R = $\|I_{+1V}\|$ / $\|I_{-1V}\|$ ≈ 350 (NaCl)	–	[28]
UiO−66-NH_2@ANM	Anion, Br^-/NO_3^- = 1240 Cl^-/NO_3^- = 509, t_+= 0.968 (1000 mM/10 mM KBr)	< 1 M KCl Surface-charge-dominated, P_{max}= 26.8 W/m^2 (100-fold KBr)	R = $\|I_{+1V}\|$ / $\|I_{-1V}\|$ ≈ 2.06 (0.001 M KCl)	–	[152]
Zn-TCPP MOF/ AAO	Cation, t_+= 0.92 (1 mM/1 mM KCl)	< 0.1 M KCl, Surface-charge-dominated, P_{max}= 6.26 W/m^2 (3000-fold KCl), $P_{max,light}$= 7.74 W/m^2	R = $\|I_{+2V}\|$ / $\|I_{-2V}\|$ ≈ 6.45 (10 mM KCl)	–	[143]
Ni_3(HITP)$_2$MOF	–	8 μF cm^{-2}	–	–	[157]
Mg-MOF−74	t_+ (Li^+) = 0.71	0.14 mS cm^{-1}	–	–	[158]
Co-HAB MOF	–	1.57 S cm^{-1}	–	–	[159]
SiO_2/Si_3N_4	Cation	< 100 μM, Surface-charge-dominated	R ≈ 83 (1 mM, V_G= −1 V, V_{CT}= 1 V)	I_{on}/ I_{off}= I(V_G= −1 V) / I(V_G= +1 V)= 10 (100 μM)	[166]
SiO_2/Al_2O_3	SiO_2 segment: K^+-selective, Al_2O_3 segment: Cl^--selective	< 1 mM KCl, Surface-charge-dominated	R = $\|I_{+1V}\|$ / $\|I_{-1V}\|$ ≈ 321 (1 mM KCl)	–	[167]
PAZT / PHEC	–	1.6 ± 0.2 mS/cm	R = $\|I_{+1V}\|$ / $\|I_{-1V}\|$ ≈ 23.11	–	[33]
PAIDs	–	218.42 μF cm^{-2}	R= $\|I_{-5V}\|$/ I_{+5V} = 10^3 (1 mM HCl)	–	[168]
Pillararene-Cyclodextrin Hybrid	Cation	P_K^+/P_{Cl}^-≈ 104.9	20.6 ± 0.3 (1 M/ 0.5 M KCl)	–	[169]
GnC7 (n = 3,4)	G3C7 : P_K^+/P_{Na}^+= 34.38 G4C7 : P_K^+/P_{Na}^+= 41.31	G3C7 : 66.2 ± 1.2 pS, G4C7 : 37.4 ± 1.6 pS (1 M KCl)	–	pH-controlled	[170]
2D Cu-TCPP	Cation, t^+> 0.85	10^{-4} M KCl, Nano-confinement enhanced ion enrichment effect, P_{max}= 16.64 W m^{-2} (0.5 M/0.01 M NaCl)	–	–	[171]
PNIPAM-GO	–	–	–	J_{25}/ J_{50}≈ 7, (12.4 vs 1.8 L m^{-2} h^{-1} bar^{-1})	[173]
PNIPAm/PPy	–	RT: ~0.02 S m^{-1}, HT (>LCST): ~0.08 S m^{-1}	–	–	[174]
hBN	Cation, K^+/Na^+ = 10^3	G(w) continuously tunable from 0 (blocked) to 1 (fully conductive)	–	–	[175]
pAMPSA/ pPEGDMA /pDADMAC	–	–	I (+1 V) / I (−1 V) ≈ 86.5 (small) | 79.0 (large)	Small device (2.5 mHz): 20.5, Large device (0.25 mHz): 8	[176]
PEDOT:PSS	–	–	R= | I (+1 V) | / | I (−1 V) | ≈ 2.5 (25 nA vs. −10 nA)	–	[177]
NASICON	$P_{Li/Na}$: 2707.4 (single) | 1325.2 (mixed), $P_{Li/K}$: 5109.8 (single) | 13695.9 (mixed), $P_{Li/Mg}$: 36161.7 (single) | 25283.7 (mixed), $P_{Li/Ca}$: 60269.6 (single) | 14048.2 (mixed)	–	–	–	[35]
N-LTO-PA−1.5	$P_{Li/Na}$≈ 13.58, $P_{Li/Ca}$≈ 173.90, (20 mM mixed salt solution)	2.14 mS/cm (20 mM NaCl/LiCl)	–	–	[178]
r-TpPa-SO_3H COF	High K^+/Li^+ and Na^+/Li^+ selectivity	J_{diff}≈ 0.4 mol·h^{-1}·m^{-2} (0.1 M KCl)	–	–	[179]
TpPa COF	Mg^{2+}/Li^+= 9.0	–	–	–	[180]
TNC-MCM	t_+= 0.91 (0.5 M/0.01 M NaCl)	J_{sc}≈ 58 A m^{-2} (Δc = 10^5, KCl), P_{max}≈ 5.9 W m^{-2} (SW/BW) | 9.8 W m^{-2} (saline lake)	–	–	[181]
V-NbP/ANF	t_+= 0.70 (1000-fold NaCl)	G ≈ 0.5 mS (1 M NaCl) | ~0.4 μS (low c, σ-dominant), P_{max}≈ 10.7 W m^{-2} (SW/RW) | 21.5 W m^{-2} (Δc = 50-fold, KCl)	–	–	[182]

devices, ion-based systems operate in liquid environments and inherently couple with chemical potential gradients, concentration

differences, electrochemical reactions, and fluid dynamics. Therefore, confined ion channels function not only as separation units but also as energy conversion units, information processing units, and functional interfaces. In practical applications, ion transport behavior is often coupled with EDL overlap effects, solvent reorganization, interfacial polarization, and non-equilibrium thermodynamic processes. This complex multi-physics coupling endows nano-confined systems with unique cross-scale functional integration capabilities. Accordingly, nano-confined ion transport systems show promising prospects in energy conversion, intelligent information processing, and sustainable separation technologies.

To contextualize the progress of nano-brick systems within practical energy frameworks, it is instructive to benchmark their performance against commercial requirements. For osmotic energy harvesting, current state-of-the-art nano-brick membranes deliver power densities of 10–30 W m^{-2} in laboratory settings, whereas large-scale blue energy installations require sustained outputs exceeding 50–100 W m^{-2} to achieve economic viability [144]. In ion separation, K^+/Mg^{2+} selectivity values of 200–600 [101] have been demonstrated for monovalent/divalent discrimination, but industrial lithium extraction from salt-lake brines demands selectivity ratios above 1000 [145] to ensure competitive recovery yields. For ion-based information processing, rectification ratios of 10–350 and gating ratios of 10^2–10^4 are achievable, yet reliable logic operations require rectification exceeding 500 and gating ratios surpassing 10^5[146–149]. These quantitative gaps underscore that nano-brick materials, while scientifically elegant, remain in the pre-competitive stage for most energy applications. The following sections detail how specific nano-brick architectures address these performance targets while acknowledging the remaining engineering barriers.

6.1. Energy harvesting and conversion

Energy conversion systems based on confined ion transport fundamentally rely on regulating the asymmetric migration of ions within nanoscale spaces to efficiently convert chemical potential differences or hydrodynamic driving forces into electrical energy output. Such systems depend on interfacial charge regulation within nanochannels and the ordered ion transport mechanisms in confined spaces, enabling the transition from stochastic thermal motion to macroscopic directional current transport.

6.1.1. Salinity gradient energy

Salinity gradient energy conversion is an important approach for harvesting energy from the salinity difference between seawater and freshwater, with its core mechanism relying on the generation of an electric potential difference induced by selective ion migration across membranes. By constructing charged nanochannel structures, differential screening and directional transport of various ions can be achieved to maximize energy recovery efficiency. Physically, this mechanism is analogous to the reverse osmosis process, but the primary driving force arises from selective ionic diffusion rather than electron transport. At the material design level, the pore size, surface charge properties, and geometric structure of nanochannels significantly influence energy conversion efficiency. Generally, constructing channel structures with high cation mobility facilitates the rapid transport of monovalent ions such as Na^+ while suppressing the migration of multivalent ions and large-sized solutes, thereby improving power density while maintaining high energy conversion efficiency. In recent years, MOF- and COF-based engineered porous materials have emerged as important platforms for salinity gradient energy harvesting. For example, a 2D Cu-tetrakis (4-carboxyphenyl) porphyrin (TCPP) MOF composite membrane integrated with silk fibroin nanofibers forms one-dimensional (1D) straight transport nanochannels, which reduce ion transport resistance and achieve relatively high osmotic energy output, reaching a power density of 29.5 W·m^{-2} in a lake–river water mixing system (Fig. 13A) [150]. Furthermore, Yang et al. constructed a metal-porphyrin COF monolayer membrane that, owing to its atomic-scale thickness, high pore density, and anion-selective transport characteristics, achieved an ultrahigh power output of 135.8–203.8 W·m^{-2} under seawater–river water salinity gradient conditions (Fig. 13B) [151]. Meanwhile, Chen et al. designed a fully sub-nanometer MOF–COF bilayer heterostructured membrane, where asymmetric pore size and charge distribution induced ion diode-like transport behavior, enabling a power density of approximately 192.9 W·m^{-2} in an acidic concentration gradient system (Fig. 13C) [28].

6.1.2. Flow-driven energy conversion

In addition to salinity gradient energy, streaming potential is also an important form of energy recovery in nano-confined systems. When

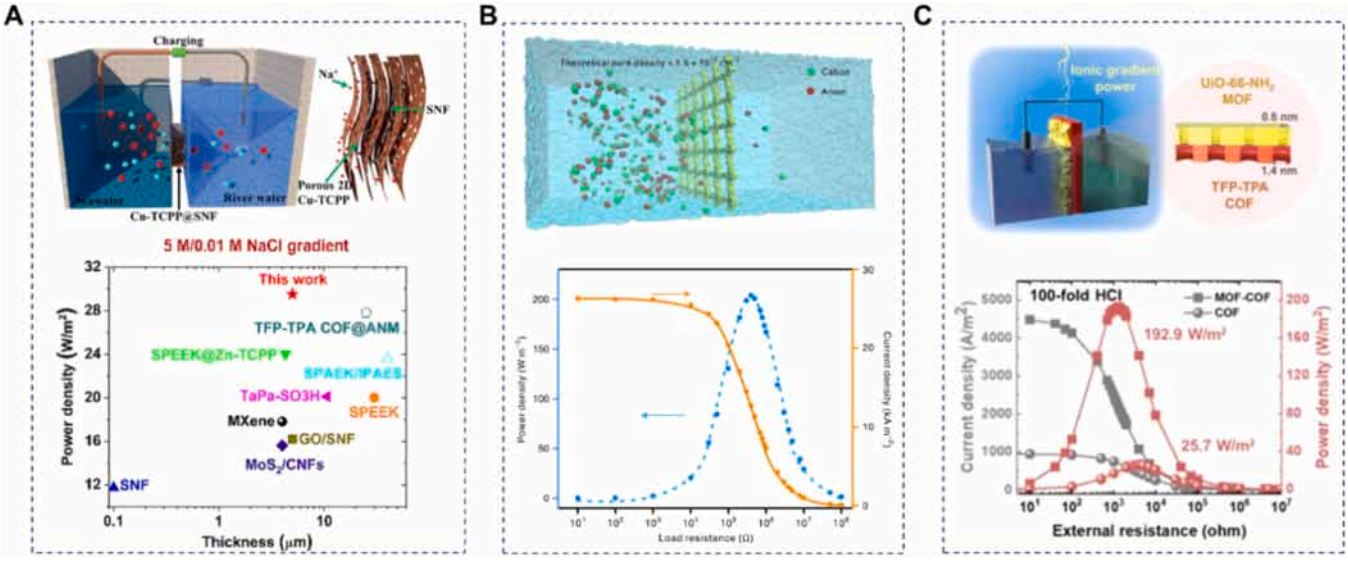


Fig. 13. Energy conversion systems based on nanoconfined system. (A) Shortened ion-channel structure of a 2D Cu-TCPP@SNF metal–organic framework/silk fibroin nanofiber composite membrane for enhanced salinity gradient energy harvesting [150]. Copyright 2024, Elsevier B.V. (B) Periodic ordered pore array structure of metal-porphyrin COF (MTPP-COF) monolayer membranes for efficient salinity-to-energy conversion [151]. Copyright 2022, Nature. (C) Sub−2 nm, acid-stable MOF-COF ion diode membrane for high-efficiency osmotic energy generation [28]. Copyright 2025, Elsevier B.V.

fluids flow through nanochannels, ion migration and separation occur under the coupled effects of shear flow and electrostatic interactions, ultimately generating a transmembrane potential difference and enabling the recovery of mechanical energy or low-grade thermal energy. Therefore, the surface charge density and structural characteristics of nanochannels are key parameters for regulating streaming potential conversion efficiency. In terms of material systems, MOF materials exhibit unique advantages in flow-driven energy conversion due to the high tunability of their pore structures. Their regularly ordered nanochannels can effectively reduce ion migration resistance while enabling precise control of ion transport pathways through interfacial charge engineering. For example, Liu et al. constructed a UiO−66-NH_2-based heterogeneous sub-nanochannel membrane, where angstrom-scale window pores synergistically enabled size sieving and electrostatic regulation, resulting in excellent ion selectivity and achieving an osmotic energy output of 26.8 $W{\cdot}m^{-2}$ under concentration gradient conditions [152]. In addition, Li et al. prepared a photoresponsive porphyrin MOF membrane via cathodic electrodeposition. By utilizing photogenerated charge carriers to modulate the surface charge density of the channels, the streaming potential was further enhanced under salinity gradient conditions, thereby improving energy conversion efficiency [153].

6.1.3. *Chemical potential difference and electrochemical coupling systems*

In addition to salinity gradient and flow-driven mechanisms, nanoconfined spaces can also utilize chemical potential differences to achieve multi-physical-field coupled energy conversion. By regulating solvation structures, temperature gradients, or chemical reaction equilibria, transmembrane potential differences can be induced within nanochannels to enable efficient energy recovery. Such coupled mechanisms are of significant importance in flow batteries and electrochemical energy storage systems [154–156]. In the design of specific electrode materials, porous structures are typically integrated with electrochemically active sites to synergistically enhance charge storage and transport efficiency. For example, Sheberla et al. (Fig. 14A) [157] reported a conductive MOF, nickel hexaiminotriphenylene framework ($Ni_3(HITP)_2$), which possesses a high specific surface area (630 $m^2\ g^{-1}$), ordered sub-nanochannel architecture, and ultrahigh electrical conductivity (>5000 S m^{-1}), achieving a mass specific capacitance of 111 F g^{-1} and an areal capacitance of 18 μF cm^{-2} while maintaining over 90% capacity retention after more than 10,000 cycles. Further studies have shown that regulating membrane thickness, channel structure, and functional group type can effectively enhance charge storage density and extend electrode lifespan. In addition, solvation structure regulation is also an important strategy for improving ion migration efficiency. Farina et al. [158] constructed a nano-confined electrolyte space using Mg-MOF−74 to optimize the solvation structure in $LiClO_4$–propylene carbonate electrolytes, reduce ion diffusion energy barriers, and increase the Li^+ transference number to $t_{Li}^{+} > 0.7$, significantly enhancing lithium-ion transport performance. In high-performance charge storage systems, 2D conductive MOFs with multiple transport pathways also exhibit excellent potential. Park et al. (Fig. 14B) [159] designed a 2D conductive MOF electrode, Co-HAB, based on hexaminobenzene ligands. Through high-density redox-active sites and ordered sub-nanochannels, it enabled synergistic fast electron–ion transport, exhibiting a high capacity of 291 mAh g^{-1} and good rate capability. First-principles calculations further revealed that 2D conductive MOFs such as copper hexaiminotriphenylene framework ($Cu_3(HITP)_2$) can regulate polysulfide adsorption and catalytic conversion through the synergy of ordered nanochannels and surface charge effects, significantly lowering the reaction energy barriers for sulfur reduction and Li_2S decomposition (approximately 0.84 eV), thereby

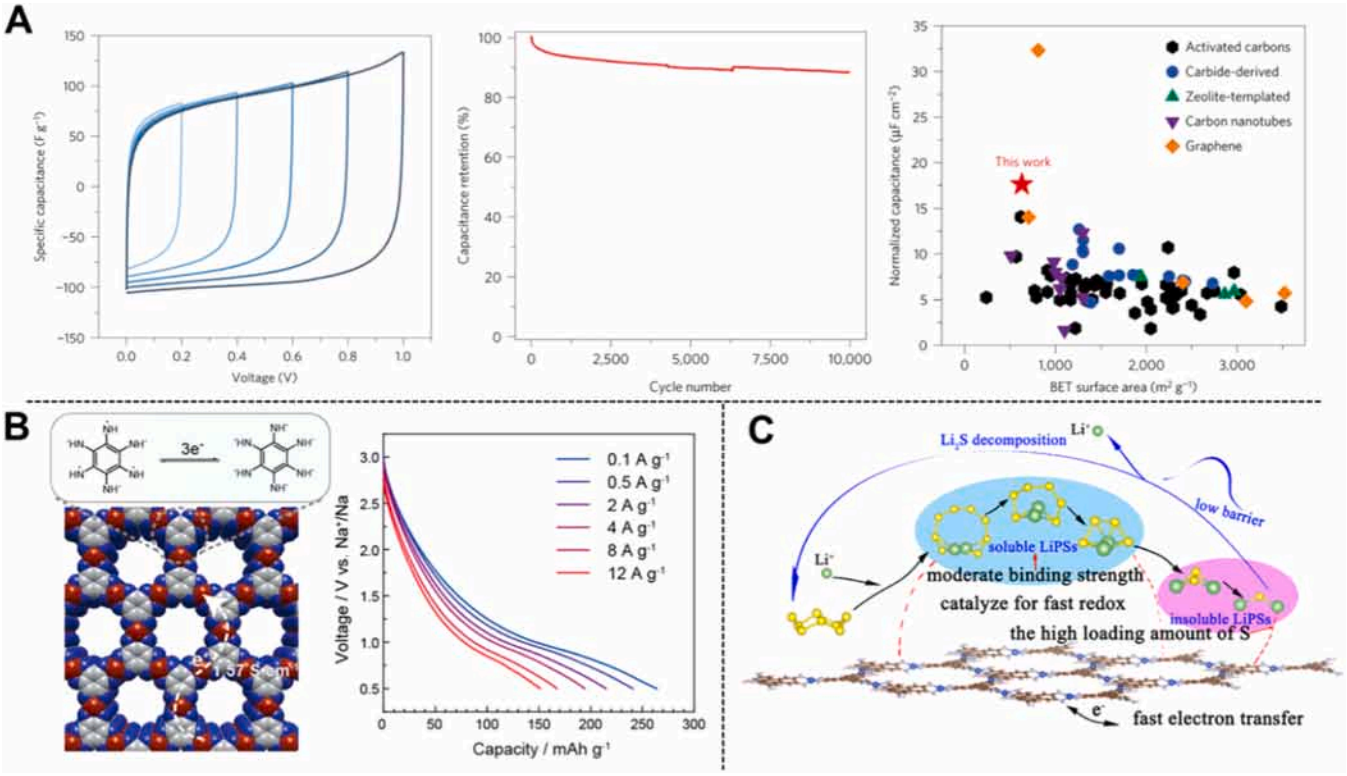


Fig. 14. Chemical potential difference and electrochemical coupling systems and their representative performance. (A) All-MOF electrode based on highly conductive $Ni_3(HITP)_2$ for electrochemical double-layer capacitors with high areal capacitance and excellent cycling stability [157]. Copyright 2017, Nature. (B) Co-HAB conductive MOF with high-density redox-active sites and high intrinsic electrical conductivity for high-power sodium-ion storage [159]. Copyright 2018, American Chemical Society. (C) 2D conductive $Cu_3(HITP)_2$ as an efficient bifunctional electrocatalyst for improving lithium–sulfur battery performance [160]. Copyright 2021, American Chemical Society.

confirming the critical role of confined structures in electrochemical reaction kinetics regulation (Fig. 14C) [160].

Overall, energy conversion technologies based on nano-confined ion transport are undergoing rapid development. With continuous advances in nanoscale structural design and interfacial regulation strategies, it is expected that energy harvesting systems with both high stability and high conversion efficiency will be constructed in the future, demonstrating broad application prospects in micro self-powered devices, environmental remediation, and waste heat recovery.

6.2. *Ion-based signal and information processing*

Ions are not only important carriers of energy transport but also serve as media for information transmission. In biological systems, the generation and propagation of neural signals rely heavily on the dynamic regulation of ion channels, providing important inspiration for the artificial construction of nano-confined ion information processing systems [161–163]. By designing nanochannel structures with nonlinear response characteristics, ion flux can be logically regulated and encoded, thereby promoting the development of ionotronic systems. From a physical mechanism perspective, ion signal processing essentially involves the dynamical regulation of non-equilibrium transport systems. Unlike conventional electronic transport, which primarily relies on directional electron migration, ion transport is usually governed by multiple factors, including electrostatic interactions, solvation structure rearrangement, thermal motion randomness, and interfacial chemical reactions. Consequently, ion transport in nano-confined spaces often exhibits pronounced nonlinear response behavior. Under external field stimulation, when the applied voltage or changes in the chemical environment exceed a specific threshold, ionic conductivity may undergo abrupt transition-like jumps. This threshold-responsive behavior is functionally analogous to the switching logic structures of electronic devices. In other words, by regulating channel interfacial charge density, hydrophilicity/hydrophobicity, and ion binding energy barriers, "on–off" controllable ion transport can be achieved, providing a physical basis for ion-based logical computation and signal modulation systems. Furthermore, such nonlinear ion transport characteristics can not only be used for information encoding but also enable the design of

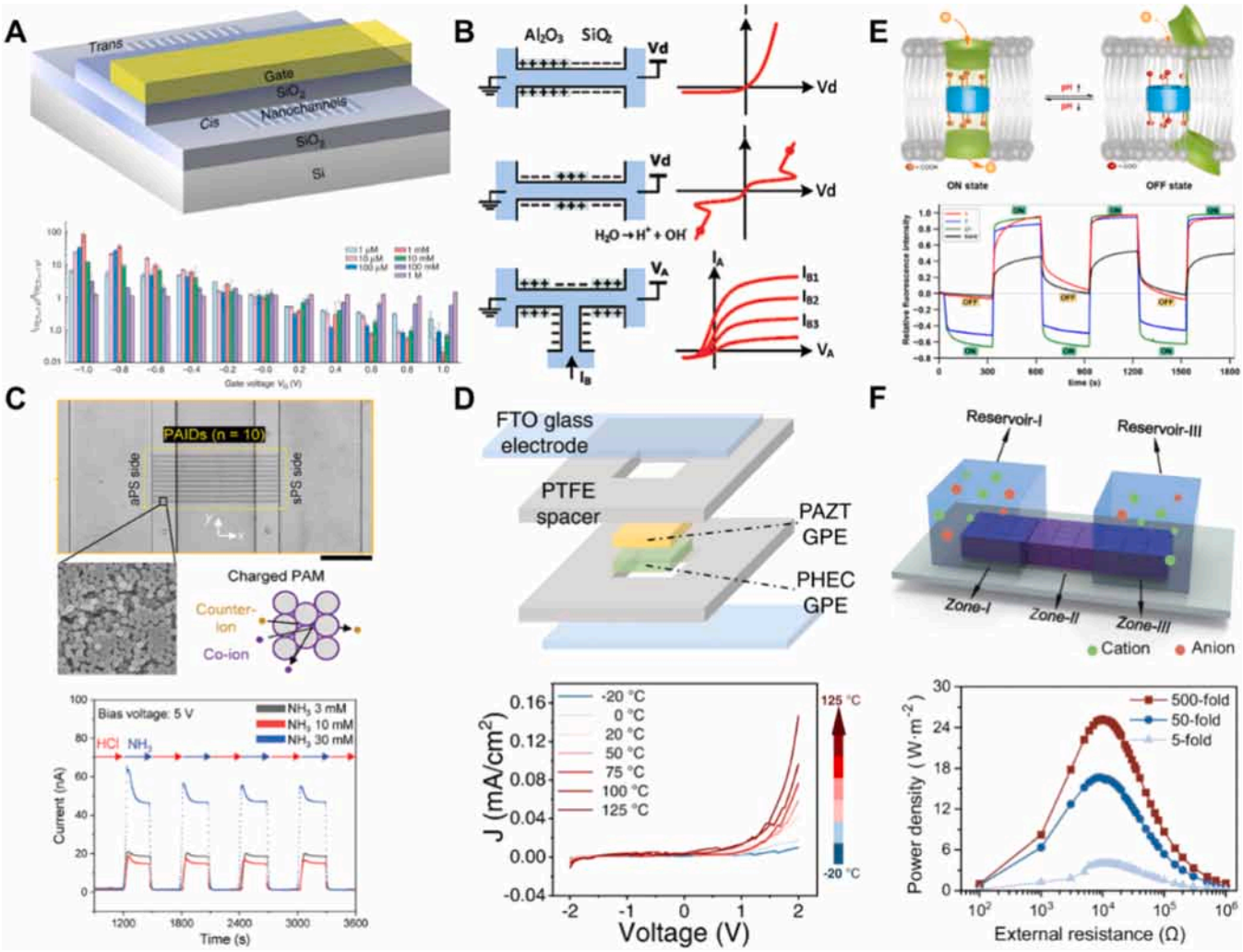


Fig. 15. Ion rectification and diode effects and their representative performance. (A) Field-effect reconfigurable nanochannel ion diode for electrostatically programmable ion transport control and logic circuit construction [166]. Copyright 2011, Nature. (B) SiO_2/Al_2O_3 heterogeneous nanochannel ion rectification and switching regulation system [167]. Copyright 2009, American Chemical Society. (C) PMMA/PVDF-HFP heterogeneous GPE ion diode and its applications in logic operations and TENG rectification [33]. Copyright 2022, Nature. (D) Particle-assembled heterogeneous charged nanopore array for in situ gas permeation-driven ionic current rectification, enabling programmable ionic signal amplification and (bio)chemical sensing. Copyright 2024, Wiley-VCH GmbH [168]. (E) Artificial acidic pocket structure constructed from pillar [5] arene–cyclodextrin hybrid molecules for millisecond-scale switching and pH-responsive bidirectional gated biomimetic ion channels [169]. Copyright 2025, Royal Society of Chemistry. (F) 2D Cu-TCPP photoresponsive nanofluidic membrane for coupled osmotic and photonic energy conversion [171]. Copyright 2024, Nature.

multifunctional integrated nanoionic devices. For example, by combining biomimetic ion channel structures, stimuli-responsive functional interfaces, and dynamically confined transport pathways, it is possible to construct ion-regulated systems with neuromorphic computing capabilities, showing promising applications in intelligent sensing, neural interfaces, and low-power information processing [164].

6.2.1. Ion rectification and diode effects

Ion rectification is one of the important physical foundations for constructing ion logic devices. In nanochannels with structural asymmetry, the uneven distribution of local electric potential leads to differences in ion migration energy barriers under forward and reverse voltages, resulting in direction-dependent transport behavior. This rectification phenomenon is usually closely related to EDL overlap effects. When the channel dimension is comparable to the Debye length, interfacial charges dominate the local ion concentration distribution, thereby forming preferential unidirectional transport pathways. Therefore, ion rectification performance can be systematically optimized by regulating nanochannel geometry, charge gradients, and interfacial wettability. At the device design level, researchers have explored various nanoionic structures capable of modulating rectification behavior [165]. For example, Guan et al. constructed a field-effect reconfigurable nanoionic diode, where the ion distribution inside nanochannels was regulated by gate voltage, enabling in situ dynamic control of rectification direction and intensity, with a maximum rectification ratio of 83, providing an important basis for programmable nanoionic circuits (Fig. 15A) [166]. Furthermore, Cheng et al. developed a SiO_2/Al_2O_3 heterogeneous nanochannel ion diode, achieving a high rectification ratio of 321 in 1 mM KCl solution and demonstrating electrically controlled ionic current modulation capability in a three-terminal structure, indicating that heterogeneous interface engineering offers significant advantages in enhancing rectification performance (Fig. 15B) [167].

In addition to fundamental rectification functions, ion diode structures can also be used for advanced information processing functions such as signal shaping and noise suppression. For example, by constructing multistage cascaded rectifying channels, the amplitude of ionic currents can be finely regulated, allowing ion signals to maintain higher stability and recognition accuracy during transmission. Based on this concept, Jiang et al. fabricated a heterojunction ion diode using a gel polymer electrolyte. The rectification behavior was induced by differences in ion migration rates between two polymer phases, achieving a rectification ratio of 23.11 under ±1 V bias and exhibiting wide temperature stability from −20 °C to 125 °C, while preliminarily demonstrating the integration potential of ion-based logic gate circuits (Fig. 15C) [33]. In addition, external field stimulation can also serve as an important means to regulate ion rectification behavior. Seo et al. dynamically and reversibly modulated ionic rectification in polymer membranes by controlling the local pH environment of microfluidic devices through gas permeation. This approach not only enabled tunable rectification coefficients but also supported reverse-operating modes of the device, further expanding the application scope of ion diodes in signal modulation and intelligent ion transport (Fig. 15D) [168].

6.2.2. Gating mechanisms and stimuli-responsive regulation

Ion gating mechanisms are an important means of endowing nanoconfined systems with active regulation of transport states, with the core principle being the reversible switching between channel open and closed states through external stimuli. Common stimulation modes include pH, light, temperature, and chemical signals. By constructing intelligent interfaces with stimulus-responsive characteristics, the electrostatic environment, spatial structure, and host–guest interaction strength within nanochannels can be dynamically regulated, enabling programmable control of ion transport behavior.

In pH-responsive regulation, nanochannels containing protonatable functional groups can modulate local potential distribution by altering their charge states. When the environment shifts from alkaline to acidic conditions, partial amino groups become protonated, changing the surface charge properties of the channel and weakening electrostatic repulsion, thereby promoting cation migration. Conversely, under alkaline conditions, deprotonation processes often enhance interfacial charge density, further improving separation selectivity. Based on this principle, Zhao et al. developed a biomimetic artificial ion channel inspired by ASICs (acid-sensing ion channels) by introducing carboxyl-functionalized structures. The reversible protonation of carboxyl groups regulated channel conformation and enabled conductivity switching behavior, exhibiting rapid and reversible gating responses under varying pH conditions (Fig. 15E) [169]. Furthermore, Wu et al. designed a dual-responsive artificial potassium ion channel that integrates mechanical force and pH responsiveness. By modulating the protonation state of inhibitor molecules to alter the electrostatic environment of the channel, reversible regulation of K^+ transport was achieved, with a K^+/Na^+ selectivity as high as 41.3, demonstrating the potential of multi-stimuli-coupled ion recognition regulation [170].

In addition to chemical stimuli-responsive systems, photoresponsive regulation has also attracted significant attention in recent years. Light stimulation offers advantages such as fast response speed, remote controllability, and flexible spatial modulation. By introducing photoisomerizable molecules or photothermal-active components, light energy can be used to induce structural or interfacial property changes within channels. For example, Wang et al. constructed a light-responsive ion regulation system based on a Cu-TCPP 2D nanochannel membrane. The photothermal effect generated a temperature gradient inside the membrane to drive directional ion migration. Meanwhile, light stimulation also regulated surface charge distribution and ion-active transport behavior within the channels, increasing osmotic energy output power from 16.64 $W{\cdot}m^{-2}$ to 31.9 $W{\cdot}m^{-2}$, demonstrating the advantages of light-assisted ion transport regulation (Fig. 15F) [171]. In addition, Wu et al. developed a programmable artificial nanochannel system based on multifunctional DNA gating strategies. This system could sequentially respond to chemical and optical stimuli, enabling intelligent recognition and regulation of multiple physiological signals such as Ca^{2+}, H_2O_2, and pH, highlighting the potential applications of ion-based information processing in complex environments [172].

On the other hand, temperature-responsive regulation mainly relies on the thermally induced phase transition behavior of smart polymers. When the temperature crosses the critical phase transition temperature of the polymer, polymer chains may undergo swelling or collapse, thereby altering the effective pore size and ion migration resistance within nanochannels. Based on this mechanism, Liu et al. constructed a poly (N-isopropylacrylamide) (PNIPAM)-grafted graphene oxide biomimetic smart membrane. The temperature-induced phase transition of PNIPAM regulated the interlayer channel size, enabling reversible gated transport of water and solutes and achieving approximately a sevenfold modulation capability of water flux (Fig. 16A) [173]. Similarly, Kim et al. designed a PNIPAM/polypyrrole (PPy) thermoresponsive composite membrane that regulated coupled electron–ion transport pathways through polymer volume changes. While maintaining structural stability, the membrane exhibited enhanced electrical conductivity and selective protein filtration performance, further expanding the application scope of thermoresponsive smart membranes (Fig. 16B) [174].

6.2.3. Neuromorphic information processing and memristive behavior

Nano-confined ion transport systems not only enable energy conversion and signal regulation but are also gradually demonstrating the potential for neuromorphic information processing. In particular, certain ion channels exhibit response characteristics similar to biological synaptic plasticity under periodic electrical stimulation, where the conductance state of the channel may undergo reversible changes depending on stimulation history, displaying pronounced hysteresis regulation behavior. This memory-like characteristic typically arises from non-equilibrium transport processes such as interfacial ion

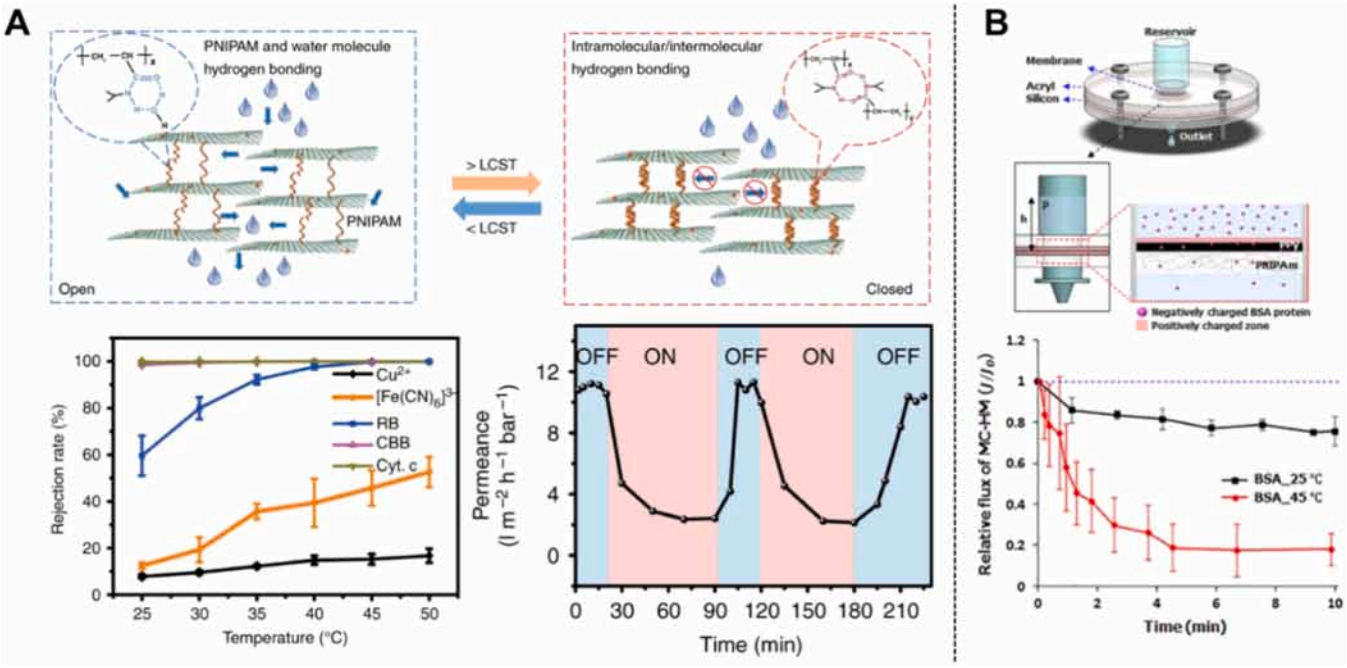


Fig. 16. Thermoresponsive and adaptive nanofluidic membrane systems. (A) Temperature-responsive graphene nanosheet membrane with tunable interlayer spacing for water gating and molecular separation [173]. Copyright 2017, Nature. (B) Nanoporous hybrid PNIPAm–PPy membrane with temperature responsiveness, deformability, and tunable surface charge for controllable transport driving, electrical sensing, and protein separation [174]. Copyright 2017, Nature.

accumulation, local structural relaxation, and spatial reconstruction of electric fields. By constructing multi-level transport network architectures, the information computing capability of the system can be further expanded. For example, multi-channel arrays can enable spatially parallel signal processing, while gradient potential structures can be used for ion signal encoding and storage [167].

In specific research examples, Noh et al. (Fig. 17A) [175] combined molecular dynamics simulations with experiments to reveal the synaptic plasticity mechanism driven by competitive ion adsorption in sub-nanometer hexagonal boron nitride (hBN) membranes. Under periodic voltage pulse stimulation, this system regulated the dynamic migration behavior of Na^+ and K^+, allowing ion flux to reversibly change with stimulation history and exhibiting stepwise conductance memory storage characteristics, reflecting the synergistic effect of competitive ion adsorption and electric field regulation within confined spaces. Furthermore, Zhang et al. (Fig. 17B) [176] constructed a trilayer bipolar polyelectrolyte gel ion memristor, where the ion concentration polarization effect within the intermediate gel layer was used to regulate the conductance state. The channel geometric scale was also designed to enable predictable regulation of memory retention time (approximately

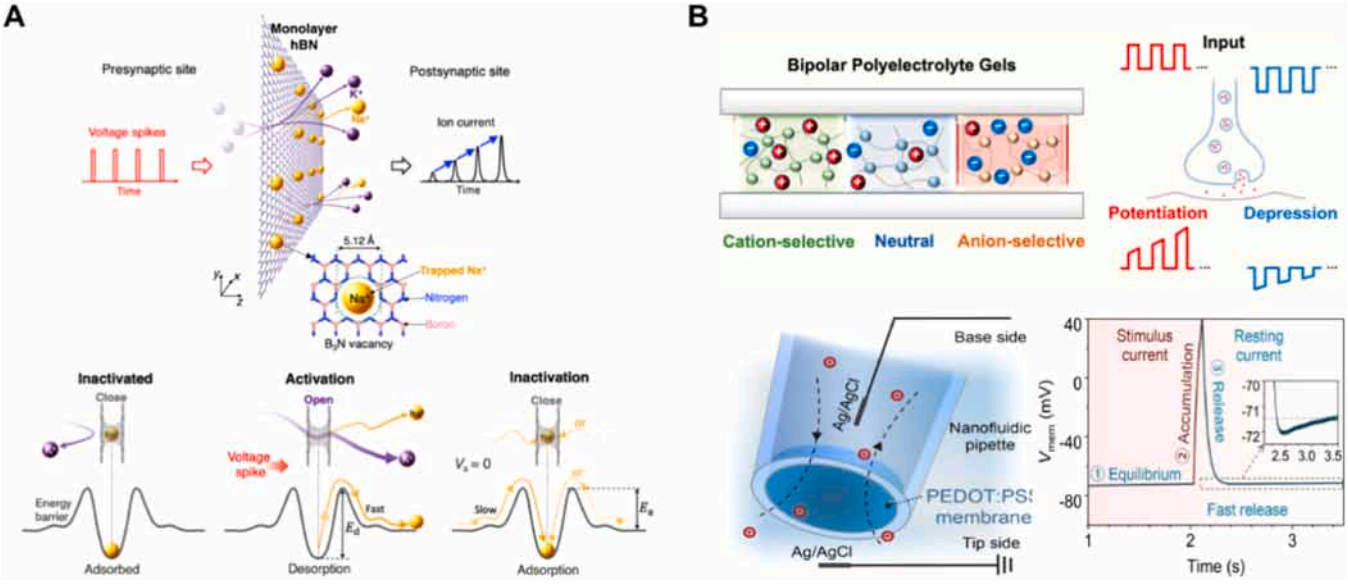


Fig. 17. Iontronics neuromorphic devices for ion information processing. (A) 2D nanoporous hBN membrane with dynamically tunable ionic conductance regulated by voltage pulses for synaptic plasticity, low-power neuromorphic computing, and ionic information processing [175]. Copyright 2024, Science. (B) Sandwich-type polyelectrolyte hydrogel ionic memristor with geometry-scalable memory time regulated by concentration polarization for neuromorphic computing and ionic information processing [176]. Copyright 2024, National Academy of Sciences.

200–4000 s). This structure not only demonstrated ion synaptic plasticity but also highlighted the important role of macroscopic structural parameters in regulating neuromorphic behavior. In addition, Xu et al. [177] developed a nano-confined ionic conductance-type biomimetic spiking synaptic device, where a geometrically asymmetric channel structure was used to induce ion concentration polarization, thereby simultaneously achieving memristive characteristics and ion rectification effects. Under electrical pulse stimulation, the device exhibited typical current response hysteresis and memory retention capability, revealing an electron–ion coupling–driven conductance regulation mechanism.

Overall, ionic memristive devices provide a new physical platform for neuromorphic computing. Compared with conventional electronic memristive systems, ionic memristive structures can operate stably in aqueous environments and are expected to directly interface with biological neural systems, thus showing significant application prospects in neural repair, intelligent sensing, and bioelectronic interfaces.

6.3. Seawater desalination and ion separation

Seawater desalination and ion resource recovery are among the most practically valuable engineering applications of nano-confined ion transport technology [37]. With the growing global shortage of freshwater resources and increasing demand for critical metal resources, the development of low-energy-consumption and high-selectivity separation technologies has gradually become a research focus. Although traditional reverse osmosis technology has achieved industrial application, it still faces limitations such as relatively high operating energy consumption, severe membrane fouling, and insufficient multivalent ion sieving capability. Therefore, membrane systems based on nano-confined transport mechanisms are considered a promising direction for future high-efficiency separation technologies. From a physical mechanism perspective, the primary advantage of nano-confined ion separation systems lies in their ability to synergistically regulate size exclusion effects, electrostatic interactions, and solvation structure reconstruction at the sub-nanometer scale. Unlike macroscopic porous membranes, ion migration within confined spaces is often accompanied by partial stripping and rearrangement of hydration shells. Since different ions exhibit significantly different hydration energies, the dehydration energy barriers required for ions to traverse confined channels also differ, providing a fundamental physical basis for achieving highly selective separation of multivalent ions. In practical separation processes, ion transmembrane migration generally involves three key stages. First, ions enter the nanochannel entrance region. Second, the hydration structure is partially disrupted and competes with interfacial adsorption sites. Finally, ions achieve directional migration within the confined space. Therefore, precise regulation of pore size, charge distribution, and interfacial chemical properties can effectively optimize the energy barrier landscape across these stages, thereby improving overall separation performance.

6.3.1. High-selectivity ion sieving mechanisms

High-selectivity ion sieving typically relies on the synergistic regulation of size exclusion effects and charge selectivity. When the nanochannel size approaches the hydrated diameter of ions, ion entry into the channel usually requires partial dehydration. Since multivalent ions possess higher hydration energies, their dehydration energy barriers are generally significantly larger than those of monovalent ions, leading to stronger migration suppression within confined systems. In terms of material design, introducing charged functional groups is an important strategy for enhancing selective regulation capability. Negatively charged channel structures usually promote cation transport while suppressing anion migration. Based on this design concept, related studies have been applied to lithium resource extraction from salt-lake brines and other complex electrolyte systems. For example, Fan et al. (Fig. 18A) [35] reported a biomimetic separation membrane based on a NASICON-type structure. Through sub-nanometer channel size optimization and surface chemical regulation, ultrahigh selective transport of Li^+ was achieved. In complex salt-lake environments, the membrane could effectively distinguish Li^+ from competing ions such as Na^+ and K^+, demonstrating the application potential of high-efficiency lithium extraction materials. Building on this, Feng et al. [178] further developed an ion-selective membrane composed of amino-functionalized lithium titanate nanoparticles embedded in a polyamide matrix. Through the synergistic effects of size sieving and charge-guided transport mechanisms, the system achieved highly selective Li^+

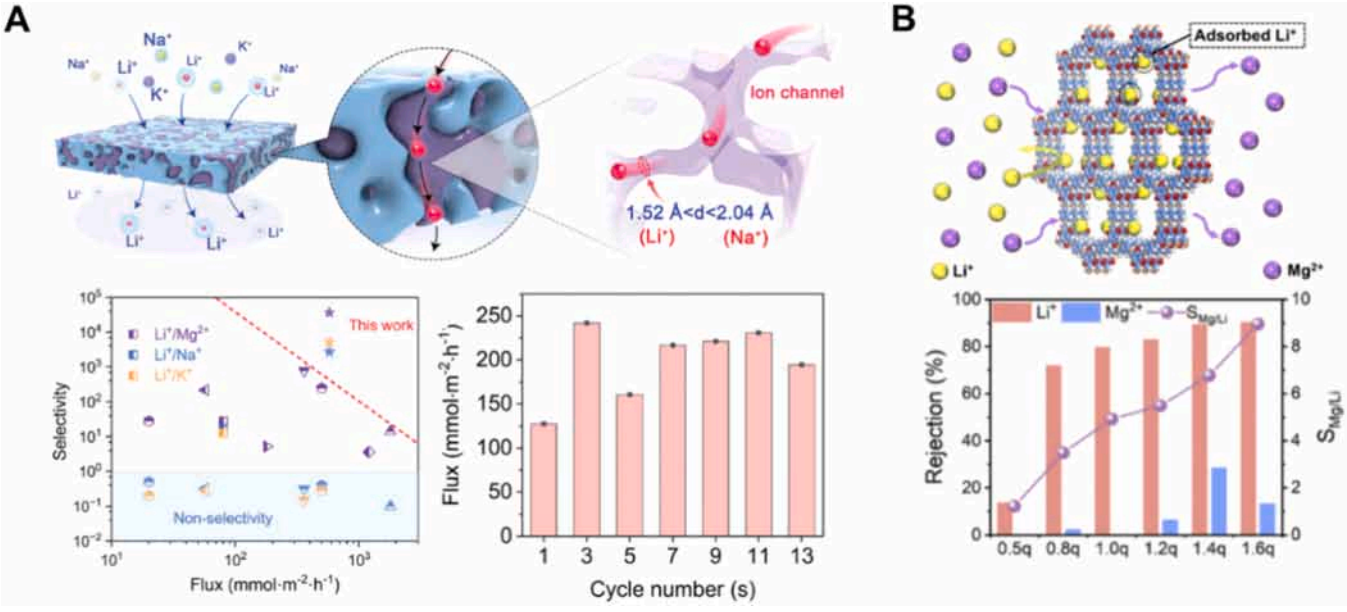


Fig. 18. Ion separation membrane systems for lithium extraction and selective ion transport. (A) Biomimetic nonporous crystalline membrane with sub-nanometer confined rigid ion channels for ultra-high Li^+/Na^+ and Li^+/K^+ selectivity and one-step lithium extraction from salt lakes [35]. Copyright 2024, Wiley-VCH GmbH. (B) Charge-regulated nanoporous COF membrane with tunable hydrophilicity for preferential Mg^{2+} permeation and Li^+ rejection in high Mg/Li ratio brines [180]. Copyright 2024, Elsevier B.V.

extraction and exhibited excellent selectivity in both LiCl/NaCl and LiCl/$CaCl_2$ systems, while maintaining good long-term operational stability under high-salinity complex environments.

With continued research progress, 2D materials and designable porous systems such as MOFs and COFs have gradually become important platforms for ion separation membranes. For example, Bao et al. [179] constructed a COF composite membrane with randomly oriented bottleneck channel structures. Through the synergistic regulation of size exclusion and sulfonic acid group chemical affinity, efficient separation of Li^+ from multiple competing ions was achieved. Further studies showed that under an applied electric field, the membrane flux was significantly enhanced, making it suitable for selective lithium enrichment from salt-lake brines. Meanwhile, Liu et al. used molecular dynamics simulations to reveal the regulation mechanism of COF membrane hydrophilicity on ion adsorption and migration behavior, finding that strongly hydrophilic pore walls could preferentially adsorb Li^+ and form localized blocking effects, thereby enhancing Mg^{2+}/Li^+ separation efficiency and providing a new interfacial chemistry design strategy for lithium extraction from salt lakes (Fig. 18B) [180].

6.3.2. Low-energy separation pathway design

Reducing the energy consumption of separation processes is one of the key objectives in promoting the industrial application of nanoseparation technologies. Confined transport systems can reduce external driving energy requirements through multiple mechanisms. First, hydrophilic low-friction channels can significantly reduce transmembrane ion migration resistance by weakening the interactions between water molecules and ions, thereby improving transport efficiency. Second, gradient potential structures can form spontaneously driven ion migration pathways within membranes, enabling directional diffusion of ions under concentration gradient conditions. In addition, some systems can also couple energy utilization with separation processes by exploiting chemical potential differences in the natural environment, which is considered an important direction for future green separation technologies. In specific studies, Zou et al. [181] proposed a Turing-type multistage nanochannel membrane design. Using a sacrificial template strategy, an interwoven transport network was constructed within a MoS_2 2D membrane. While maintaining high cation transport selectivity (with a transference number of approximately 0.91), the design significantly enhanced ion flux and achieved stable osmotic energy output under natural salinity gradient conditions. Safaei et al. [182] further introduced phosphorus vacancy structures into 2D niobium phosphate nanosheets via acid etching. This approach increased the membrane surface negative charge density and hydrophilicity, reduced ion diffusion energy barriers, and achieved an osmotic energy power density of approximately 10.7 $W{\cdot}m^{-2}$ in a seawater–freshwater gradient system.

6.3.3. Anti-fouling capability and long-term stability optimization

Membrane fouling is a major bottleneck restricting the engineering application of separation membranes. Biofouling, organic fouling, and inorganic salt deposition can all lead to channel blockage and reduced separation efficiency; therefore, improving interfacial anti-fouling performance is of great importance. One effective strategy is to construct interfaces with low surface energy and stable hydration layer structures to reduce contaminant adsorption. For example, hydration layers can form a stable protective barrier on the membrane surface, suppressing the adhesion of proteins, bacteria, and organic molecules. He et al. [183] constructed a dynamic sliding supramolecular anti-fouling interface composed of cyclodextrin and polydimethylsiloxane (PDMS) chains. By stabilizing the hydrophilic hydration layer to reduce the binding strength of hydrophobic pollutants, the membrane exhibited a flux decline rate of only 14.2% under low-speed stirring filtration conditions, with an initial water flux reaching 550 L m^{-2} h^{-1}.

On the other hand, regulating the surface chemical structure and roughness of the membrane can further enhance anti-fouling performance. For example, Taghipour et al. (Fig. 19A) [184] fabricated an anti-fouling modification layer enriched with sulfonic acid and carboxyl groups on the surface of a nanofiltration membrane via an ultrasonic aerosol interfacial polymerization method. By reducing surface roughness and enhancing electrostatic repulsion, the adsorption of protein and polysaccharide contaminants was effectively suppressed, achieving approximately 90% flux recovery. Meanwhile, improving the intrinsic stability of membrane materials is also crucial. The adoption of covalently cross-linked structures, in situ growth synthesis methods, or multilayer composite architectures can enhance the mechanical and chemical stability of membranes, enabling their application in high-salinity and complex contaminated water environments. For example, Liao et al. (Fig. 19B) [185] constructed a thiazole-linked covalent organic framework membrane using a “monomer–solvent dual engineering” strategy. The irreversible covalent bonding significantly improved chemical resistance and structural stability, allowing the membrane to maintain high separation performance under strongly acidic and organic solvent conditions. Li et al. fabricated a high-salinity-resistant distillation membrane via interfacial polymerization using tetraaldehyde-functionalized calixarene monomers, forming a rigid three-dimensional porous network that achieved the synergistic optimization of high water flux and low salt rejection (Fig. 19C) [186]. Furthermore, Yuan et al. constructed an interdigitated ultramicroporous crystalline COF desalination membrane through an acid-regulated interfacial synthesis strategy. Hydrogen-bond-regulated reaction diffusion kinetics enhanced membrane crystallinity and cross-linking density, enabling a NaCl rejection rate of 99.7% and significantly improving long-term operational stability (Fig. 19D) [187].

Overall, through the synergistic optimization of multiscale structural regulation and interfacial chemical engineering, nano-confined ion separation membranes are expected to play a more important role in complex water purification, salt-lake resource recovery, and low-energy seawater desalination.

6.4. Practical challenges and engineering considerations

While the nano-brick framework provides a powerful conceptual paradigm for designing programmable ion transport systems, translating these laboratory demonstrations into practical energy technologies requires addressing several critical engineering challenges. In this section, we systematically analyze the scalability, stability, and fabrication barriers that currently limit the deployment of nanoconfined iontronic systems, and identify strategies to bridge the gap between proof-of-concept materials and device-level implementation.

6.4.1. Scalability and manufacturing precision

A fundamental challenge in nano membranes is achieving large-area, defect-free fabrication while maintaining the precise structural control that defines their transport properties. For 2D material membranes, vacuum filtration and layer-by-layer assembly methods are simple and scalable, yet they often suffer from inhomogeneous stacking, wrinkles, and interlayer spacing fluctuations across macroscopic areas. For example, MXene membranes exhibit excellent intrinsic properties in small-scale tests, but large-area fabrication remains plagued by nonuniform channel dimensions and mechanical fragility (Table 1). Similarly, MOF and COF membranes require precise control over crystallization kinetics to avoid grain boundaries and misaligned pores that compromise selectivity. Recent advances such as the inverse microemulsion interfacial polymerization strategy for rapid COF membrane preparation (Fig. 12A), enabling highly crystalline, large-area membranes within seconds. However, the reproducibility of sub-nanometer pore dimensions across batches and the elimination of pinhole defects remain significant hurdles for industrial manufacturing. The trade-off between fabrication throughput and structural precision must be carefully balanced, rapid synthesis methods may introduce disorder, whereas overly stringent conditions reduce yield and increase cost.

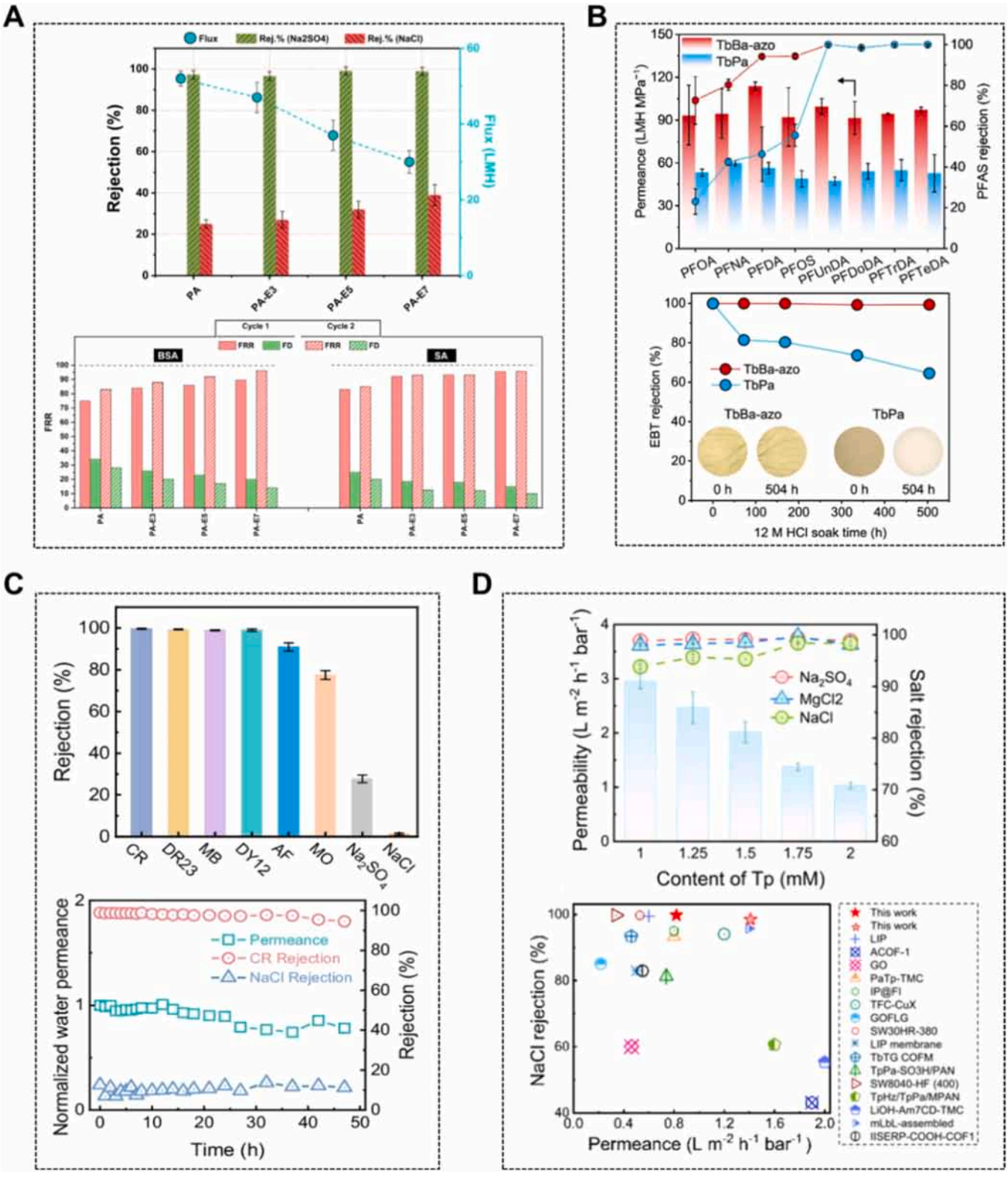


Fig. 19. High-performance separation membrane systems. (A) Composite nanofiltration membrane with enhanced negative charge constructed via ultrasonic atomization interfacial polymerization of spot-like polyester coatings for mitigating membrane fouling while maintaining separation performance [184]. Copyright 2024, American Chemical Society. (B) Thiazole-based COF membrane with spatially exposed N/S heteroatoms for highly selective separation and stable chemical transport under strong acidic conditions [185]. Copyright 2026, Nature. (C) TACA calixarene nanofilm constructed via unidirectional diffusion-assisted interfacial polymerization for efficient dye/salt separation [186]. Copyright 2026, Nature. (D) ABC staggered-stacking, acetic acid-regulated ultramicroporous COF membrane for high-efficiency reverse osmosis desalination [187]. Copyright 2025, American Chemical Society.

6.4.2. Long-term operational stability

The aqueous instability of many nano materials, particularly MOFs, poses a severe constraint for practical deployment. Water molecules can hydrolyze metal-ligand coordination bonds or induce framework collapse, especially under extreme pH, high salinity, or elevated temperatures. For instance, ZIF−8 membranes demonstrate exceptional ion selectivity but degrade in acidic or alkaline environments due to ligand protonation/deprotonation. To address this, recent strategies have focused on strengthening intrinsic coordination bonds, as exemplified by UiO−66-$(OH)_2$, where Zr–O bond reinforcement enables excellent structural stability in acidic aqueous solutions (Fig. 10C). Alternatively, Al-MOF monolayer membranes exploit π–π interaction-induced self-locking to enhance long-term operational durability (Fig. 10B). For 2D materials, interlayer spacing controlled by hydration or molecular intercalants is sensitive to environmental humidity fluctuations, causing channel dimension drift and compromised sieving reliability over time. Sub-nanometer channels are particularly vulnerable to structural collapse or pore clogging under pressure fluctuations, fouling conditions, or mechanical stress, necessitating robust interlayer reinforcement strategies.

6.4.3. Performance trade-offs and system optimization

Nano-brick systems inherently face device-level trade-offs between selectivity, permeability, and stability that must be balanced in practical operation. Narrower interlayer spacing or pore apertures enhance molecular sieving precision but exponentially increase hydraulic resistance, reducing ion flux and power density below commercially viable thresholds. Higher surface charge density improves cation selectivity through enhanced EDL overlap, yet simultaneously intensifies electrostatic repulsion that diminishes effective pore volume and transport rates (Table 1), as reflected in the sub−30 W m^{-2} power outputs of current state-of-the-art membranes. These gaps highlight the need for system-level multidimensional optimization rather than single-parameter materials tuning. Furthermore, in real-world high-salinity operation, concentration polarization at membrane interfaces reduces effective driving forces, necessitating engineered module designs with optimized flow geometries to mitigate boundary layer effects, an aspect rarely addressed in laboratory-scale demonstrations.

6.4.4. Device integration and anti-fouling engineering

Beyond material-level performance, practical iontronic devices require hierarchical integration of nano-brick units into scalable modules with optimized flow configurations. The assembly of heterogeneous nano-bricks, such as MOF-COF bilayers or 2D material composites, demands precise interfacial matching to avoid transport bottlenecks and mechanical delamination. In continuous operation, membrane fouling by organic matter, biofilms, or inorganic scaling progressively degrades channel performance. Anti-fouling strategies must therefore be co-designed with the nano-brick architecture. For example, sulfonic acid and carboxyl group-enriched surfaces reduce protein adsorption through enhanced electrostatic repulsion and hydrophilic hydration layers (Fig. 19A), while dynamic sliding supramolecular interfaces maintain stable flux decline rates below 15% (Section 6.3.3). The development of self-cleaning or regenerable nano-brick surfaces represents a critical future direction for extending operational lifespan.

6.4.5. Cost effectiveness and lifecycle assessment

Finally, the economic viability of nano-brick membranes depends on raw material costs, synthesis complexity, and recyclability. Precursor chemicals for MOFs and COFs can be expensive, and multistep post-synthetic functionalization adds manufacturing overhead. Conductive MOFs such as $Ni_3(HITP)_2$ offer exceptional electrochemical performance but require costly ligands and controlled redox conditions (Fig. 14A). For widespread energy applications, low-cost, earth-abundant alternatives, such as GO derivatives or clay-based 2D materials, may provide more sustainable pathways, albeit with moderated performance. Lifecycle assessment frameworks should be integrated early in the design process to evaluate the environmental footprint of nano-brick fabrication, operation, and disposal, ensuring that technological advances align with sustainable energy goals.

In summary, while the nano-brick framework enables unprecedented precision in ion transport regulation, its practical impact hinges on overcoming these engineering challenges through interdisciplinary collaboration across materials synthesis, process engineering, and device architecture. Future research should prioritize scalable manufacturing protocols, robust anti-fouling interfaces, and system-level performance benchmarking to accelerate the transition from laboratory innovation to real-world energy solutions.

7. Conclusion

This review systematically summarizes recent progress in nano-confined iontronics, emphasizing the modular nano-brick framework, core research challenges, and quantitative benchmarks for practical applications. Focusing on ion selectivity, rectification, and gating, it outlines the fundamental principles of ion transport regulation. At the materials level, 2D materials, MOFs, and COFs are highlighted as key platforms for constructing sub-nanochannel architectures. The regulatory roles of pore size, charge distribution, and interfacial chemistry in governing ion migration pathways and energy barriers are analyzed. Strategies including surface charge engineering, functional group modification, and chemical recognition enable the programmable construction of ion transport systems. Based on these structure-property relationships, the review discusses the application potential of nano-building block networks in energy harvesting, ion-based information processing, seawater desalination, and ion separation. It reveals the pathway from molecular-scale design to system-level integration, and highlights key challenges toward practical translation. Nano-confined iontronics stands at the frontier of materials science, nanofluidics, and electrochemistry. Precise control of sub-nanochannels, electrical double layer, and interfacial states enables molecular-scale ion transport control, transforming confined systems from passive separators into multifunctional platforms. However, scaling to large-scale applications faces core bottlenecks: fabrication scalability, long-term operational stability, and multifunctional performance balancing. Future research should advance the nano-building block concept, strengthen cross-scale modeling, and foster the synergistic convergence of energy, water desalination, and bioelectronics. With progress in nanofabrication, interface regulation, and multiscale simulation, nano-confined iontronics will evolve toward practical integrated systems, enabling efficient energy conversion, precise separation, and intelligent response, opening new paradigms for sustainable energy, water management, and information processing.

CRediT authorship contribution statement

Di Wei: Writing – review & editing, Funding acquisition, Conceptualization. **Carita Kvarnström:** Conceptualization. **Zhong Lin Wang:** Conceptualization. **Lixue Yang:** Writing – review & editing, Writing – original draft, Methodology, Investigation, Data curation, Conceptualization. **Ari Ivaska:** Conceptualization. **Zhe Wang:** Funding acquisition, Conceptualization.

Declaration of Competing Interest

The authors declare that they have no known competing financial interests or personal relationships that could have appeared to influence the work reported in this paper.

Acknowledgements

This work was funded by the National Natural Science Foundation

(grant number 22479016, U24A20505, and 52473205).

Data Availability

No data was used for the research described in the article.

References

[1] D. Wei, F. Yang, Z. Jiang, Z. Wang, Flexible iontronics based on 2D nanofluidic material, Nat. Commun. 13 (2022) 4965, https://doi.org/10.1038/s41467-022-32699-x.

[2] H. Qian, D. Wei, Z. Wang, Bionic iontronics based on nano-confined structures, Nano Res. 16 (2023) 11718–11730, https://doi.org/10.1007/s12274-023-5705-z.

[3] P. Peng, H. Qian, J. Liu, Z. Wang, D. Wei, Bioinspired ionic control for energy and information flow, Int. J. Smart Nano Mater. 15 (2024) 198–221, https://doi.org/10.1080/19475411.2024.2305393.

[4] P. Peng, F. Yang, X. Li, S. Li, Z. Wang, D. Wei, High-power iontronics enabled by nanoconfined ion dynamics, Cell. Rep. Phys. Sci. 5 (2024) 101824, https://doi.org/10.1016/j.xcrp.2024.101824.

[5] L. Yang, L.N.Y. Cao, S. Li, P. Peng, H. Qian, G. Amaratunga, F. Yang, Z.L. Wang, D. Wei, MOFs/MXene nano-hierarchical porous structures for efficient ion dynamics, Nano Energy 129 (2024) 110076, https://doi.org/10.1016/j.nanoen.2024.110076.

[6] H. Qian, P. Peng, H. Fan, Z. Yang, L. Yang, Y. Zhou, D. Tan, F. Yang, M. Willatzen, G. Amaratunga, Z. Wang, D. Wei, Horizontal transport in Ti_3C_2Tx MXene for highly efficient osmotic energy conversion from saline-alkali environments, Angew. Chem. Int. Ed. 63 (2024) e202414984, https://doi.org/10.1002/anie.202414984.

[7] L. Yang, S. Li, H. Qian, Z. Wang, Z.L. Wang, D. Wei, Osmotic power generation based on nanoconfined materials, MRS Energy Sustain. 11 (2024) 193–218, https://doi.org/10.1557/s43581-024-00104-3.

[8] P. Peng, H. Qian, F. Yang, D. Wei, Scalable, Light rechargeable energy storage based on osmotic effects and photochemical reactions in a hair-thin filament, Adv. Energy Mater. 15 (2025) 2405547, https://doi.org/10.1002/aenm.202405547.

[9] L. Yang, Z. Wang, Z.L. Wang, D. Wei, Porous organic framework membranes with nanostructures for osmotic power conversion, water desalination, and selective separation, ChemNanoMat 11 (2025) e202400629, https://doi.org/10.1002/cnma.202400629.

[10] H. Qian, P. Peng, Y. Liu, Z.L. Wang, D. Wei, Balancing selectivity and permeability in nanofluidic membranes for osmotic power generation, Prog. Energy 7 (2025) 042001, https://doi.org/10.1088/2516-1083/ae0117.

[11] D. Wei, Writable electrochemical energy source based on graphene oxide, Sci. Rep. 5 (2015) 15173, https://doi.org/10.1038/srep15173.

[12] P. Peng, Z.L. Wang, D. Wei, Modulating multi-ion dynamics for high-performance iontronic systems, Iontronics 2 (2026) 5, https://doi.org/10.20517/iontronics.2026.05.

[13] M. Gao, M.-J. Zheng, A.F.M. El-Mahdy, C.-W. Chang, Y.-C. Su, W.-H. Hung, S.-W. Kuo, L.-H. Yeh, A bioinspired ionic diode membrane based on sub-2 nm covalent organic framework channels for ultrahigh osmotic energy generation, Nano Energy 105 (2023) 108007, https://doi.org/10.1016/j.nanoen.2022.108007.

[14] Y. Liu, P. Peng, H. Qian, Z.L. Wang, D. Wei, Nanoconfined iontronics and its electronic applications, Nano Res. Energy 4 (2025) e9120156, https://doi.org/10.26599/NRE.2025.9120156.

[15] Y. Liu, P. Peng, F. Yang, Z.L. Wang, D. Wei, Printable high-performance iontronic power source based on osmotic effects, Energy Mater. 5 (2025) 500059, https://doi.org/10.20517/energymater.2024.187.

[16] A. Wang, S. Feng, T. Xiao, G. Wang, B. Zhu, W. Zhou, L. Wang, Microenvironment-engineered piezoionic hydrogel nanogenerators for enhanced energy harvesting and sensing, SmartSys 1 (2025) e70004, https://doi.org/10.1002/sys3.70004.

[17] H. Daiguji, Ion transport in nanofluidic channels, Chem. Soc. Rev. 39 (2010) 901–911, https://doi.org/10.1039/B820556F.

[18] D. Stein, M. Kruithof, C. Dekker, Surface-charge-governed ion transport in nanofluidic channels, Phys. Rev. Lett. 93 (2004) 035901, https://doi.org/10.1103/PhysRevLett.93.035901.

[19] R.B. Schoch, J. Han, P. Renaud, Transport phenomena in nanofluidics, Rev. Mod. Phys. 80 (2008) 839–883, https://doi.org/10.1103/RevModPhys.80.839.

[20] Y. Chen, Y. Wang, Z. Wen, G. Wang, H. Zhang, C.C. Yang, Q. Jiang, $CuInSe_2$ nanoparticles@3D N-doped carbon nanosheet framework for highly-efficient sodium ion battery, Chem. Eng. J. 519 (2025) 165572, https://doi.org/10.1016/j.cej.2025.165572.

[21] X. Davoy, A. Gellé, J.-C. Lebreton, H. Tabuteau, A. Soldera, A. Szymczyk, A. Ghoufi, High water flux with ions sieving in a desalination 2D sub-nanoporous boron nitride material, ACS Omega 3 (2018) 6305–6310, https://doi.org/10.1021/acsomega.8b01076.

[22] E. Hoenig, Y. Han, K. Xu, J. Li, M. Wang, C. Liu, situ generation of (sub) nanometer pores in MoS2 membranes for ion-selective transport, Nat. Commun. 15 (2024) 7911, https://doi.org/10.1038/s41467-024-52109-8.

[23] B. Clayville, J.Y. Choi, C. Wagner, W. Warren, J. Park, Selective Li ion transport via interpenetrated crystal growth on ZIF-8 seeded nanocomposite membranes, J. Mater. Chem. C. 12 (2024) 13816–13821, https://doi.org/10.1039/D4TC01399A.

[24] H. Zhang, J. Hou, Y. Hu, P. Wang, R. Ou, L. Jiang, J.Z. Liu, B.D. Freeman, A. J. Hill, H. Wang, Ultrafast selective transport of alkali metal ions in metal organic frameworks with subnanometer pores, Sci. Adv. 4 (2018) eaaq0066, https://doi.org/10.1126/sciadv.aaq0066.

[25] R. Xu, X. Xu, A. Alowasheeir, Y. Yamauchi, D. Jiang, Carboxyl-functionalized covalent organic framework for high-performance capacitive deionization, Bull. Chem. Soc. Jpn. 98 (2025), https://doi.org/10.1093/bulcsj/uoaf053.

[26] L. Cao, I.C. Chen, Z. Li, X. Liu, M. Mubashir, R.A. Nuaimi, Z. Lai, Switchable Na+ and K+ selectivity in an amino acid functionalized 2D covalent organic framework membrane, Nat. Commun. 13 (2022) 7894, https://doi.org/10.1038/s41467-022-35594-7.

[27] T. Zhu, Y. Kong, B. Lyu, L. Cao, B. Shi, X. Wang, X. Pang, C. Fan, C. Yang, H. Wu, Z. Jiang, 3D covalent organic framework membrane with fast and selective ion transport, Nat. Commun. 14 (2023) 5926, https://doi.org/10.1038/s41467-023-41555-5.

[28] N.C.R. Chen, P.-C. Han, L.-H. Yeh, Y.-H. Peng, C.-A. Lung, Y. Yamauchi, K.C. W. Wu, A full sub-2 nm and acid-resistant MOF-COF ionic diode membrane for efficient ionic gradient power generation, Chem. Eng. J. 525 (2025) 170303, https://doi.org/10.1016/j.cej.2025.170303.

[29] Y. Zheng, J. Shen, J. Yuan, N.A. Khan, X. You, C. Yang, S. Zhang, A. El-Gendi, H. Wu, R. Zhang, Z. Jiang, 2D nanosheets seeding layer modulated covalent organic framework membranes for efficient desalination, Desalination 532 (2022) 115753, https://doi.org/10.1016/j.desal.2022.115753.

[30] Y. Chu, F. Liu, B. Jian, Y. Hou, F. Huo, Molecular dynamics for nanoconfined ion and water transport: mechanisms and applications in functional nanofluidic devices, ACS Appl. Mater. Interfaces 17 (2025) 68841–68868, https://doi.org/10.1021/acsami.5c15216.

[31] H. Zhang, J. Xing, G. Wei, X. Wang, S. Chen, X. Quan, Electrostatic-induced ion-confined partitioning in graphene nanolaminate membrane for breaking anion–cation co-transport to enhance desalination, Nat. Commun. 15 (2024) 4324, https://doi.org/10.1038/s41467-024-48681-8.

[32] Z. Zhang, C. Li, J. Zhang, M. Eikerling, J. Huang, Dynamic response of ion transport in nanoconfined electrolytes, Nano Lett. 23 (2023) 10703–10709, https://doi.org/10.1021/acs.nanolett.3c02560.

[33] F. Jiang, W.C. Poh, J. Chen, D. Gao, F. Jiang, X. Guo, J. Chen, P.S. Lee, Ion rectification based on gel polymer electrolyte ionic diode, Nat. Commun. 13 (2022) 6669, https://doi.org/10.1038/s41467-022-34429-9.

[34] C. Chen, D. Liu, L. He, S. Qin, J. Wang, J.M. Razal, N.A. Kotov, W. Lei, Bio-inspired nanocomposite membranes for osmotic energy harvesting, Joule 4 (2020) 247–261, https://doi.org/10.1016/j.joule.2019.11.010.

[35] F. Fan, Y. Ren, S. Zhang, Z. Tang, J. Wang, X. Han, Y. Yang, G. Lu, Y. Zhang, L. Chen, Z. Wang, K. Zhang, J. Gao, J. Zhao, G. Cui, B. Tang, A bioinspired membrane with ultrahigh Li^+/Na^+ and Li^+/K^+ separations enables direct lithium extraction from brine, Adv. Sci. 11 (2024) 2402898, https://doi.org/10.1002/advs.202402898.

[36] N.R. Aluru, F. Aydin, M.Z. Bazant, D. Blankschtein, A.H. Brozena, J.P. de Souza, M. Elimelech, S. Faucher, J.T. Fourkas, V.B. Koman, M. Kuehne, H.J. Kulik, H.-K. Li, Y. Li, Z. Li, A. Majumdar, J. Martis, R.P. Misra, A. Noy, T.A. Pham, H. Qu, A. Rayabharam, M.A. Reed, C.L. Ritt, E. Schwegler, Z. Siwy, M.S. Strano, Y. Wang, Y.-C. Yao, C. Zhan, Z. Zhang, Fluids and electrolytes under confinement in single-digit nanopores, Chem. Rev. 123 (2023) 2737–2831, https://doi.org/10.1021/acs.chemrev.2c00155.

[37] H. You, T.-N. Kim, J. Hwang, Nanochannel membranes for ion-selective electrodialysis: principles, materials, and environmental applications, Environ. Sci. Nano 13 (2026) 208–241, https://doi.org/10.1039/D5EN00815H.

[38] J.A. Hossain, B. Kim, Unveiling unique ion transport mechanisms in nanopores beyond the continuum framework, Desalination 614 (2025) 119162, https://doi.org/10.1016/j.desal.2025.119162.

[39] M. Queralt-Martín, L.M. Alvero-González, D.A. Perini, E. García-Giménez, A. Alcaraz, Ion transport in biological ion channels beyond classical electrostatics. Nanoscale confinement, non-linear concentration patterns and interfacial effects, Biophys. Rev. (2026), https://doi.org/10.1007/s12551-026-01413-2.

[40] W. Pu, Z. Sun, Synergistic effects of confinement size and interface on anomalous ultrafast transport in nanofluidics, Commun. Phys. 8 (2025) 167, https://doi.org/10.1038/s42005-025-02085-2.

[41] W. Zhang, A. Zhang, W. Zhou, Y. Ji, Z. Xu, P. Sun, Revisiting ion transport through micropores: significant and non-negligible surface transport, Nanoscale Horiz. 11 (2026) 795–802, https://doi.org/10.1039/D5NH00582E.

[42] X. Li, Z.L. Wang, Iontronic logic control driven by dynamic electrical double layer regulation, Iontronics 1 (2025) 2, https://doi.org/10.20517/iontronics.2025.02.

[43] G. Zhang, G. Hu, J. Li, G. Feng, Y. Cui, Z. Chen, Z. Liu, Y. Cui, Design strategies for ion-sieving charge mosaic membranes toward sustainable lithium extraction, Proc. Natl. Acad. Sci. 122 (2025) e2511666122, https://doi.org/10.1073/pnas.2511666122.

[44] Q. Guo, M. Xu, Q. Tang, Y. Liu, W. Zhang, C. Guo, X. Zhao, Y. Zhu, S. Ye, D. Liu, W. Lei, C. Chen, Advanced hybrid nanosheet membranes with stable nanochannels for ultrafast molecular separation, npj Clean. Water 6 (2023) 38, https://doi.org/10.1038/s41545-023-00250-0.

[45] C. Chen, J. Chen, Y. Peng, M. Wang, D. Luo, Y. Li, R.S. Ruoff, S.H. Lee, Multifunctional coatings of graphene oxide: New membranes for proton permeation and salt rejection, Matter 7 (2024) 1259–1274, https://doi.org/10.1016/j.matt.2024.01.014.

[46] X. Liu, W. Lin, K.B. Al Mohawes, N.M. Khashab, Guanidinium-based covalent organic framework membranes for superior mono- and divalent cations

separation, Small Struct. 6 (2025) 2400496, https://doi.org/10.1002/sstr.202400496.
[47] H. Qian, H. Fan, P. Peng, Y. Du, X. Li, Y. Liu, F. Yang, Y. Zhou, Z.L. Wang, D. Wei, Biomimetic Janus MXene membrane with bidirectional ion permselectivity for enhanced osmotic effects and iontronic logic control, Sci. Adv. 11 (2025) eadx1184, https://doi.org/10.1126/sciadv.adx1184.
[48] N. Kavokine, R.R. Netz, L. Bocquet, Fluids at the Nanoscale: From Continuum to Subcontinuum Transport, Annu. Rev. Fluid. Mech. 53 (2021) 377–410, https://doi.org/10.1146/annurev-fluid-071320-095958.
[49] L. Bocquet, E. Charlaix, Nanofluidics, from bulk to interfaces, Chem. Soc. Rev. 39 (2010) 1073–1095, https://doi.org/10.1039/B909366B.
[50] T.A. Zangle, A. Mani, J.G. Santiago, Theory and experiments of concentration polarization and ion focusing at microchannel and nanochannel interfaces, Chem. Soc. Rev. 39 (2010) 1014–1035, https://doi.org/10.1039/B902074H.
[51] X. Li, Y. Wei, Z.L. Wang, D. Wei, Iontronic regulation of nanoconfined electrical double layers on dielectric solids, Small Sci. 5 (2025) 2500371, https://doi.org/10.1002/smsc.202500371.
[52] R.B. Schoch, P. Renaud, Ion transport through nanoslits dominated by the effective surface charge, Appl. Phys. Lett. 86 (2005), https://doi.org/10.1063/1.1954899.
[53] H. Daiguji, P. Yang, A. Majumdar, Ion transport in nanofluidic channels, Nano Lett. 4 (2004) 137–142, https://doi.org/10.1021/nl0348185.
[54] Z. Zhang, L. Wen, L. Jiang, Nanofluidics for osmotic energy conversion, Nat. Rev. Mater. 6 (2021) 622–639, https://doi.org/10.1038/s41578-021-00300-4.
[55] A. Siria, P. Poncharal, A.-L. Biance, R. Fulcrand, X. Blase, S.T. Purcell, L. Bocquet, Giant osmotic energy conversion measured in a single transmembrane boron nitride nanotube, Nature 494 (2013) 455–458, https://doi.org/10.1038/nature11876.
[56] M.A. Brown, A. Goel, Z. Abbas, Effect of Electrolyte Concentration on the Stern Layer Thickness at a Charged Interface, Angew. Chem. Int. Ed. 55 (2016) 3790–3794, https://doi.org/10.1002/anie.201512025.
[57] C.G. Gray, P.J. Stiles, Nonlinear electrostatics: the Poisson–Boltzmann equation, Eur. J. Phys. 39 (2018) 053002, https://doi.org/10.1088/1361-6404/aaca5a.
[58] J. Chen, W. Xin, X.-Y. Kong, Y. Qian, X. Zhao, W. Chen, Y. Sun, Y. Wu, L. Jiang, L. Wen, Ultrathin and robust silk fibroin membrane for high-performance osmotic energy conversion, ACS Energy Lett. 5 (2020) 742–748, https://doi.org/10.1021/acsenergylett.9b02296.
[59] Z. Zhang, X. Sui, P. Li, G. Xie, X.-Y. Kong, K. Xiao, L. Gao, L. Wen, L. Jiang, Ultrathin and ion-selective Janus membranes for high-performance osmotic energy conversion, J. Am. Chem. Soc. 139 (2017) 8905–8914, https://doi.org/10.1021/jacs.7b02794.
[60] J.-R. Li, R.J. Kuppler, H.-C. Zhou, Selective gas adsorption and separation in metal–organic frameworks, Chem. Soc. Rev. 38 (2009) 1477–1504, https://doi.org/10.1039/B802426J.
[61] S. Qiu, M. Xue, G. Zhu, Metal–organic framework membranes: from synthesis to separation application, Chem. Soc. Rev. 43 (2014) 6116–6140, https://doi.org/10.1039/C4CS00159A.
[62] H. Furukawa, K.E. Cordova, M. O'Keeffe, O.M. Yaghi, The chemistry and applications of metal-organic frameworks, Science 341 (2013) 1230444, https://doi.org/10.1126/science.1230444.
[63] S. Hou, W. Ji, J. Chen, Y. Teng, L. Wen, L. Jiang, Free-standing covalent organic framework membrane for high-efficiency salinity gradient energy conversion, Angew. Chem. Int. Ed. 60 (2021) 9925–9930, https://doi.org/10.1002/anie.202100205.
[64] L.-J. Cheng, L.J. Guo, Nanofluidic diodes, Chem. Soc. Rev. 39 (2010) 923–938, https://doi.org/10.1039/B822554K.
[65] K. Xiao, L. Jiang, M. Antonietti, on transport in nanofluidic devices for energy harvesting, Joule 3 (2019) 2364–2380, https://doi.org/10.1016/j.joule.2019.09.005.
[66] Z.S. Siwy, Ion-current rectification in nanopores and nanotubes with broken symmetry, Adv. Funct. Mater. 16 (2006) 735–746, https://doi.org/10.1002/adfm.200500471.
[67] P. Liu, G. Xie, P. Li, Z. Zhang, L. Yang, Y. Zhao, C. Zhu, X.-Y. Kong, L. Jiang, L. Wen, A universal tunable nanofluidic diode via photoresponsive host–guest interactions, NPG Asia Mater. 10 (2018) 849–857, https://doi.org/10.1038/s41427-018-0079-5.
[68] I. Vlassiouk, Z.S. Siwy, Nanofluidic diode, Nano Lett. 7 (2007) 552–556, https://doi.org/10.1021/nl062924b.
[69] M. Li, Y. Cao, Y. Xiong, G. Qing, Hierarchically engineered nanochannel systems with pore-in/on-pore structures, NPG Asia Mater. 15 (2023) 16, https://doi.org/10.1038/s41427-022-00451-y.
[70] Z.-J. Yang, L.-H. Yeh, Y.-H. Peng, Y.-P. Chuang, K.C.W. Wu, Enhancing ionic selectivity and osmotic energy by using an ultrathin Zr-MOF-based heterogeneous membrane with trilayered continuous porous structure, Angew. Chem. Int. Ed. 63 (2024) e202408375, https://doi.org/10.1002/anie.202408375.
[71] Y. Du, Z.L. Wang, D. Chu, G. Amaratunga, D. Wei, Iontronics for adaptive and flexible pressure sensing, Iontronics 2 (2026) 13, https://doi.org/10.20517/iontronics.2026.13.
[72] Y. Du, Z.L. Wang, D. Wei, Intelligent wearable technologies enabled by triboelectric nanogenerators, Soft Sci. 6 (2026) 12, https://doi.org/10.20517/ss.2025.136.
[73] Z. Zhou, Y. Du, Y. Zhang, J. Fu, Y. Ouyang, Z.L. Wang, D. Wei, Bioinspired omnidirectional iontronic sensors based on triboelectric charge, Small 22 (2026) e10157, https://doi.org/10.1002/smll.202510157.
[74] Y. Ouyang, X. Li, Y. Du, Y. Zhang, Z.L. Wang, D. Wei, Mechano-driven neuromimetic logic gates established by geometrically asymmetric hydrogel iontronics, Small 21 (2025) 2409998, https://doi.org/10.1002/smll.202409998.
[75] Y. Jiang, R. Wang, C. Ye, X. Wang, D. Wang, Q. Du, H. Liang, S. Zhang, P. Gao, Stimuli-responsive ion transport regulation in nanochannels by adhesion-induced functionalization of macroscopic outer surface, ACS Appl. Mater. Interfaces 16 (2024) 35666–35674, https://doi.org/10.1021/acsami.4c02299.
[76] B. Sabbagh, N.E. Fraiman, A. Fish, G. Yossifon, Designing with iontronic logic gates—from a single polyelectrolyte diode to an integrated ionic circuit, ACS Appl. Mater. Interfaces 15 (2023) 23361–23370, https://doi.org/10.1021/acsami.3c00062.
[77] J. Li, M. Li, K. Zhang, L. Hu, D. Li, High-performance integrated iontronic circuits based on single nano/microchannels, Small 19 (2023) 2208079, https://doi.org/10.1002/smll.202208079.
[78] W. Liu, T. Mei, Z. Cao, C. Li, Y. Wu, L. Wang, G. Xu, Y. Chen, Y. Zhou, S. Wang, Y. Xue, Y. Yu, X.-Y. Kong, R. Chen, B. Tu, K. Xiao, Bioinspired carbon nanotube–based nanofluidic ionic transistor with ultrahigh switching capabilities for logic circuits, Sci. Adv. 10 (2024) eadj7867, https://doi.org/10.1126/sciadv.adj7867.
[79] Z. Shen, D. Zhu, M. Zhang, Synergy of smart materials and structures toward intelligent metamaterials, SmartSys 1 (2025) e70007, https://doi.org/10.1002/sys3.70007.
[80] J. Liu, S. Wang, T. Huang, P. Manchanda, E. Abou-Hamad, S.P. Nunes, Smart covalent organic networks (CONs) with "on-off-on" light-switchable pores for molecular separation, Sci. Adv. 6 (2020) eabb3188, https://doi.org/10.1126/sciadv.abb3188.
[81] C. Zhao, J. Hou, M. Hill, B. Freeman, H. Wang, H. Zhang, Enhanced gating effects in responsive sub-nanofluidic ion channels, Acc. Mater. Res. 4 (2023) 786–797, https://doi.org/10.1021/accountsmr.3c00067.
[82] I. Vlassiouk, C.-D. Park, S.A. Vail, D. Gust, S. Smirnov, Control of nanopore wetting by a photochromic spiropyran: a light-controlled valve and electrical switch, Nano Lett. 6 (2006) 1013–1017, https://doi.org/10.1021/nl060313d.
[83] H. Cong, X. Xu, B. Yu, Z. Yang, X. Zhang, A smart temperature and magnetic-responsive gating carbon nanotube membrane for ion and protein transportation, Sci. Rep. 6 (2016) 32130, https://doi.org/10.1038/srep32130.
[84] F. Sheng, B. Wu, X. Li, T. Xu, M.A. Shehzad, X. Wang, L. Ge, H. Wang, T. Xu, Efficient ion sieving in covalent organic framework membranes with sub-2-nanometer channels, Adv. Mater. 33 (2021) 2104404, https://doi.org/10.1002/adma.202104404.
[85] J. Fang, G. Zhang, M.-A. Goulet, P. Zuo, Y. Zhou, H. Li, J. Jiang, M.D. Guiver, Z. Yang, T. Xu, High selectivity framework polymer membranes chemically tuned towards fast anion conduction, Nat. Commun. 16 (2025) 3282, https://doi.org/10.1038/s41467-025-58638-0.
[86] J. Wang, J. Zhang, P. Jin, H. Wen, Z. Dai, H. Tan, S. Yuan, J. Yang, M. Elimelech, A covalent organic framework membrane with highly selective and permeable artificial sodium channels via ion recognition, Nat. Commun. 16 (2025) 7346, https://doi.org/10.1038/s41467-025-62329-1.
[87] R.K. Tonnah, S. Foorginezhad, B.W. Nyande, F. Arshadi, M. Razbin, M. Chai, A. Razmjou, M. Asadnia, Bioinspired and engineered ion-selective membranes toward high-flux and high-selectivity energy devices, Small 22 (2026) e10500, https://doi.org/10.1002/smll.202510500.
[88] X. Liu, J. Wang, Y. Shang, C.T. Yavuz, N.M. Khashab, Ionic covalent organic framework-based membranes for selective and highly permeable molecular sieving, J. Am. Chem. Soc. 146 (2024) 2313–2318, https://doi.org/10.1021/jacs.3c11542.
[89] Y. Zhao, J. Wang, X.-Y. Kong, W. Xin, T. Zhou, Y. Qian, L. Yang, J. Pang, L. Jiang, L. Wen, Robust sulfonated poly (ether ether ketone) nanochannels for high-performance osmotic energy conversion, Natl. Sci. Rev. 7 (2020) 1349–1359, https://doi.org/10.1093/nsr/nwaa057.
[90] I. Sadeghi, J. Kronenberg, A. Asatekin, Selective transport through membranes with charged nanochannels formed by scalable self-assembly of random copolymer micelles, ACS Nano 12 (2018) 95–108, https://doi.org/10.1021/acsnano.7b07596.
[91] G. Zhao, Y. Zhang, Y. Li, G. Pan, Y. Liu, Positively charged nanofiltration membranes for efficient Mg^{2+}/Li^{+} separation from high Mg^{2+}/Li^{+} ratio brine, Adv. Membr. 3 (2023) 100065, https://doi.org/10.1016/j.advmem.2023.100065.
[92] Y. Wang, Y. Zhang, M. Zhang, S. Jiang, X. Tang, H. Liang, Advanced biomimetic nanofiltration membranes for lithium recovery with anti-janus charge structure, Nat. Commun. 17 (2025) 202, https://doi.org/10.1038/s41467-025-66887-2.
[93] Z. Zhao, N. Di, Z. Zha, J. Wang, Z. Wang, S. Zhao, Positively charged polyamine nanofiltration membrane for precise ion–ion separation, ACS Appl. Mater. Interfaces 15 (2023) 48695–48704, https://doi.org/10.1021/acsami.3c11076.
[94] Z. Zhang, X. Xiao, Y. Zhou, L. Huang, Y. Wang, Q. Rong, Z. Han, H. Qu, Z. Zhu, S. Xu, J. Tang, J. Chen, Bioinspired graphene oxide membranes with pH-responsive nanochannels for high-performance nanofiltration, ACS Nano 15 (2021) 13178–13187, https://doi.org/10.1021/acsnano.1c02719.
[95] J. Hou, H. Zhang, H. Wang, A.W. Thornton, K. Konstas, Amphoteric metal–organic framework subnanochannels with pH-tuneable cation and anion sieving properties, J. Mater. Chem. A 11 (2023) 13223–13230, https://doi.org/10.1039/D3TA01901B.
[96] Y. Du, D. Lei, X. Hao, Z. Liu, X. Du, Crown ether-functionalized 3D COF membrane with ion-recognition sites for enhanced monovalent cation selectivity, Sep. Purif. Technol. 376 (2025) 133979, https://doi.org/10.1016/j.seppur.2025.133979.

[97] T. Ye, G. Hou, W. Li, C. Wang, K. Yi, N. Liu, J. Liu, S. Huang, J. Gao, Artificial sodium-selective ionic device based on crown-ether crystals with subnanometer pores, Nat. Commun. 12 (2021) 5231, https://doi.org/10.1038/s41467-021-25597-1.
[98] Z. Jing, G. Wang, Y. Zhou, D. Pang, F. Zhu, H. Liu, Selectivity of 18-crown-6 ether to alkali ions by density functional theory and molecular dynamics simulation, J. Mol. Li. 311 (2020) 113305, https://doi.org/10.1016/j.molliq.2020.113305.
[99] H. Zhang, J. Zhang, D. Wang, H. Fan, Y. Xu, F. Zhao, Q. Chen, J. Wang, Z. Xu, Advances in metal organic framework-based membranes for ion–selective sieving, Sep. Purif. Technol. 374 (2025) 133623, https://doi.org/10.1016/j.seppur.2025.133623.
[100] H.-Y. Chi, S. Song, K. Zhao, K.-J. Hsu, Q. Liu, Y. Shen, A.F. Sido Belin, A. Allaire, R. Goswami, W.L. Queen, K.V. Agrawal, Non-van-der-waals oriented two-dimensional UiO-66 films by rapid aqueous synthesis at room temperature, J. Am. Chem. Soc. 147 (2025) 7255–7263, https://doi.org/10.1021/jacs.4c11134.
[101] R.-J. Mo, S. Chen, L.-Q. Huang, X.-L. Ding, S. Rafique, X.-H. Xia, Z.-Q. Li, Regulating ion affinity and dehydration of metal-organic framework sub-nanochannels for high-precision ion separation, Nat. Commun. 15 (2024) 2145, https://doi.org/10.1038/s41467-024-46378-6.
[102] A. Wang, C. Breakwell, F. Foglia, R. Tan, L. Lovell, X. Wei, T. Wong, N. Meng, H. Li, A. Seel, M. Sarter, K. Smith, A. Alvarez-Fernandez, M. Furedi, S. Guldin, M. M. Britton, N.B. McKeown, K.E. Jelfs, Q. Song, Selective ion transport through hydrated micropores in polymer membranes, Nature 635 (2024) 353–358, https://doi.org/10.1038/s41586-024-08140-2.
[103] R. Shevate, D.L. Shaffer, Large-area 2D covalent organic framework membranes with tunable single-digit nanopores for predictable mass transport, ACS Nano 16 (2022) 2407–2418, https://doi.org/10.1021/acsnano.1c08804.
[104] Y.-C. Lin, H.-H. Chen, C.-W. Chu, L.-H. Yeh, Massively enhanced charge selectivity, ion transport, and osmotic energy conversion by antiswelling nanoconfined hydrogels, Nano Lett. 24 (2024) 11756–11762, https://doi.org/10.1021/acs.nanolett.4c03836.
[105] S. Liao, Y. Liu, L. Li, L. Ding, Y. Wei, H. Wang, Theoretical framework for confined ion transport in two-dimensional nanochannels, Nat. Commun. 16 (2025) 6675, https://doi.org/10.1038/s41467-025-61735-9.
[106] J. Lu, H. Zhang, J. Hou, X. Li, X. Hu, Y. Hu, C.D. Easton, Q. Li, C. Sun, A. W. Thornton, M.R. Hill, X. Zhang, G. Jiang, J.Z. Liu, A.J. Hill, B.D. Freeman, L. Jiang, H. Wang, Efficient metal ion sieving in rectifying subnanochannels enabled by metal–organic frameworks, Nat. Mater. 19 (2020) 767–774, https://doi.org/10.1038/s41563-020-0634-7.
[107] Y. Lou, Z. Wang, W. Yang, S. Lang, J. Fan, Q. Ke, R. Wang, Z. Zhang, W. Chen, J. Xue, Covalent organic framework membranes for ion separation: a review, Membranes 15 (2025), https://doi.org/10.3390/membranes15070211.
[108] S. Su, Y. Zhang, S. Peng, L. Guo, Y. Liu, E. Fu, H. Yao, J. Du, G. Du, J. Xue, Multifunctional graphene heterogeneous nanochannel with voltage-tunable ion selectivity, Nat. Commun. 13 (2022) 4894, https://doi.org/10.1038/s41467-022-32590-9.
[109] Y. Cui, H. Guo, X. Yan, W. Zhou, Q. Ye, C. Ying, Z. Liu, J. Tian, Nonlinear and anisotropic ion transport in black phosphorus nanochannels, Nano Lett. 23 (2023) 5886–5893, https://doi.org/10.1021/acs.nanolett.3c00078.
[110] T. Ying, N. Onofrio, L. Mei, H. Peng, Z. Zhang, M. Gu, C. Ma, Y. Chen, J. Zhou, K. M.Y. Leung, C. Cheng, S. Li, B. Liu, C.Y. Tang, D. Voiry, Z. Zeng, Vacancy functionalized MoS_2 nanolaminated membranes for efficient sieving in forward osmosis, Adv. Mater. 37 (2025) e04781, https://doi.org/10.1002/adma.202504781.
[111] Y. Liu, R. Wang, X. Ma, Y. Wang, S. Shen, B. Bai, C. Sun, Two-dimensional lamellar nanosheet membranes with intrinsic size-sieving nanopores for ultrafast hydrogen separation, Sci. Adv. 12 (2026) eadz5523, https://doi.org/10.1126/sciadv.adz5523.
[112] S. Hong, F. Ming, Y. Shi, R. Li, I.S. Kim, C.Y. Tang, H.N. Alshareef, P. Wang, Two-dimensional Ti_3C_2Tx MXene membranes as nanofluidic osmotic power generators, ACS Nano 13 (2019) 8917–8925, https://doi.org/10.1021/acsnano.9b02579.
[113] D. Shi, L. Zhou, Z. Li, Nanofluidic systems for ion transport with tunable surface charges: fabrications, characterizations, and applications, Front. Lab. Chip. Technol. 3 (2024), https://doi.org/10.3389/frlct.2024.1356800.
[114] L. Chen, G. Shi, J. Shen, B. Peng, B. Zhang, Y. Wang, F. Bian, J. Wang, D. Li, Z. Qian, G. Xu, G. Liu, J. Zeng, L. Zhang, Y. Yang, G. Zhou, M. Wu, W. Jin, J. Li, H. Fang, Ion sieving in graphene oxide membranes via cationic control of interlayer spacing, Nature 550 (2017) 380–383, https://doi.org/10.1038/nature24044.
[115] R.K. Joshi, P. Carbone, F.C. Wang, V.G. Kravets, Y. Su, I.V. Grigorieva, H.A. Wu, A.K. Geim, R.R. Nair, Precise and ultrafast molecular sieving through graphene oxide membranes, Science 343 (2014) 752–754, https://doi.org/10.1126/science.1245711.
[116] M. Zhang, K. Guan, Y. Ji, G. Liu, W. Jin, N. Xu, Controllable ion transport by surface-charged graphene oxide membrane, Nat. Commun. 10 (2019) 1253, https://doi.org/10.1038/s41467-019-09286-8.
[117] C. Cheng, G. Jiang, C.J. Garvey, Y. Wang, G.P. Simon, J.Z. Liu, D. Li, Ion transport in complex layered graphene-based membranes with tuneable interlayer spacing, Sci. Adv. 2 (2016) e1501272, https://doi.org/10.1126/sciadv.1501272.
[118] S. Chen, G.S.X. Tan, A. Ivanov, T.M. Savilov, K. Yang, X. Leng, M. Chen, K. S. Novoselov, D.V. Andreeva, Tunable anion transport and the chemical transistor effect in functionalized graphene oxide membranes, npj 2D Mater. Appl. 9 (2025) 62, https://doi.org/10.1038/s41699-025-00585-x.
[119] P. Sun, M. Zhu, K. Wang, M. Zhong, J. Wei, D. Wu, Z. Xu, H. Zhu, Selective ion penetration of graphene oxide membranes, ACS Nano 7 (2013) 428–437, https://doi.org/10.1021/nn304471w.
[120] Z. Zhang, W. Shen, L. Lin, M. Wang, N. Li, Z. Zheng, F. Liu, L. Cao, Vertically transported graphene oxide for high-performance osmotic energy conversion, Adv. Sci. 7 (2020) 2000286, https://doi.org/10.1002/advs.202000286.
[121] X. He, W. Xin, C. Yang, S. Wan, T. Liu, S. Huang, Y. Deng, L. Shi, L. Wen, T. Zhou, Two-dimensional molybdenum disulfide/graphene oxide composite membrane for stable osmotic energy conversion, J. Membr. Sci. 732 (2025) 124251, https://doi.org/10.1016/j.memsci.2025.124251.
[122] X. Liu, L. Zhang, X. Cui, Q. Zhang, W. Hu, J. Du, H. Zeng, Q. Xu, 2D material nanofiltration membranes: from fundamental understandings to rational design, Adv. Sci. 8 (2021) 2102493, https://doi.org/10.1002/advs.202102493.
[123] X. Li, H. Zhang, P. Wang, J. Hou, J. Lu, C.D. Easton, X. Zhang, M.R. Hill, A. W. Thornton, J.Z. Liu, B.D. Freeman, A.J. Hill, L. Jiang, H. Wang, Fast and selective fluoride ion conduction in sub-1-nanometer metal-organic framework channels, Nat. Commun. 10 (2019) 2490, https://doi.org/10.1038/s41467-019-10420-9.
[124] Y. Peng, H. Huang, Y. Zhang, C. Kang, S. Chen, L. Song, D. Liu, C. Zhong, A versatile MOF-based trap for heavy metal ion capture and dispersion, Nat. Commun. 9 (2018) 187, https://doi.org/10.1038/s41467-017-02600-2.
[125] D.T. Sun, L. Peng, W.S. Reeder, S.M. Moosavi, D. Tiana, D.K. Britt, E. Oveisi, W. L. Queen, Rapid, selective heavy metal removal from water by a metal–organic framework/polydopamine composite, ACS Cent. Sci. 4 (2018) 349–356, https://doi.org/10.1021/acscentsci.7b00605.
[126] X. Yang, Q. An, X. Li, Y. Fu, S. Yang, M. Liu, Q. Xu, G. Zeng, Charging modulation of the pyridine nitrogen of covalent organic frameworks for promoting oxygen reduction reaction, Nat. Commun. 15 (2024) 1889, https://doi.org/10.1038/s41467-024-46291-y.
[127] Y. Wu, Y. Qian, B. Niu, J. Chen, X. He, L. Yang, X.-Y. Kong, Y. Zhao, X. Lin, T. Zhou, L. Jiang, L. Wen, Surface charge regulated asymmetric ion transport in nanoconfined space, Small 17 (2021) 2101099, https://doi.org/10.1002/smll.202101099.
[128] R.K. Tonnah, M. Chai, M. Khedri, M. Razbin, R. Maleki, A. Razmjou, M. Asadnia, Bilayer asymmetric-based metal-organic frameworks membrane for blue energy conversion, Desalination 591 (2024) 117968, https://doi.org/10.1016/j.desal.2024.117968.
[129] R.J. Marshall, Y. Kalinovskyy, S.L. Griffin, C. Wilson, B.A. Blight, R.S. Forgan, Functional versatility of a series of Zr metal–organic frameworks probed by solid-state photoluminescence spectroscopy, J. Am. Chem. Soc. 139 (2017) 6253–6260, https://doi.org/10.1021/jacs.7b02184.
[130] D. Yang, Y. Yang, T. Wong, S. Iguodala, A. Wang, L. Lovell, F. Foglia, P. Fouquet, C. Breakwell, Z. Fan, Y. Wang, M.M. Britton, D.R. Williams, N. Shah, T. Xu, N. B. McKeown, M.-M. Titirici, K.E. Jelfs, Q. Song, Solution-processable polymer membranes with hydrophilic subnanometre pores for sustainable lithium extraction, Nat. Water 3 (2025) 319–333, https://doi.org/10.1038/s44221-025-00398-8.
[131] E.B. Nordquist, Z. Jia, J. Chen, Inner pore hydration free energy controls the; activation of big potassium channels, Biophys. J. 122 (2023) 1158–1167, https://doi.org/10.1016/j.bpj.2023.02.005.
[132] S. Wannapaiboon, A. Schneemann, I. Hante, M. Tu, K. Epp, A.L. Semrau, C. Sternemann, M. Paulus, S.J. Baxter, G. Kieslich, R.A. Fischer, Control of structural flexibility of layered-pillared metal-organic frameworks anchored at surfaces, Nat. Commun. 10 (2019) 346, https://doi.org/10.1038/s41467-018-08285-5.
[133] M. Jian, R. Qiu, Y. Xia, J. Lu, Y. Chen, Q. Gu, R. Liu, C. Hu, J. Qu, H. Wang, X. Zhang, Ultrathin water-stable metal-organic framework membranes for ion separation, Sci. Adv. 6 (2020) eaay3998, https://doi.org/10.1126/sciadv.aay3998.
[134] R. Akai, S. Kitajima, K. Okubo, N. Serizawa, H. Nishihara, H. Kasai, K. Oka, Water-resistant redox-active metal–organic framework, Nat. Commun. 16 (2025) 10798, https://doi.org/10.1038/s41467-025-65849-y.
[135] H. Wang, Y. Zhai, Y. Li, Y. Cao, B. Shi, R. Li, Z. Zhu, H. Jiang, Z. Guo, M. Wang, L. Chen, Y. Liu, K.-G. Zhou, F. Pan, Z. Jiang, Covalent organic framework membranes for efficient separation of monovalent cations, Nat. Commun. 13 (2022) 7123, https://doi.org/10.1038/s41467-022-34849-7.
[136] S. Zheng, X. Liu, C. Wang, Z. Ouyang, X. Zhang, S. Bi, G. Shi, Q. Xu, J.S. Francisco, G. Zeng, Quantitative skeletal-charge engineering of anion-selective COF membrane for ultrahigh osmotic power output, J. Am. Chem. Soc. 147 (2025) 15777–15786, https://doi.org/10.1021/jacs.5c03492.
[137] Y. Yusran, B. Miao, S. Qiu, Q. Fang, Functional covalent organic frameworks: design principles to potential application, Acc. Mater. Res. 5 (2024) 1263–1278, https://doi.org/10.1021/accountsmr.4c00195.
[138] Y. Yusran, X. Guan, H. Li, Q. Fang, S. Qiu, Postsynthetic functionalization of covalent organic frameworks, Natl. Sci. Rev. 7 (2019) 170–190, https://doi.org/10.1093/nsr/nwz122.
[139] H. Liu, S. Zhu, Y. Zhi, H. Yue, X. Liu, Donor–acceptor type covalent organic frameworks: design, optimization strategies and applications, Chem. Sci. 16 (2025) 12768–12803, https://doi.org/10.1039/D5SC01267H.
[140] X.-F. Hu, T. Jiang, H. Fan, Y.-F. Guan, J.-J. Chen, H.-Q. Yu, M. Elimelech, Dual-regulated covalent organic framework membranes with near-theoretical pore sizes for angstrom-scale ion separations, Sci. Adv. 11 (2025) eady3587, https://doi.org/10.1126/sciadv.ady3587.
[141] X. You, L. Cao, Y. Liu, H. Wu, R. Li, Q. Xiao, J. Yuan, R. Zhang, C. Fan, X. Wang, P. Yang, X. Yang, Y. Ma, Z. Jiang, Charged nanochannels in covalent organic

framework membranes enabling efficient ion exclusion, ACS Nano 16 (2022) 11781–11791, https://doi.org/10.1021/acsnano.2c04767.
[142] Y. Pan, G. Yu, L. Gao, X. Li, L. Yang, H. Gao, T. Wang, W. Zhang, S. Ma, H. Meng, Ultra-rapid preparation of large-area high-crystallinity covalent organic framework membranes, Nat. Commun. 17 (2025) 857, https://doi.org/10.1038/s41467-025-67569-9.
[143] Y.J. Shin, M. Kim, H. Kim, Y.Y. Kim, N.H. Kwon, A. Machida, Y. Nakahira, S. Kim, K. Sakaki, W.B. Lee, E.S. Cho, Surface-engineered asymmetric covalent organic framework membranes with polymers for improved ion transport, ACS Nano 19 (2025) 34150–34162, https://doi.org/10.1021/acsnano.5c10521.
[144] P. Wang, W. Tao, T. Zhou, J. Wang, C. Zhao, G. Zhou, Y. Yamauchi, Nanoarchitectonics in advanced membranes for enhanced osmotic energy harvesting, Adv. Mater. 36 (2024) 2404418, https://doi.org/10.1002/adma.202404418.
[145] Y. Zhang, K. Zhou, S. Su, J. Gao, J. Liu, L. Jiang, Congener-welded crystalline carbon nitride membrane for robust and highly selective Li/Mg separation, Sci. Adv. 10 (2024) eadm9620, https://doi.org/10.1126/sciadv.adm9620.
[146] J. Luo, A. Remy, Y. Zhang, Iontronic devices from biological nanopores to artificial systems: emerging applications and future perspectives, Chem. Rev. 125 (2025) 11840–11877, https://doi.org/10.1021/acs.chemrev.5c00579.
[147] P. Xu, X. Wu, Z. Zhang, P. Pan, X. Liu, Enhancing the rectification effect of hydrogel-based stretchable ionic diodes through incorporating cations with high valence, Microsyst. Nanoeng. 11 (2025) 139, https://doi.org/10.1038/s41378-025-00943-1.
[148] A. Bahrawy, P. Galek, C. Gellrich, N. Niese, M.A.A. Mohamed, M. Hantusch, J. Grothe, S. Kaskel, Nanostructured h-WO_3-based ionologic gates with enhanced rectification and transistor functionality, ACS Nano 19 (2025) 20655–20671, https://doi.org/10.1021/acsnano.5c02035.
[149] S. Shimizu, H. Shioya, T. Hatano, K. Miwa, A. Oiwa, S. Ono, Electrically induced insulator-to-metal transition in InP-based ion-gated transistor, Sci. Rep. 14 (2024) 30364, https://doi.org/10.1038/s41598-024-81685-4.
[150] V.-P. Mai, A.R. Fauziah, C.-R. Gu, Z.-J. Yang, K.C.W. Wu, L.-H. Yeh, R.-J. Yang, Two-dimensional metal–organic framework nanocomposite membranes with shortened ion pathways for enhanced salinity gradient power harvesting, Chem. Eng. J. 484 (2024) 149649, https://doi.org/10.1016/j.cej.2024.149649.
[151] J. Yang, B. Tu, G. Zhang, P. Liu, K. Hu, J. Wang, Z. Yan, Z. Huang, M. Fang, J. Hou, Q. Fang, X. Qiu, L. Li, Z. Tang, Advancing osmotic power generation by covalent organic framework monolayer, Nat. Nanotechnol. 17 (2022) 622–628, https://doi.org/10.1038/s41565-022-01110-7.
[152] Y.-C. Liu, L.-H. Yeh, M.-J. Zheng, K.C.-W. Wu, Highly selective and high-performance osmotic power generators in subnanochannel membranes enabled by metal-organic frameworks, Sci. Adv. 7 (2021) eabe9924, https://doi.org/10.1126/sciadv.abe9924.
[153] Z.-Q. Li, G.-L. Zhu, R.-J. Mo, M.-Y. Wu, X.-L. Ding, L.-Q. Huang, Z.-Q. Wu, X.-H. Xia, Light-enhanced osmotic energy harvester using photoactive porphyrin metal–organic framework membranes, Angew. Chem. Int. Ed. 61 (2022) e202202698, https://doi.org/10.1002/anie.202202698.
[154] Y. Wu, Y. Liu, C. Zhu, X.-Y. Kong, L. Wen, Olfactory-inspired nanofluidic sensor: molecular recognition and transport in confined space, Iontronics 2 (2026) 14, https://doi.org/10.20517/iontronics.2026.001.
[155] X. Chen, Y. Liu, T. Deng, M. Wang, Bioinspired mechanosensitive ion channels: design principles and emerging applications, Iontronics 2 (2026) 12, https://doi.org/10.20517/iontronics.2026.12.
[156] Y. Lyu, Y. Su, K. Nan, Y. Zhang, Bioinspiration for bioiontronics, Iontronics 2 (2026) 9, https://doi.org/10.20517/iontronics.2026.09.
[157] D. Sheberla, J.C. Bachman, J.S. Elias, C.-J. Sun, Y. Shao-Horn, M. Dincă, Conductive MOF electrodes for stable supercapacitors with high areal capacitance, Nat. Mater. 16 (2017) 220–224, https://doi.org/10.1038/nmat4766.
[158] M. Farina, B.B. Duff, C. Tealdi, A. Pugliese, F. Blanc, E. Quartarone, Li^+ dynamics of liquid electrolytes nanoconfined in metal–organic frameworks, ACS Appl. Mater. Interfaces 13 (2021) 53986–53995, https://doi.org/10.1021/acsami.1c16214.
[159] J. Park, M. Lee, D. Feng, Z. Huang, A.C. Hinckley, A. Yakovenko, X. Zou, Y. Cui, Z. Bao, Stabilization of hexaaminobenzene in a 2D conductive metal–organic framework for high power sodium storage, J. Am. Chem. Soc. 140 (2018) 10315–10323, https://doi.org/10.1021/jacs.8b06020.
[160] J. Wang, F. Li, Z. Liu, Z. Dai, S. Gao, M. Zhao, Two-dimensional conductive metal–organic frameworks as highly efficient electrocatalysts for lithium–sulfur batteries, ACS Appl. Mater. Interfaces 13 (2021) 61205–61214, https://doi.org/10.1021/acsami.1c19381.
[161] L. Zhai, Z. Xu, Information processing by digitalizing confined ion transport, Iontronics 2 (2026) 11, https://doi.org/10.20517/iontronics.2026.11.
[162] L. Li, W. Chen, X.-Y. Kong, L. Wen, Nanofluidic neuromorphic iontronics: a nexus for biological signal transduction, Iontronics 2 (2026) 4, https://doi.org/10.20517/iontronics.2026.04.
[163] C. Luo, L. Zhou, R. Xu, Y. Hou, X. Hou, CNT array-based aluminum bipolar electrode iontronic memristors, Iontronics 2 (2026) 6, https://doi.org/10.20517/iontronics.2026.06.
[164] B. Xie, P. Yu, Ion-shuttling memristor: towards ionic computing and neuromorphic sensing, Iontronics 2 (2026) 2, https://doi.org/10.20517/iontronics.2026.02.
[165] Y. Ouyang, Z.L. Wang, D. Wei, Ionic rectification via electrical double layer modulation at hydrogel interfaces, RSC Appl. Interfaces 2 (2025) 873–896, https://doi.org/10.1039/D5LF00098J.
[166] W. Guan, R. Fan, M.A. Reed, Field-effect reconfigurable nanofluidic ionic diodes, Nat. Commun. 2 (2011) 506, https://doi.org/10.1038/ncomms1514.
[167] L.-J. Cheng, L.J. Guo, Ionic current rectification, breakdown, and switching in heterogeneous oxide nanofluidic devices, ACS Nano 3 (2009) 575–584, https://doi.org/10.1021/nn8007542.
[168] S. Seo, T. Kim, In-situ gas permeation-driven ionic current rectification of heterogeneously charged nanopore arrays, Small 20 (2024) 2402188, https://doi.org/10.1002/smll.202402188.
[169] W. Zhao, L. Shi, J. Chen, J. Ma, Q. Lv, Y. Sun, N. Lv, X. Chang, P. Xin, Fast-switching pH-responsive biomimetic ion channels with bidirectional gating control, Chem. Sci. 17 (2026) 2273–2280, https://doi.org/10.1039/D5SC07123B.
[170] Y. Wu, Q. Xu, Y. Chen, C. Li, Y. Wu, X. Yu, H. Li, Z. Xu, J. Xu, Z. Ni, Y. Ge, T. Yan, Z. Qi, J. Liu, Mechanosensitive and pH-gated butterfly-shaped artificial ion channel for high-selective K^+ transport and cancer cell apoptosis, Adv. Mater. 37 (2025) 2416852, https://doi.org/10.1002/adma.202416852.
[171] J. Wang, Z. Song, M. He, Y. Qian, D. Wang, Z. Cui, Y. Feng, S. Li, B. Huang, X. Kong, J. Han, L. Wang, Light-responsive and ultrapermeable two-dimensional metal-organic framework membrane for efficient ionic energy harvesting, Nat. Commun. 15 (2024) 2125, https://doi.org/10.1038/s41467-024-46439-w.
[172] M.-S. Wu, X.-C. Du, Z.-R. Zhou, X.-Y. Wang, S.-Y. Zheng, J. Lv, B.-B. Chen, D.-W. Li, R.-C. Qian, Chemically gated artificial nanochannels for programmable subcellular signal modulated transport regulation, Nat. Commun. 16 (2025) 11423, https://doi.org/10.1038/s41467-025-66239-0.
[173] J. Liu, N. Wang, L.-J. Yu, A. Karton, W. Li, W. Zhang, F. Guo, L. Hou, Q. Cheng, L. Jiang, D.A. Weitz, Y. Zhao, Bioinspired graphene membrane with temperature tunable channels for water gating and molecular separation, Nat. Commun. 8 (2017) 2011, https://doi.org/10.1038/s41467-017-02198-5.
[174] H. Kim, K. Kim, S.J. Lee, Nature-inspired thermo-responsive multifunctional membrane adaptively hybridized with PNIPAm and PPy, e445, NPG Asia Mater. 9 (2017) e445, https://doi.org/10.1038/am.2017.168.
[175] Z. Sun, T. He, Z. Ren, C. Wang, X. Liu, Z. Zhang, J. Zhou, X. Guo, Y. Yang, C. Lee, Moving toward human-like perception and sensation systems—from integrated intelligent systems to decentralized smart devices, SmartSys 1 (2025) e4, https://doi.org/10.1002/sys3.4.
[176] Y. Noh, A. Smolyanitsky, Synaptic-like plasticity in 2D nanofluidic memristor from competitive bicationic transport, Sci. Adv. 10 (2024) eadr1531, https://doi.org/10.1126/sciadv.adr1531.
[177] Z. Zhang, B. Sabbagh, Y. Chen, G. Yossifon, Geometrically scalable iontronic memristors: employing bipolar polyelectrolyte gels for neuromorphic systems, ACS Nano 18 (2024) 15025–15034, https://doi.org/10.1021/acsnano.4c01730.
[178] Y.-T. Xu, S.-Y. Yu, Z. Li, B.-H. Kou, J.-X. Pang, W.-W. Zhao, H.-Y. Chen, J.-J. Xu, A nanofluidic spiking synapse, Sci. Adv. 121 (2024) e2403143121, https://doi.org/10.1073/pnas.2403143121.
[179] Y. Feng, Y. Zhu, W. Chen, X. Huang, X. Weng, M.D. Meyer, T.-H. Chen, Y. Liu, Z. He, C.-H. Hou, K. Zuo, N.Y. Yip, K. Gong, J. Lou, Q. Li, A rationally designed scalable thin film nanocomposite cation exchange membrane for precise lithium extraction, Nat. Commun. 16 (2025) 8618, https://doi.org/10.1038/s41467-025-63660-3.
[180] S. Bao, Z. Ma, L. Yu, Q. Li, J. Xia, S. Song, K. Sui, Y. Zhao, X. Liu, J. Gao, Randomly oriented covalent organic framework membrane for selective Li+ sieving from other ions, Nat. Commun. 16 (2025) 3896, https://doi.org/10.1038/s41467-025-59188-1.
[181] M. Liu, M. Wei, G. Liu, D. Li, Z. Zhang, Y. Wang, Covalent organic framework membranes achieving Mg/Li separation by permeating Mg^{2+} while retaining Li^+, J. Membr. Sci. 712 (2024) 123247 https://doi.org/10.1016/j.memsci.2024.123247.
[182] K. Zou, H. Ling, Q. Wang, C. Zhu, Z. Zhang, D. Huang, K. Li, Y. Wu, W. Xin, X.-Y. Kong, L. Jiang, L. Wen, Turing-type nanochannel membranes with extrinsic ion transport pathways for high-efficiency osmotic energy harvesting, Nat. Commun. 15 (2024) 10231, https://doi.org/10.1038/s41467-024-54622-2.
[183] J. Safaei, Y. Gao, M. Hosseinpour, X. Zhang, Y. Sun, X. Tang, Z. Zhang, S. Wang, X. Guo, Y. Wang, Z. Chen, D. Zhou, F. Kang, L. Jiang, G. Wang, Vacancy engineering for high-efficiency nanofluidic osmotic energy generation, J. Am. Chem. Soc. 145 (2023) 2669–2678, https://doi.org/10.1021/jacs.2c12936.
[184] M. He, Y. He, D. Lu, M. Wang, J. Yang, T. Wu, J. Ma, Supramolecular dynamics-enhanced synergistic antifouling mechanisms for enhanced membrane antifouling and permeability, Nat. Commun. 16 (2025) 6956, https://doi.org/10.1038/s41467-025-62231-w.
[185] A. Taghipour, P. Karami, M. Manikantan Sandhya, M. Sadrzadeh, An innovative surface modification technique for antifouling polyamide nanofiltration membranes, ACS Appl. Mater. Interfaces 16 (2024) 37197–37211, https://doi.org/10.1021/acsami.4c06082.
[186] Y. Liao, S. Fang, J. Tang, M. Tang, F. Zheng, Z. Pan, J. Zhan, G. Han, Thiazole-conjugated covalent organic framework membranes enable ultraselective molecular desalination under strongly acidic conditions, Nat. Commun. 17 (2026) 1424, https://doi.org/10.1038/s41467-025-68171-9.
[187] Y. Li, Y. Duan, J. Yuan, L. Ge, X. Zhang, J. Hou, Y. Zhang, B. Van der Bruggen, J. Zhu, M. Elimelech, Macrocycle-assembled membranes for high-salinity organic wastewater treatment, Nat. Commun. 17 (2026) 1731, https://doi.org/10.1038/s41467-026-68430-3.